Uniwersytet Gdański

Wydział Biologii
Uniwersytetu Gdańskiego

mgr Mariola Gimła

Mechanizmy działania pochodnej kwasu usninowego wobec komórek nowotworu trzustki

Praca przedstawiona
Radzie Dyscypliny Nauki biologiczne Uniwersytetu Gdańskiego
celem uzyskania stopnia doktora
w dziedzinie nauk ścisłych i przyrodniczych
w dyscyplinie nauki biologiczne

Promotor: prof. dr hab. Anna Herman-Antosiewicz

Promotor pomocniczy: dr Aleksandra Hać

Katedra Biologii i Genetyki Medycznej, Wydział Biologii,
Uniwersytet Gdański

GDAŃSK 2025

Faculty of Biology
University of Gdansk

Mariola Gimła, MSc

Mechanisms of action of usnic acid derivative against pancreatic cancer cells

PhD thesis
presented to the Biological Sciences Discipline Board
of the University of Gdansk
to obtain a doctoral degree in the field of exact and natural sciences in the discipline of biological sciences

Supervisor: Anna Herman-Antosiewicz, PhD

Co-supervisor: Aleksandra Hać, PhD

Department of Medical Biology and Genetics, Faculty of Biology, University of Gdansk

GDAŃSK 2025

Składam serdeczne podziękowania
Mojej Pani Promotor Profesor Annie Herman-Antosiewicz
za cenne uwagi, za wszechstronną pomoc,
za wsparcie podczas każdego etapu tworzenia tej pracy,
a także za cały poświęcony czas.

Dziękuję Pani Promotor dr Aleksandrze Hać
za wsparcie merytoryczne,
życzliwość i słowa otuchy
w czasie powstawania pracy.

Dziękuję Rodzicom i Bratu
za ogrom cierpliwości,
nieustanną motywację oraz
oparcie w trudnych chwilach.

Dziękuję Przyjaciołom i Rodzinie
za przypominanie mi, że po burzy zawsze wychodzi słońce
i to dopiero początek.

Spis treści

1. Wykaz prac wchodzących w skład rozprawy doktorskiej

1. **Gimła Mariola**, Herman-Antosiewicz Anna (2024) Multifaceted properties of usnic acid in disrupting cancer hallmarks, *Biomedicines* 12 (10): 2199. DOI:10.3390/biomedicines12102199.
2. **Gimła Mariola**, Pyrczak-Felczykowska Agnieszka, Malinowska Marcelina, Hać Aleksandra, Narajczyk Magdalena, Bylińska Irena, Reekie Tristan, Herman-Antosiewicz Anna (2023) The pyrazole derivative of usnic acid inhibits the proliferation of pancreatic cancer cells in vitro and in vivo, *Cancer Cell International* 23(1): 210., DOI:10.1186/s12935-023-03054.
3. **Gimła Mariola**, Hać Aleksandra, Reekie Tristan, Herman-Antosiewicz Anna. Impact of usnic acid pyrazole derivative on the metastatic potential and mitochondria of pancreatic cancer cells - manuskrypt złożony do redakcji *BMC Cancer*, w trakcie recenzji.

2. Źródła finansowania

1. Projekt: “Nowe pochodne kwasu usninowego jako leki antynowotworowe” finansowany przez Narodowe Centrum Nauki w programie Harmonia 9 (2019/35/N/NZ2/00505). Kierownik projektu: prof. dr hab. Anna Herman-Antosiewicz.
2. Projekt: „Wpływ pochodnej kwasu usninowego na proces inwazji w komórkowym modelu nowotworu trzustki” finansowany w Konkursie Projektów Badawczych Młodych Naukowców Uniwersytetu Gdańskiego (grant nr 539-D130-B859-21). Kierownik projektu: mgr Mariola Gimła.
3. Projekt: „Działanie terapii łączonej na zmiany metabolizmu energetycznego w komórkowym modelu nowotworu trzustki” finansowany w Konkursie Projektów Badawczych Młodych Naukowców Uniwersytetu Gdańskiego (grant nr 539-D130-B953-22). Kierownik projektu: mgr Mariola Gimła.

3. Wykaz skrótów

2-APB: ang. 2-Aminoethoxydiphenylborane, 2-aminoetoksydifenyloboran, inhibitor receptora trifosforanu inozytolu

3-BrPA: ang. 3-Bromopyruvic Acid, kwas 3-bromopirogronowy, inhibitor glikolizy

3-PGK: ang. 3-Phosphoglycerate Kinase, kinaza 3-fosfoglicerynianowa, enzym glikolityczny

7-AAD: ang. 7-amino-actinomycin D, 7-amino-aktynomycyna D, barwnik znakujący DNA

ATP: ang. Adenosine triphosphate, adenozynotrójfosforan

BAPTA: ang. 1,2-Bis(2-aminophenoxy)ethane-N,N,N',N'-tetraacetic acid, 1,2-Bis(2-aminofenoksy)etano-N,N,N',N'-kwas tetraoctowy, chelator jonów wapnia

Bax: ang. Bcl-2–associated X protein, białko proapoptotyczne

Bcl-2: ang. B-cell lymphoma 2, białko antyapoptotyczne

BiP: ang. Binding Immunoglobin Protein, marker stresu siateczki śródplazmatycznej

CCL2 (MCP-1): ang. Monocyte Chemoattractant Protein-1, chemokina regulująca migrację monocytów/makrofagów.

CDKN2A/p16: ang. Cyclin Dependent Kinase Inhibitor 2A, gen kodujący białko p16 będące inhibitorem kinaz zależnych od cyklin, supresor nowotworzenia

CI: ang. Combination Index, współczynnik kombinacji

COX-2: ang. Cyclooxygenase-2, cyklooksygenaza-2 indukowana pod wpływem czynników związanych ze stanem zapalnym

c-PARP: Cleaved PARP, cięta forma polimerazy poli-ADP rybozy, marker apoptozy

CTL: ang. Cytotoxic T lymphocytes, Limfocyty T cytotoksyczne

CXCL10: ang. Interferon gamma-induced protein 10, białko 10 indukowane interferonem gamma, cytokina prozapalna

CXCL8: interleukina 8, białko zaangażowane w adhezję i migrację komórek

DMEM: ang. Dulbecco's Modified Eagle Medium, pożywka hodowlana

DMSO: ang. Dimethyl Sulfoxide, dimetylosulfotlenek

DNMT: ang. DNA Methyltransferase, metylofransferaza DNA

ECM: ang. Extracellular Matrix, macierz zewnątrzkomórkowa

EMT: ang. Epithelial- Mesenchymal Transition, przejście epitelialno-mezenchymalne

EGFR: ang Epidermal Growth Factor Receptor, receptor naskórkowego czynnika wzrostu

ER: ang. Endoplasmic Reticulum, retikulum endoplazmatyczne

FAK: ang. Focal Adhesion Kinase, kinaza płytek przylegania

GADD153: ang. Growth Arrest DNA Damage 153, marker stresu ER

GAPDH: ang. Glyceraldehyde 3-Phosphate Dehydrogenase, dehydrogenaza aldehydu 3-fosfoglicerynowego, enzym glikolityczny

GSH: ang. Glutathione, glutation

HDFa : ang. Human Dermal Fibroblasts adult, ludzkie fibroblasty skóry

HK2: ang. Hexokinase 2, heksokinaza2, enzym metabolizmu glukozy

IC_{50}: ang. Half Maximal Inhibitory Concentration, połowa maksymalnego stężenia hamującego

IL-2: Interleukina 2, reguluje różnicowanie i funkcję komórek T CD4(+)

IL-6: Interleukina 6, działa zarówno jako cytokina prozapalna, jak i miokina przeciwzapalna

iNOS : ang. Inducible Nitric Oxide Synthase, indukowana syntaza tlenku azotu

IRE1α: ang. Inositol Requiring Enzyme 1 alpha, kinaza białkowa serynowo-treoninowa/endorybonukleaza, marker stresu ER

LDH: ang. Lactate Dehydrogenase, dehydrogenaza mleczanowa, enzym szlaku glikolizy

MAPK: ang. Mitogen-Activated Protein Kinase, kinaza białkowa aktywowana mitogenem

MCF-7: linia komórek ludzkiego gruczolakoraka piersi

MDA: ang. Malondialdehyde, dialdehyd malonowy, marker peroksydacji lipidów

Mia PaCa-2: linia komórek ludzkiego nowotworu trzustki pochodzenia epitelialnego

MMP: ang. Matrix Metalloproteinase, metaloproteinaza macierzy

MTT: ang. 3-(4,5-dimethylthiazol-2-yl)-2,5-diphenyltetrazolium bromide, Bromek 3-(4,5-dimetylotiazol-2-ylo)-2,5-difenylotetrazoliowy, barwnik wykorzystywany w testach cytotoksyczności

NK: ang. Natural Killer, komórki układu odpornościowego zaangażowane w niszczenie nieprawidłowych komórek

NO: ang. Nitric Oxide, tlenek azotu

OCR: ang. Oxygen Consumption Rate, szybkość zużycia tlenu, marker funkcji mitochondriów

OXPHOS: ang. Oxidative Phosphorylation, fosforylacja oksydacyjna

p53: ang. protein 53, białko p53, czynnik transkrypcyjny, białko supresorowe nowotworów

PANC-1: linia komórek ludzkiego nowotworu trzustki pochodzenia epitelialnego

PBS: ang. Phosphate-Buffered Saline, buforowana fosforanem sól fizjologiczna

PDAC: ang. Pancreatic Ductal Adenocarcinoma, gruczolakorak, rak przewodu trzustkowego

PDH: ang. Pyruvate Dehydrogenase, dehydrogenaza pirogronianowa, enzym przekształcający pirogronian w acetylo-CoA

PD-L1 : ang. Programmed Death Ligand 1, ligand 1 programowanej śmierci komórek, białko immunologicznego punktu kontrolnego

PGE2; ang. prostaglandin E2, prostaglandyna E2, marker stanu zapalnego

PVDF: ang. Polyvinylidene Fluoride, membrana PVDF używana w technice Western blot

RAS: Rat Sarcoma Virus, protoonkogen, koduje białko Ras zaangażowane w szlaki przekazywania sygnałów do przeżycia i proliferacji komórek

Rb: ang. Retinoblastoma Protein, białko retinoblastomy, białko supresorowe nowotworu

RFT: Reaktywne Formy Tlenu

SDS–PAGE: ang. Sodium Dodecyl Sulfate–Polyacrylamide Gel Electrophoresis, elektroforeza poliakrylamidowa w warunkach denaturujących

SE: ang. Standard Error, błąd standardowy

SEM: ang. Standard Error of the Mean, błąd standardowy średniej

SGI-1027: ang. N-[4-[(2-amino-6-methyl-4-pyrimidinyl)amino]phenyl]-4-(4-quinolinyl-amino)-benzamide, inhibitor metylotransferazy DNA

SMAD4: ang. Mothers Against Decapentaplegic Homolog 4, białko biorące udział w przekazywaniu sygnału od transformującego czynnika wzrostu beta

SRB: ang. Sulforhodamine B, sulforodamina B, barwnik wykorzystywany w testach żywotności komórek

TAZ: Trójmiejska Zwierzętarnia Akademicka

TCA: ang. Tricarboxylic Acid Cycle, cykl kwasów trójkarboksylowych

TEM: ang. Transmission Electron Microscopy, transmisyjna mikroskopia elektronowa

TGF-β: ang. Transforming Growth Factor beta, transformujący czynnik wzrostu beta, czynnik wzrostu

TNF-α: ang. Tumor Necrosis Factor alpha, czynnik martwicy nowotworu alfa, cytokina prozapalna

UA: ang. Usnic Acid, kwas usninowy

uPA: ang. Urokinase-type Plasminogen Activator, aktywator plazminogenu typu urokinazy, białko zaangażowane w migrację komórek

UPR: ang. Unfolded Protein Response, odpowiedź na błędnie sfałdowane białka

VEGF: ang. Vascular Endothelial Growth Factor, czynnika wzrostu śródbłonka naczyniowego

4. Streszczenie w języku polskim

Choroby nowotworowe stanowią obecnie jedno z najpoważniejszych zdrowotnych wyzwań w skali całego świata. Nowotwór trzustki jest trzecim pod względem śmiertelności nowotworem, zaraz po raku płuca i jelita grubego. W 2022 r. prawie pół miliona osób zmarło z powodu tej choroby. Wzrost zachorowalności i zgonów z powodu nowotworów złośliwych, w tym nowotworu trzustki, jest przyczyną ciągłych poszukiwań i rozwoju nowych leków, również w oparciu o związki naturalnie występujące w przyrodzie.

Kwas usninowy (ang. usnic acid, UA, 2,6-diacetylo-7,9-dihydroksy-8,9b-dimetylodibenzo[b,d]furan-1,3(2H,9bH)-dion) należy do benzofuranowych metabolitów wtórnych porostów i wykazuje szereg aktywności biologicznych, w tym działanie antynowotworowe. Liczne badania wskazują, że UA posiada potencjał antyproliferacyjny i zatrzymuje cykl komórkowy w fazie G0/G1, S lub G2/M, a także powoduje śmierć komórek nowotworowych. Mimo tej obiecującej aktywności, UA ma także wady. Przede wszystkim musi być stosowany w wysokich stężeniach, aby wykazywać działanie antynowotworowe, a wówczas cechuje się również silną hepatotoksycznością. W celu ulepszenia działania UA, w tym zwiększenia jego aktywności i selektywności wobec komórek nowotworowych oraz zwiększenia rozpuszczalności w wodzie i biodostępności, badacze projektują jego syntetyczne pochodne.

Jedną z takich pochodnych, która silniej niż UA obniża żywotność różnych typów komórek nowotworowych, jest (*R*)-8-acetylo-5,7-dihydroksy-3,4a,6-trimetylo-2,4a-dihydro-4*H*-benzofuro[3,2-*f*]indazol-4-on, pirazolowa pochodna UA oznaczona jako **5.**

Celem niniejszej pracy było porównanie jej aktywności wobec komórek ludzkiego nowotworu trzustki z aktywnością związku wyjściowego i poznanie mechanizmów jej działania. Otrzymane wyniki wskazują, że pochodna **5** działa wielokierunkowo w komórkach raka trzustki linii Mia PaCa-2 i PANC-1. Wykazuje ona silniejszy niż UA potencjał antyproliferacyjny i cytotoksyczny poprzez hamowanie cyklu komórkowego w fazie G0/G1 oraz indukcję śmierci komórek. U podłoża tych procesów leży stres retikulum endoplazmatycznego (ER). Co ważne, działanie to jest również widoczne *in vivo*. U myszy z przeszczepionymi ludzkimi komórkami nowotworowymi trzustki pochodna **5** skutecznie hamuje wzrost guza i nie powoduje widocznych skutków ubocznych. Co więcej,

pochodna **5** efektywnie ogranicza migrację i inwazję komórek raka trzustki. Towarzyszy temu modulacja poziomu markerów przejścia epitelialno-mezenchymalnego (EMT), zwłaszcza zwiększenie poziomu białka Klaudyny-1, co sugeruje, że związek ten poprzez utrzymanie integralności nabłonka mógłby zapobiegać lub odwracać proces EMT i redukować tym samym potencjał metastatyczny.

Pochodna **5** normalizuje także morfologię mitochondriów, co wiąże się ze spadkiem poziomu ATP w komórkach nowotworowych. Połączenie pochodnej **5** z inhibitorem glikolizy, 3-BrPA, potęguje spadek poziomu ATP (efekt synergii), co wpływa na natężenie i rodzaj śmierci komórek.

Podsumowując, poprzez wpływ na takie procesy jak cykl komórkowy, śmierć komórek, ich migrację, inwazję, EMT i metabolizm energetyczny, pochodna **5** ogranicza wiele kluczowych etapów w progresji raka trzustki. Fakt, że jest efektywna i bezpieczna w modelu *in vivo*, skłania do dalszych badań nad jej wykorzystaniem w terapii tego nowotworu.

5. Streszczenie w języku angielskim

Cancer is currently one of the most serious health challenges worldwide. Pancreatic cancer is the third most deadly neoplasia, after lung and colon cancer. In 2022, almost half a million people died from this disease. The increase in morbidity and mortality due to malignant tumors, including pancreatic cancer, is the reason for the continuous search and development of new drugs, also based on naturally occurring compounds.

Usnic acid (UA 2,6-diacetyl-7,9-dihydroxy-8,9b-dimethyldibenzo[b,d]furan 1,3(2H,9bH)-dione) belongs to the benzofuran secondary metabolites of lichens and exhibits many biological activities, including anticancer activity. Numerous studies indicate that UA has antiproliferative potential by arresting the cell cycle at the G0/G1, S or G2/M phase, and also causes the death of cancer cells through apoptosis or necrosis. Despite its promising activity, UA also has disadvantages. First of all, it must be used in high concentrations to exhibit anticancer activity, and it is also characterized by hepatotoxicity. To improve its properties, including increasing its activity and selectivity towards cancer cells, as well as enhancing its water solubility and bioavailability, researchers are designing its synthetic derivatives.

One of such derivatives, which more strongly than UA reduces the viability of various types of cancer cells, is (R)-8-acetyl-5,7-dihydroxy-3,4a,6-trimethyl-2,4a-dihydro-4H benzofuro[3,2-f]indazol-4-one, a pyrazole derivative of UA, designated as **5**.

This study aimed to compare activity of derivative **5** with the parent compound against human pancreatic cancer cells and to understand the mechanisms of its action.

The obtained results indicate that derivative **5** acts multidirectionally in pancreatic cancer cells of the Mia PaCa-2 and PANC-1 lines. It exhibits stronger antiproliferative and cytotoxic potential than UA by inhibiting the cell cycle at the G0/G1 phase and inducing cell death. The basis of these processes is endoplasmic reticulum (ER) stress. Importantly, this effect is also visible *in vivo*. In mice transplanted with human pancreatic cancer cells, derivative **5** effectively inhibits tumor growth and causes no visible side effects.

Moreover, derivative **5** effectively limits the migration and invasion of pancreatic cancer cells. This is accompanied by modulation of the levels of epithelial-mesenchymal transition (EMT) markers, especially the increase in the level of Claudin-1 protein,

suggesting that this compound, by maintaining the integrity of the epithelium, could prevent or reverse the EMT process and thus reduce the metastatic potential of cancer cells. Derivative **5** also normalizes mitochondrial morphology, which is associated with a decrease in ATP levels in cancer cells. Combination of derivative **5** with a glycolysis inhibitor, 3-BrPA, decreases ATP levels in a synergistic way, which affects the intensity and type of cell death.

In summary, by affecting processes such as the cell cycle, cell death, migration, invasion, EMT and energy metabolism, derivative **5** limits many key stages in the progression of pancreatic cancer. The fact that it is effective and safe in the in vivo model encourages further research on its use in the therapy of this cancer.

6. Wprowadzenie

Choroby nowotworowe stanowią obecnie jedno z najpoważniejszych zdrowotnych wyzwań w skali całego świata [1]. W samym 2022 roku były przyczyną prawie 10 milionów zgonów [2]. Szacuje się, że jedna na pięć osób zostanie dotknięta tą chorobą w ciągu swojego życia. Prognozy wskazują też, że globalna liczba zachorowań na nowotwory znacznie wzrośnie w najbliższych latach. Do 2050 r. spodziewanych jest ponad 35 milionów nowych przypadków rocznie, co stanowi wzrost o 77% w porównaniu z 2022 r [3].

Nowotwory to zróżnicowana grupa chorób charakteryzujących się niekontrolowanymi podziałami zmienionych, transformowanych nowotworowo komórek i ich rozprzestrzenianiem się w organizmie chorego oraz tworzeniem kolejnych ognisk, czyli tzw. przerzutów. Powstawanie przerzutów uznaje się za główną przyczyną śmiertelności związanej z chorobami nowotworowymi [4].

Nowotwór trzustki jest trzecim pod względem śmiertelności nowotworem, zaraz po raku płuca i jelita grubego [5]. Oszacowano, że zapadalność na tę chorobę na świecie wynosiła 510 566 przypadków w 2022 r., a prognozy przewidują utrzymujący się wzrostowy trend [2]. Liczba zgonów z powodu nowotworów trzustki w 2022 roku wyniosła 467 005, co odzwierciedla wysoki wskaźnik śmiertelności tej choroby [2,3]. Jest też jedną z najczęstszych przyczyn zgonów spowodowanych nowotworami, zarówno u mężczyzn jak i kobiet na całym świecie, według danych GLOBOCAN [2].

Znaczna część pacjentów diagnozowana jest w późnym wieku - mediana wynosi 71 lat, ale 20% diagnoz stawianych jest już przed 60 rokiem życia [6]. 5-letni wskaźnik przeżycia pacjenta od chwili postawienia diagnozy wynosi poniżej 10%, a powodem niskiej przeżywalności jest występowanie nieresekcyjnych form guza oraz znaczne zaawansowanie choroby w momencie jej wykrycia [7,8].

Nowotwory trzustki dzieli się na dwa główne typy - zewnątrzwydzielnicze oraz neuroendokrynne, z których każdy ma odrębne charakterystyczne cechy i dzieli się na podtypy [9]. Najczęściej diagnozowanymi są rodzaje zewnątrzwydzielnicze, stanowiące ponad 90% wszystkich przypadków nowotworów trzustki. Tego typu guzy powstają z komórek produkujących enzymy trawienne lub wyścielających przewody trzustki.

Gruczolakorak (rak przewodowy, ang. pancreatic ductal adenocarcinoma, PDAC) jest najczęstszym typem, stanowiąc ponad 90% przypadków [10].

U podłoża PDAC leżą zmiany w sekwencji lub ekspresji wielu genów. Praca Grutzmann i wsp. pokazała, że zmiany w ekspresji genów w raku trzustki dotyczyły 568 genów, przy czym 364 wykazywało zwiększoną, a 204 zmniejszoną ekspresję [11]. Niektóre z nich są klasyfikowane jako geny napędowe (ang. driver genes). Mutacje w tych genach dają przewagę selekcyjną komórkom nowotworowym w podziałach i żywotności, co przekłada się na wzrost guza i progresję choroby. Inne zmiany dotyczą genów pasażerskich (ang. passenger genes), które nie są kluczowe i nie przyczyniają się bezpośrednio do procesu nowotworzenia [12]. Główne geny napędowe w PDAC to onkogen *KRAS* kodujący białko Ras oraz geny supresorowe - *SMAD4* kodujący czynnik transkrypcyjny, *CDKN2A* kodujący białko p16 będące inhibitorem kinaz zależnych od cyklin fazy G1 cyklu komórkowego i *TP53* kodujące białko p53 [13,14]. Onkogenne mutacje w *KRAS* występują w 80–95% przypadków tego nowotworu, szczególnie w populacjach zachodnich. W przypadkach, w których wykryto dziki typ *KRAS*, inne geny, m.in. *BRAF, GNAS, FGFR2 i CTNNB1* odgrywają główną rolę w progresji tego raka. [15,16]. Jeśli chodzi o geny supresorowe nowotworów, to ponad 90% przypadków PDAC charakteryzuje się mutacjami w *CDKN2A* oraz *SMAD4,* a następnie zmniejszeniem ekspresji *TP53*, które występuje w sześciu z dziesięciu diagnozowanych nowotworów [17,18]. Jednocześnie około jedna na dziesięć osób z PDAC ma mutacje linii zarodkowej w genach naprawy DNA, *BRCA2* i *MLH1*, podczas gdy prawie 40% wykazuje nadmierną ekspresję *EGFR* [19,20]. Na podstawie tych markerów i analizy RNA-seq PDAC dzieli się na kilka podtypów molekularnych, co ma znaczenie w odpowiednim doborze terapii [21]. Co ważne, oprócz dużej różnorodności na poziomie DNA i RNA między podtypami tego nowotworu, w obrębie guza u danego pacjenta występują heterogenne populacje komórek [22]. Przyczynia się to oporności tych nowotworów na leczenie.

Do braku sukcesu obecnych terapii przyczynia się również nadmierna desmoplazja będącą charakterystyczną cechą PDAC. Cechuje ją gęsta macierz zewnątrzkomórkowa (ang. Extracellular Matrix, ECM), która razem z licznymi czynnikami wzrostu wydzielanymi przez fibroblasty i inne komórki tam obecne, sprzyja proliferacji i inwazyjności komórek nowotworowych, hamuje odpowiedź ze strony komórek układu immunologicznego oraz utrudnia penetrację leków do komórek rakowych [23,24].

Ostatnie 10 lat postępu w metodach diagnostycznych, postępowaniu okołooperacyjnym, technikach radioterapii i systemowych terapiach spowodował istotny postęp w leczeniu pacjentów z rakiem trzustki, choć ciągle niesatysfakcjonująco wydłużają czas przeżycia [25–27]. Możliwość operacyjnego usunięcia guza dotyczy 15-20% przypadków, ale pomimo resekcji chirurgicznej, u 75% pacjentów choroba nawraca w ciągu dwóch lat, co wymaga pooperacyjnej chemioterapii [27]. Lekiem stosowanym w chemioterapii pierwszego rzutu jest gemcytabina, ale zaledwie 5,4% pacjentów dotkniętych nowotworem trzustki odpowiada na leczenie tym związkiem. W celu poprawy skuteczności leczenia zaleca się zatem terapie skojarzone, np. z użyciem FOLFIRINOX (kombinacja kwasu foliowego, 5-fluorouracylu, irynotekanu, oksaliplatyny), gemcytabiny w połączeniu z cisplatyną lub nab-paklitakselem oraz 5-fluorouracyl (lub doustny wariant, S-1) w monoterapii [28–30]. Wybór schematu leczenia dla każdego pacjenta może się różnić w zależności od stanu zdrowia i stadium raka [31]. Analiza bazy danych Cochrane sugeruje, że łączenie wielu środków chemioterapeutycznych w zaawansowanym raku trzustki jest skuteczniejsze niż pojedyncze leczenie, pomimo zwiększonych działań niepożądanych [32]. Dla przykładu, zmodyfikowany FOLFIRINOX (5-fluorouracyl, irynotekan, oksaliplatyna i leukoworyna), który jest oferowany głównie po operacji kwalifikującym się pacjentom, wydłużał czas przeżycia pacjentów bez progresji raka do sześciu miesięcy w porównaniu do pacjentów poddanych wyłącznie resekcji guza [33].

Wzrost zachorowalności i zgonów z powodu nowotworów złośliwych, w tym nowotworu trzustki, jest przyczyną ciągłych poszukiwań i rozwoju leków o działaniu przeciwnowotworowym. Substancje pochodzenia naturalnego, w tym obecne w diecie, są od lat szeroko badane pod kątem aktywności antyproliferacyjnej. Naturalne związki są często źródłem inspiracji do projektowania syntetycznych pochodnych lub formulacji leków o lepszym działaniu terapeutycznym niż związki macierzyste, w tym o wyższej aktywności, lepszej selektywności wobec zmienionych komórek oraz większej biodostępności.

Kwas usninowy (ang. usnic acid, UA; 2,6-diacetylo-7,9-dihydroksy-8,9b-dimetylodibenzo[b,d]furan-1,3(2H,9bH)-dion, Ryc. 1) należy do benzofuranowych metabolitów wtórnych porostów. Obficie występuje w rodzajach *Alectoria, Cladonia, Evernia, Lecanora, Ramalina* i *Usnea*. Stanowi około 4–8% suchej masy plechy porostowej,

jednakże zawartość ta może się różnić w zależności od warunków środowiskowych [34,35]. W przyrodzie występuje w postaci izomerów różniących się orientacją grupy metylowej w pozycji 9b: (–)-UA i (+)-UA oraz jako mieszanina racemiczna [36,37]. Enancjomery mogą wykazywać różne aktywności biologiczne i interakcje [38].

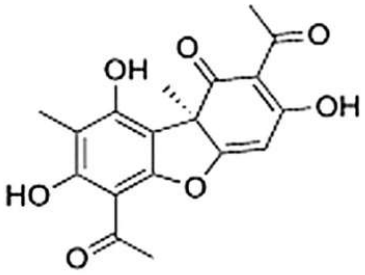

Ryc. 1 Struktura (+)-kwasu usninowego

UA to jeden z najlepiej zbadanych związków bioaktywnych występujących w porostach. Wykazuje szereg aktywności biologicznych, takich jak działanie przeciwbakteryjne, przeciwwirusowe, przeciwgrzybicze, przeciwpierwotniakowe, przeciwzapalne, przeciwbólowe, neuroprotekcyjne i przeciwnowotworowe [39–43]. Działanie przeciwnowotworowe (–)-UA opisano po raz pierwszy w 1975 r., kiedy Kupchan i Kopperman wyizolowali ten związek z *Cladonia* i podali myszom z rakiem płuca Lewisa. Okazało się, że (–)-UA zastosowany w zakresie dawek 20–200 mg/kg wydłużył życie zwierząt nawet o 52% w porównaniu z nieleczoną grupą kontrolną [44].

Od tamtej pory związek ten jest szeroko badany w kontekście działania na komórki nowotworowe różnego pochodzenia. Wyniki tych badań wykazują, że UA ma potencjał antyproliferacyjny przez zatrzymanie cyklu komórkowego w fazie G0/G1, S lub G2/M, a także powoduje śmierć komórek poprzez apoptozę lub nekrozę [45–47]. Dodatkowo, wpływa też na inne cechy komórek nowotworowych. Dla przykładu, ekspozycja ludzkich komórek raka okrężnicy linii Caco2 i HTC116 oraz mysich komórek raka okrężnicy linii CT26 na UA powodowała obniżenie ich inwazyjnego potencjału [48]. Efekt w postaci ograniczenia zdolności komórek do migracji i inwazji zaobserwowano także w przypadku traktowania kwasem usninowym komórek linii A549 niedrobnokomórkowego raka płuca [49]. Galanty et al. wykazali hamujący wpływ UA na migrację komórek ludzkiego raka prostaty linii DU-145 oraz ludzkiego czerniaka linii HTB-140 [50]. UA również hamował angiogenezę *in vivo* w modelu z wykorzystaniem błony kosmówkowo-omoczniowej

zarodka kurzego, w modelu angiogenezy indukowanej przez VEGF w rogówce myszy oraz u myszy z ksenoprzeszczepem komórek raka sutka Bcap-37 [51,52].

Antynowotworowe działanie UA może obejmować również środowisko guza. Dla przykładu, badania prowadzone przez Yildirim et al. pokazują rolę UA w regulacji odpowiedzi przeciwzapalnej. Naukowcy wykazali, że UA obniżał poziomy tlenku azotu (NO), VEGF, prostaglandyny E2 (PGE2), poziomy ekspresji genu cyklooksygenazy-2 (*COX-2*) i indukowanej syntazy tlenku azotu (*iNOS*), dodatkowo szeregu cytokin (IL-2, CXCL 10, CXCL8, CCL2 (MCP-1), TNF-α, IL-6) na modelu raka piersi [53].

Kwas usninowy jest lipofilowym słabym kwasem, który może dyfundować przez błony. UA może działać jako transporter protonów i bezpośrednio rozpraszać potencjał na wewnętrznej błonie mitochondrialnej, wpływając na fosforylację oksydacyjną [54–56]. Wykazano, że UA obniża poziom ATP w komórkach raka sutka linii T47D [55]. Dodatkowo, odkryto, że UA hamuje mitochondrialne kompleksy łańcucha oddechowego (I i III) w komórkach raka płaskonabłonkowego płuc, prowadząc do zmniejszenia produkcji ATP i wzrostu produkcji reaktywnych form tlenu (RFT) [56].

Efekty działania UA w różnych typach komórek nowotworowych, zarówno i*n vitro*, jak i *in vivo*, zostały szczegółowo opisane w Gimła & Herman-Antosiewicz, 2024 **[Artykuł nr 1]** [57]**.** Plejotropowe działanie UA wobec komórek nowotworowych przedstawia Rycina 2.

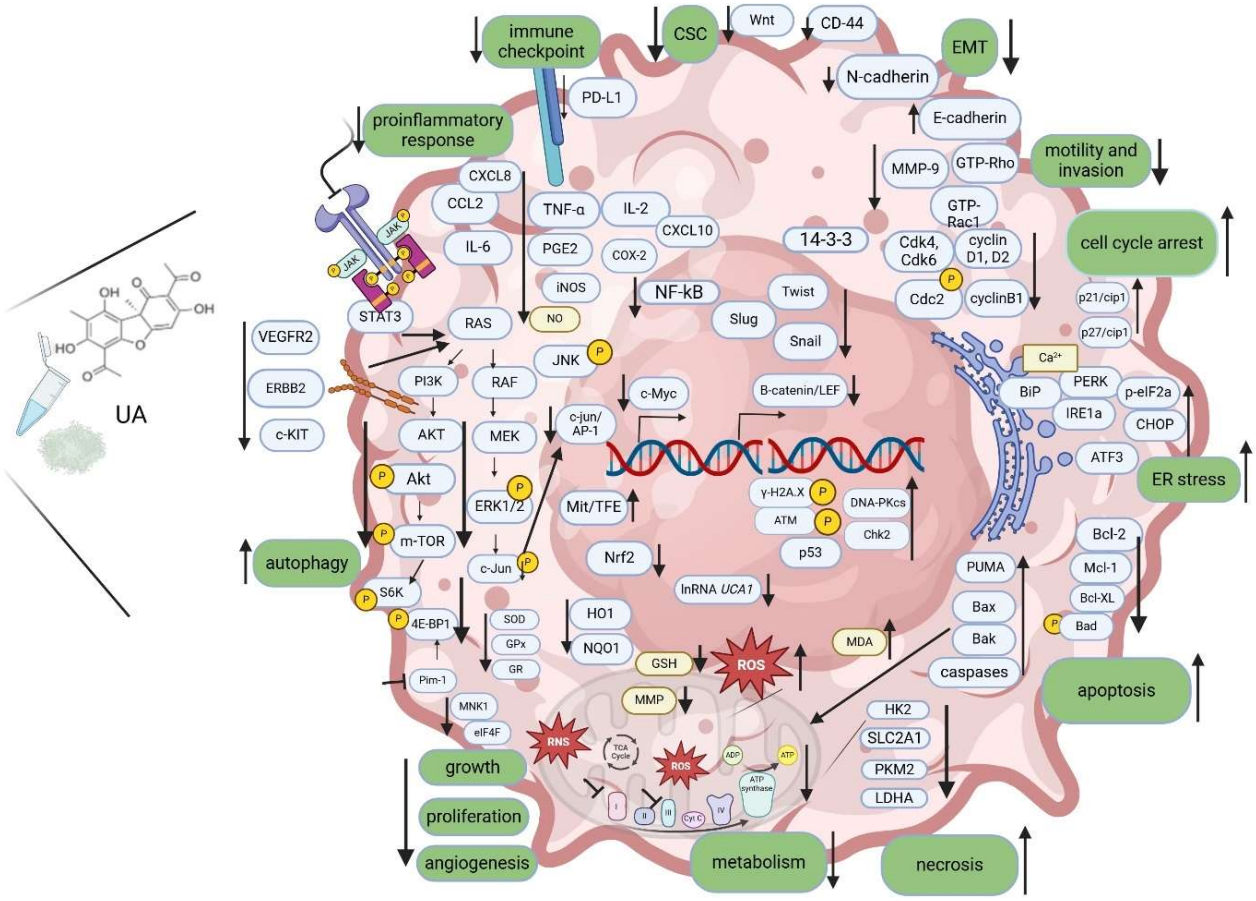

Ryc. 2 Mechanizmy działania UA w komórkach nowotworowych. UA hamuje proliferację i indukuje apoptozę komórek nowotworowych, hamuje angiogenezę, migrację i inwazję komórek, ułatwia immunologiczną destrukcję komórek nowotworowych, tłumi stan zapalny, który promuje wzrost guza i moduluje metabolizm komórkowy. Ponadto UA indukuje stres ER i autofagię oraz hamuje EMT i cechy komórek macierzystych (rycina pochodzi z publikacji Gimła & Herman-Antosiewicz, 2024 ***[Artykuł nr 1]*** [57]***.***

Mimo obiecującej aktywności wobec komórek nowotworowych, UA ma także wady. Przede wszystkim musi być stosowany w dość wysokich stężeniach, aby wykazywać działanie antynowotworowe, a wówczas cechuje się również silną hepatotoksycznością [42,58–61]. W celu ulepszenia działania UA, w tym jego większej aktywności i selektywności wobec komórek nowotworowych oraz zwiększenia rozpuszczalności w wodzie i biodostępności, badacze projektują jego syntetyczne pochodne. Opisano wiele pochodnych UA, które wykazują wyższą cytotoksyczność wobec komórek nowotworowych niż związek macierzysty, co jest podsumowane w licznych pracach przeglądowych, m.in. w [62]. Również nasz zespół ma dokonania w syntezie aktywnych pochodnych UA [63–66]. Wykazaliśmy, że izoksazolowa pochodna UA [(R)-8-acetylo-5,7-dihydroksy-3,4a,6-trimetylobenzo[2,3]benzofuro[5,6-*d*]izooksazol-4(4a*H*)]-on indukuje

wakuolizację komórek raka piersi linii MCF-7, co wynika ze stresu retikulum endoplazmatycznego (ER) i prowadzi do śmierci komórek przypominającej paraptozę [65]. Dzieje się tak na skutek zaburzenia działania mitochondrialnego łańcucha oddechowego, gdyż związek ten jest inhibitorem kompleksu II [67]. Inną pochodną, która silniej niż UA obniża żywotność różnych typów komórek nowotworowych, jest (*R*)-8-acetylo-5,7-dihydroksy-3,4a,6-trimetylo-2,4a-dihydro-4*H*-benzofuro[3,2-*f*]indazol-4-on (Ryc. 3), pirazolowa pochodna oznaczona jako **5** [63].

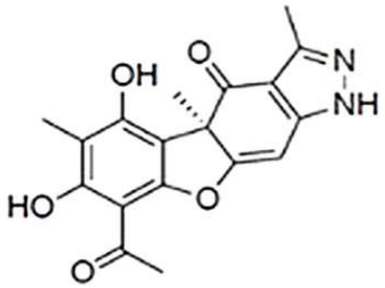

*Ryc. 3 Strukura pirazolowej pochodnej kwasu usninowego - **5***

W niniejszej pracy badano wpływ pochodnej **5** na komórki nowotworu trzustki.

7. Cele pracy

Celem pracy była weryfikacja hipotezy badawczej, że modyfikacja struktury kwasu usninowego prowadząca do powstania pirazolowej pochodnej **5**, zwiększy aktywność antyproliferacyjną i antynowotworową tego związku wobec ludzkich komórek nowotworu trzustki.

Cele szczegółowe:

1. Ocena wpływu pochodnej **5** na komórki nowotworu trzustki w porównaniu do działania UA, z uwzględnieniem takich aspektów jak: żywotność i morfologia komórek, przebieg cyklu komórkowego, indukcja śmierci, zdolność migracji i inwazji, wpływ na ER i mitochondria, wzrost guza *in vivo*.

2. Określenie skuteczności terapii łączonej z wykorzystaniem pochodnej **5** i inhibitora glikolizy (3-BrPA) w komórkowym modelu nowotworu trzustki.

8. Materiały i metody

1. Pochodna 5

Pirazolowa pochodna kwasu usninowego **5** [(*R*)-8-acetylo-5,7-dihydroksy-3,4a,6-trimetylo-2,4a-dihydro-4*H*-benzofuro[3,2-*f*]indazol-4-on] została zsyntetyzowana przez zespół chemików pod kierownictwem dr Tristana Reekie ze School of Science University of New South Wales Canberra, Australia. Szczegóły dotyczące syntezy chemicznej związku zostały szczegółowo omówione w artykule Gunawan et al., 2023 [63]. W cytowanej publikacji mam również swój udział polegający na przeprowadzeniu biologicznej części eksperymentów.

2. Linie komórkowe i warunki hodowli

Linię komórek ludzkiego gruczolakoraka piersi MCF-7 uzyskano od CLS Cell Lines Service GmbH (Eppelheim, Niemcy), ludzkie fibroblasty skórne HDFa uzyskano od Thermo Fisher Scientific (Product Line Cascade Biologics™), a linie komórek ludzkiego raka trzustki Mia PaCa-2 i PANC-1 pochodzą z kolekcji pani prof. dr hab. Iwony Inkielewicz-Stępniak z Gdańskiego Uniwersytetu Medycznego. Wszystkie linie komórkowe zostały przetestowane pod kątem infekcji mykoplazmą przed ich użyciem. Hodowle monowarstwowe komórek MCF-7 prowadzono w pożywce RPMI 1640; komórki HDFa, Mia PaCa-2 i PANC-1 hodowano w DMEM (z 4 mM L-glutaminą i 4500 mg/l glukozą). Podstawowe media uzupełniono 10% (v/v) płodową surowicą bydlęcą i 1% mieszaniną penicyliny–streptomycyny. Komórki były utrzymywane w temperaturze 37°C w atmosferze 5% wysycenia CO_2 oraz stałej wilgotności.

3. Ocena żywotności komórek

Żywotność oceniano w komórkach poddanych działaniu odpowiednich stężeń UA, pochodnej UA lub samego rozpuszczalnika (DMSO) oraz inhibitora glikolizy 3-BrPA i kombinacji **5** z 3-BrPA. W tym celu zastosowano test MTT, który mierzy aktywność metaboliczną komórek. Komórki były eksponowane na badane związki przez 24 lub 48 godzin, a ilość powstałego formazanu, będącego produktem redukcji soli tetrazolowej (bromku 3-(4,5-dimetylotiazol-2-yl)-2,5-difenylotetrazoliowego) przez komórkowe dehydrogenazy, określana była spektrofotometrycznie (przy długości fali 570 nm).

Żywotność komórek kontrolnych, traktowanych wyłącznie rozpuszczalnikiem (DMSO) przyjmowano jako 100%.

4. Analiza morfologii komórek

Analizy morfologii komórek poddanych działaniu UA lub pochodnej **5** dokonano na dwa sposoby: wykorzystując mikroskopię świetlną z kontrastem fazowym (powiększenie 200x) i transmisyjną elektronową mikroskopię (TEM). W celu przygotowania prób do analizy TEM, komórki traktowano DMSO (kontrola) lub pochodną **5** przez 24 lub 48 godzin i utrwalano je w lodowatym 2,5% glutaraldehydzie. Następnie próby przekazywano do Laboratorium Bioobrazowania na Wydziale Biologii UG w celu dalszych analiz. Zdjęcia komórek w TEM wykonane zostały przez panią dr hab. Magdalenę Narajczyk. Analiza ultrastruktury komórek na podstawie otrzymanych zdjęć, w tym pomiar wielkości mitochondriów, zostały przeprowadzone przeze mnie przy użyciu programu ImageJ.

5. Analiza cyklu komórkowego i śmierci komórek

Wpływ badanych związków na śmierć komórek określono za pomocą analizatora komórek Muse™ Cell Analyzer (Millipore). Komórki po 48 godzinach traktowania pochodną **5**, UA lub 3-BrPA, a także kombinacją **5** i 3-BrPA lub równoważną ilością DMSO wybarwiono za pomocą zestawu Muse™ Annexin-V & Dead Cell Assay Kit i zliczono za pomocą cytometrii przepływowej. Odsetek żywych, apoptotycznych i nekrotycznych komórek określono za pomocą detekcji aneksyny V związanej z fosfatydyloseryną na powierzchni komórek apoptotycznych oraz przez akumulację barwnika 7-aminoaktynomycyny D (7-AAD) zachodzącą w komórkach w wyniku permeabilizacji błony.

6. Oznaczanie poziomu wybranych białek

Oznaczenia poziomu białek zaangażowanych w proces śmierci komórkowej (c-PARP), stres związany z retikulum endoplazmatycznym (IRE1α, GADD 153 i BiP) oraz proces przejścia epitelialno-mezenchymalnego (E-kadherynę, Klaudynę 1, N-kadherynę, Wimentynę, Snail, Slug, ZEB-1) dokonano, wykorzystując technikę Western blot. β-aktynę zastosowano jako białko referencyjne. Komórki traktowano pochodną **5**, UA lub DMSO (kontrola). Lizaty białkowe oczyszczono przez wirowanie. Białka rozdzielono metodą SDS–PAGE i przeniesiono na membranę PVDF. Membranę blokowano i inkubowano

z pożądanym przeciwciałem pierwszego rzędu, a następnie traktowano odpowiednim przeciwciałem drugorzędowym. Immunoreaktywne prążki wykrywano za pomocą odczynnika o wzmocnionej chemiluminescencji (Thermo Scientific). Membrany po oczyszczeniu inkubowano z przeciwciałami anty-β-aktyna w celu normalizacji różnic w ilości białka w poszczególnych próbkach. Analizę densytometryczną wykonano przy użyciu oprogramowania Quantity One 1-D Analysis (Bio-Rad).

7. Ocena zdolności komórek do migracji i inwazji

Zdolność komórek od migracji oceniono z wykorzystaniem testu zarysowań. Komórki Mia PaCa-2 i PANC-1 wysiano na płytki w konfluencji ok. 90%. Przez środek dołka przeprowadzono rysę, a następnie komórki zostały poddane działaniu DMSO (kontrola) lub pochodnej **5** przez 48 godzin. Zdolność komórek do migracji zbadano pod mikroskopem świetlnym (powiększenie 20x). Zmiany powierzchni zarysowania analizowano przy użyciu programu ImageJ.

Do oceny zdolności komórek do inwazji wykorzystano eksperyment z użyciem komór Boydena. Komory opłaszczono matrigelem (rozpuszczonym preparatem błony podstawnej firmy Corning) i umieszczono w nich komórki. Jako atraktant wykorzystano 10% roztwór surowicy bydlęcej w medium hodowlanym. Następnie po 16-godzinnym traktowaniu pochodną **5,** UA lub DMSO (grupa kontrolna) komórki, które przeszły zasymulowaną błonę podstawną, zliczono przy użyciu mikroskopu świetlnego.

8. Oznaczenie poziomu Ca^{2+} w komórkach

Poziom wewnątrzkomórkowego wapnia oznaczano w komórkach traktowanych pochodną **5** przez 6 (MCF-7) lub 12 godzin (Mia PaCa-2, PANC-1). W niektórych eksperymentach komórki były wstępnie traktowane przez 24 godziny 2-APB (30 μM) lub BAPTA (10 μM). Poziom Ca^{2+} oceniano przy użyciu zestawu Fluo-4 Direct Assay Kit (Invitrogen) zgodnie z instrukcją producenta. Eksperyment z wykorzystaniem inhibitorów 2-APB i BAPTA na linii MCF-7 został przeprowadzony przez panią dr A. Pyrczak-Felczykowską. Z kolei działanie wspomnianych wcześniej inhibitorów w komórkach trzustki zbadała pani dr A. Hać (materiały te zostały zamieszczone w suplemencie do publikacji Gimla et al., (2023) [66]).

9. Oznaczanie poziomu ATP w komórkach

Komórki wysiano na płytki hodowlane i inkubowano przez noc. Medium podstawowe zastąpiono świeżym z dodatkiem pochodnej **5**, 3-BrPA lub kombinacją obu na 48 godzin. Poziom ATP oznaczano za pomocą systemu ATPlite Luminescence ATP Assay System (PerkinElmer), zgodnie z protokołem producenta. Współczynnik kombinacji (CI) wyliczono według wzoru: $CI = CD5/(IC_{50})D5 + CBr/(IC_{50})Br$, gdzie CD5 i CBr to odpowiednio stężenia pochodnej **5** i 3-BrPA, które w połączeniu powodują 50% spadek poziomu ATP; $(IC_{50})D5$ i $(IC_{50})Br$ to odpowiednio stężenia pochodnej **5** i 3-BrPA, które indywidualnie zmniejszają ATP do 50% w stosunku do poziomu obserwowanego w komórkach kontrolnych.

10. Ocena aktywności pochodnej 5 *in vivo*

W celu wyjaśnienia, czy pochodna **5** wykazuje antynowotworowe właściwości *in vivo* wykorzystano mysi model. Eksperyment został przeprowadzony w Trójmiejskiej Zwierzętarni Akademickiej (TZA). Myszom szczepu BALB/c z deficytem odporności podskórnie zaszczepiono komórki linii Mia PaCa-2. Zwierzęta losowo rozdzielono na dwie grupy eksperymentalne i podawano im przez zgłębnik doustny 3 razy w tygodniu olej kukurydziany (grupa kontrolna) lub zawiesinę pochodnej **5** w oleju kukurydzianym (400 mg/kg) przez 4 tygodnie. Ocenę zmian w wielkości guzów i masie ciała dokonywano co 2 lub 3 dni. Pobrane pośmiertnie guzy nowotworowe, nerki i wątroby poddano barwieniu eozyną-hematoksyliną w celu określenia struktury tkanki i stopnia wakuolizacji komórek. Mój udział w tej części doświadczeń polegał na przygotowaniu do ksenoprzeszczepów komórek linii Mia PaCa-2 oraz ich zawiesiny w matrigelu, która była dostarczona do zwierzętarni. Podawanie pochodnej lub nośnika, ocena wielkości guzów i masy ciała zwierząt oraz pośmiertne zebranie materiału zwierzęcego został przeprowadzony przez panią dr Marcelinę Malinowską.

11. Analiza statystyczna

Wszystkie dane przedstawiono zostały jako średnie ± błąd standardowy średniej (SEM) z co najmniej trzech niezależnych eksperymentów. Istotność różnic między komórkami kontrolnymi i traktowanymi pochodną **5** określono z wykorzystaniem testów t-Studenta lub ANOVA i testów post hoc wielokrotnych porównań Dunnetta lub Sidaka

przy użyciu GraphPad Prism (wersja 8). Różnice uznano za istotne przy *p < 0,05; **p < 0,01; ***p < 0,001; ****p < 0,0001.

9. Omówienie prac wchodzących w skład rozprawy

I. Publikacja 1

Gimła Mariola, Herman-Antosiewicz Anna (2024) Multifaceted properties of usnic acid in disrupting cancer hallmarks, *Biomedicines* 12 (10): 2199.

Przeciwnowotworowa aktywność kwasu usninowego została odkryta po raz pierwszy w 1975 roku i od tego czasu jego antyproliferacyjny potencjał względem komórek nowotworowych i prawidłowych oraz mechanizmy działania są przedmiotem wielu badań. Jak dotąd, dokładne mechanizmy jego działania nie zostały w pełni poznane, jednak UA zdaje się być obiecującym związkiem jako środek do interwencji terapeutycznej. Znajomość wpływu UA na wspólne, charakterystyczne cechy nowotworów (ang. cancer hallmarks), zaprezentowane przez Douglasa Hanahana i Roberta Weinberga, staje się kluczowa dla zrozumienia potencjału tego związku oraz opracowania nowych terapii antynowotworowych z jego użyciem [68–70].

Celem naszej pracy był przegląd literatury, usystematyzowanie i podsumowanie wiedzy na temat aktywności UA w kontekście wpływu na cechy i procesy charakterystyczne dla komórek nowotworowych różnego pochodzenia, opierając się na artykułach przedstawiających molekularne mechanizmy tej aktywności. Praca ta omawia przykłady działania UA w komórkach nowotworowych na etapie hamowania nieprawidłowej sygnalizacji, reaktywacji supresorów nowotworzenia, zapobiegania migracji i inwazji, hamowania angiogenezy, ograniczania nieśmiertelności replikacyjnej, modulacji układu odpornościowego, indukowania apoptozy, wpływu na niestabilność genomu i regulacji energetyki komórkowej.

Zdolność do nadmiernej proliferacji jest jedną z kluczowych cech charakterystycznych wśród komórek nowotworowych. Liczne badania wykazały, że UA może zaburzać szlaki sygnałowe promujące podziały komórkowe. Kwas usninowy hamuje szlak MAPK - kinazy białkowej aktywowanej mitogenem, odgrywający rolę w różnicowaniu komórek, regulacji ich wzrostu, przeżycia i podziałach komórkowych [46]. Co więcej, związek ten może też wpływać na szlak sygnałowy receptora naskórkowego czynnika wzrostu (EGFR). Szlak ten jest nadmiernie aktywny w wielu typach

nowotworów. Dzięki hamowaniu sygnalizacji EGFR, kwas usninowy może powodować zmniejszenie rozmiaru guza i ograniczyć przerzuty [49] .

Kolejną cechą charakterystyczną komórek nowotworowych jest zdolność zahamowanie ekspresji genów supresorowych. Jako przykład mogą posłużyć geny kodujące białka p53 czy białko retinoblastomy (Rb). Przedstawione supresory nowotworzenia są kluczowe w regulacji cyklu komórkowego oraz zapobiegają niekontrolowanym podziałom komórek. UA aktywuje ekspresję genu p53, tym samym zwiększa zdolność komórek do indukowania procesu apoptozy i jednocześnie ogranicza przeżycie zmienionych komórek [71]. Wykazano także, że UA może zwiększać ekspresję genów białek proapoptotycznych Bax i kaspazy-3 [72,73].

Komórki nowotworowe często nabywają mechanizmy opierania się śmierci komórkowej, co pozwala im przetrwać w niekorzystnych warunkach. UA indukuje apoptozę w różnych liniach komórek nowotworowych. Badania wskazują, że aktywuje on wewnętrzną ścieżkę apoptozy, czemu towarzyszy zaburzenie funkcjonowania mitochondriów oraz wzrost produkcji reaktywnych form tlenu (RFT) [56,74]. Ponadto wykazano, że związek ten hamuje białka antyapoptotyczne, takie jak Bcl-2, które są często nadprodukowane w komórkach nowotworowych. Poprzez negatywną regulację tych białek UA zwiększa wrażliwość komórek nowotworowych na czynniki apoptotyczne [71,75].

Angiogeneza jest procesem powstawania nowych naczyń krwionośnych, wspomagającym wzrost guza i proces przerzutowania. Kwas usninowy ma zdolność hamowania angiogenazy przez modulację szlaku sygnałowego czynnika wzrostu śródbłonka naczyniowego (VEGF). VEGF jest kluczowym czynnikiem stymulującym wzrost naczyń krwionośnych w środowisku guza. Kwas usninowy niweluje ekspresję genu VEGF, tym samym ograniczając sygnalizację dla jego receptora. Zapobiega tym samym powstawaniu naczyń krwionośnych i dopływowi krwi do tkanek guza, co przekłada się na ograniczenie jego wzrostu [76]. Co więcej, wykazano, że związek ten zmniejsza ekspresję metaloproteinaz macierzy zewnątrzkomórkowej (MMP), enzymów zaangażowanych w procesy przebudowy macierzy pozakomórkowej i migrację komórek, co dodatkowo hamuje angiogenezę i proces tworzenia przerzutów [77].

Komórki nowotworowe cechuje zmieniony metabolizm, a fenomen ten jest znany jako efekt Warburga. Mają one zdolność produkcji ATP, bazując głównie na procesie

glikolizy, także w warunkach tlenowych. Ten zabieg metaboliczny pozwala na wzmożoną proliferację komórek nowotworu. UA moduluje ten proces, hamując enzymy glikolityczne, takie jak heksokinaza-2 (HK2) i dehydrogenaza mleczanowa (LDH) [78]. Enzymy te są kluczowe w procesie glikolizy, a ich hamowanie zmniejsza ilość energii w komórkach, wpływając na ograniczenie ich wzrostu. Dowiedziono także, że UA zaburza funkcje mitochondriów i zwiększa produkcję RFT, co dodatkowo przekłada się na zakłócenie równowagi energetycznej komórek nowotworowych [56].

W progresji raka inwazja i przerzuty są kluczowymi etapami, w których komórki nowotworowe rozprzestrzeniają się do odległych miejsc i tworzą guzy wtórne. UA wykazuje zdolność hamowania inwazji komórek nowotworowych i przerzutów poprzez tłumienie ekspresji genów metaloproteinaz macierzy (MMP) i białek adhezyjnych [79]. Białka te ułatwiają degradację macierzy zewnątrzkomórkowej i umożliwiają komórkom nowotworowym inwazję otaczających tkanek i tworzenie przerzutów.

Komórki nowotworowe posiadają zdolność wymykania się spod nadzoru immunologicznego dzięki nadprodukcji białek punktów kontrolnych, takich jak PD-L1. Zabieg ten ogranicza liczbę limfocytów T, powodując ich śmierć. UA wpływa na odpowiedź immunologiczną zwiększając aktywności komórek NK (ang. Natural Killer) i cytotoksycznej frakcji limfocytów T (CTL) [77]. Działanie to wspomaga rozpoznanie i eliminację komórek nowotworowych. UA wpływa także na hamowanie wydzielania immunosupresyjnych cytokin, jak TGF-β. Cytokiny te hamują odpowiedź immunologiczną i sprzyjają rozwojowi nowotworu [80].

UA wykazuje właściwości przeciwnowotworowe, oddziałując na szereg charakterystycznych cech raka. Jego plejotropowe działanie wskazuje, że jest on cennym związkiem do opracowywania nowych terapii antynowotworowych. Dodatkowo może również sprawdzić się do stosowania w połączeniu z innymi środkami terapeutycznymi. Konieczne są jednak dalsze badania, w tym badania kliniczne, aby w pełni zrozumieć jego potencjał terapeutyczny. Wiedza ta również stanowi podstawę do projektowania syntetycznych pochodnych UA, które miałyby działać bardziej selektywnie i jednocześnie cechować się wyższą aktywnością w stosunku do komórek nowotworowych niż związek wyjściowy.

II. Publikacja 2

Gimła Mariola, Pyrczak-Felczykowska Agnieszka, Malinowska Marcelina, Hać Aleksandra, Narajczyk Magdalena, Bylińska Irena, Reekie Tristan, Herman-Antosiewicz Anna (2023) The pyrazole derivative of usnic acid inhibits the proliferation of pancreatic cancer cells in vitro and in vivo, *Cancer Cell International* 23(1): 210.

W wyniku realizacji grantu NCN „Harmonia" uzyskano szereg pochodnych UA, które początkowo były testowane na komórkach nowotworu szyjki macicy linii HeLa, co zostało opisane w pracach [63,64]. Tylko kilka z nich okazało się być bardziej aktywnymi niż związek wyjściowy, m.in. pirazolowa pochodna kwasu usninowego, oznaczona jako pochodna **5** ((R)-8-acetylo-5,7-dihydroxy-3,4a,6-trimetylo-1,4a-dihydro-4H-benzofuro[3,2-f]indazol-4-on), która wykazała silniejsze właściwości antyproliferacyjne wobec komórek HeLa niż pochodne **2** i **3a** (wartości IC_{50} określone po 24 godzinach traktowania były odpowiednio około czterokrotnie i dziewięciokrotnie niższe) [63]. Co więcej, podobnie jak pochodna izoksazolowa **2**, pochodna pirazolowa **5** indukowała stres ER w komórkach raka piersi MCF-7.

Ponieważ komórki trzustki wykazują funkcje wydzielnicze, charakteryzują się wysoce rozwiniętymi ER. W związku z tym, zaostrzenie stresu ER zostało zaproponowane jako obiecujący cel w terapii nowotworu tego narządu [81,82]. Mając na uwadze ten aspekt, celem dalszej pracy było zbadanie aktywności związku **5** wobec komórek raka trzustki w modelach *in vitro* i *in vivo* oraz poznanie mechanizmów jego działania.

W pracy wykazano, że pochodna **5** skuteczniej zmniejszała żywotność komórek nowotworowych - w tym komórek nowotworu trzustki linii Mia PaCa-2 i PANC-1 - w porównaniu do działania na zdrowe fibroblasty, wykazując tym samym stosunkowo selektywne działanie. W badanym zakresie stężeń pochodna **5** powodowała obniżenie żywotności komórek nowotworowych w sposób zależny od dawki i czasu ekspozycji, w przeciwieństwie do wyjściowego związku - UA. Pochodna indukowała wakuolizację komórek raka trzustki, podobnie jak w przypadku testowanych wcześniej komórek raka piersi MCF-7. Dodatkowo, markery stresu ER, takie jak BIP, IRE1α, GADD153, były podwyższone. Co więcej, pochodna **5** zwiększała poziom Ca^{2+} w cytoplazmie komórek raka trzustki, co było hamowane przez 2-APB, ale nie przez BAPTA, wskazując

na retikularne, a nie zewnątrzkomórkowe pochodzenie tych jonów. Opróżnianie pokładów wewnątrzsiateczkowego Ca^{2+} może być przyczyną indukcji stresu ER. Morfologiczna ocena ultrastruktury komórek raka trzustki po ekspozycji na działanie pochodnej **5** ujawniła zależną od dawki i czasu ekspozycji wakuolizację komórek, przy czym nie zaobserwowano takich cech w komórkach traktowanych UA w tych samych stężeniach. W przypadku komórek PANC-1 zaobserwowano także komórki z uszkodzoną plazmalemmą, co może wskazywać na śmierć nekrotyczną.

W celu pogłębienia wiedzy na temat mechanizmów antyproliferacyjnego działania pochodnej **5**, zbadano jej wpływ na cykl komórkowy i śmierć komórkową. Traktowanie pochodną **5** przez 24 godziny zwiększało odsetek komórek w fazie G0/G1 w sposób zależny od dawki, przy jednoczesnym zmniejszeniu liczby komórek w fazach S i G2/M. UA zastosowany w tych samych stężeniach wykazał minimalny wpływ na przebieg cyklu komórkowego. Co więcej, analiza profilu śmierci komórkowej pokazała, że pochodna **5** zmniejszała liczbę żywych komórek, jednocześnie zwiększając liczbę komórek apoptotycznych, szczególnie w przypadku linii komórkowej Mia PaCa-2. W przypadku linii PANC-1 udział procentowy żywych komórek spadł, a po traktowaniu pochodną **5** w wysokim stężeniu (5 μg/ml) wzrosła liczba komórek apoptotycznych i nekrotycznych. Kaspazo-zależne cięcie polimerazy PARP potwierdziło, że związek **5** jest bardziej aktywny niż UA w indukcji procesu apoptozy, szczególnie w komórkach Mia PaCa-2.

Testowano również działanie pochodnej **5** *in vivo* z wykorzystaniem myszy szczepu BALB/c-Nude. Oceniono działanie pochodnej **5** na wielkość guzów z komórek Mia PaCa-2. Doustne podanie pochodnej hamowało wzrost nowotworu, ale co ważne - nie wpłynęło na zmianę masy ciała zwierząt. Analiza histopatologiczna tkanek wykazała, że pochodna **5** zmienia strukturę guza, co można powiązać z indukcją śmierci komórek nowotworowych. Wakuolizację komórek nowotworowych w tkance guza obserwowano jedynie u zwierząt leczonych pochodną **5**. Co ważne, takich zmian nie zaobserwowano w wątrobach i nerkach tych zwierząt [66].

Przedstawiona praca pokazuje, że nowa pochodna pirazolowa **5** indukuje zatrzymanie cyklu komórkowego oraz śmierć komórek raka trzustki powiązaną z indukcją stresu ER. Testowany związek jest znacznie bardziej aktywny niż macierzysty UA, który przy stosowaniu w tych samych stężeniach nie ma prawie żadnego wpływu na komórki nowotworu trzustki.

III. Publikacja nr 3

Gimła Mariola, Hać Aleksandra, Reekie Tristan, Herman-Antosiewicz Anna: Impact of usnic acid pyrazole derivative on the metastatic potential and mitochondria of pancreatic cancer cells; manuskrypt złożony do redakcji *BMC Cancer*.

We wspomnianych wcześniej pracach, tj. Gunawan i wsp. (2024) oraz Gimła i wsp. (2023), zostały przedstawione informacje na temat syntezy i aktywności antyproliferacyjnej pirazolowej pochodnej kwasu usninowego **5**. Pokazano, że obniża ona żywotność różnych komórek nowotworowych przy stężeniach niższych niż UA, a co ważne, komórki nienowotworowe są mniej wrażliwe na jej działanie. Odkryto również mechanizmy leżące u podłoża tej aktywności.

W kolejnej pracy skupiono się na zbadaniu zdolności pochodnej **5** do hamowania kolejnych stadiów progresji raka prowadzących do przerzutów. Zbadano wpływ pochodnej **5** na migrację i inwazję komórek raka trzustki, a także ekspresję markerów przejścia nabłonkowo-mezenchymalnego (EMT). EMT jest kluczowym procesem w progresji raka, umożliwiającym komórkom nowotworowym pochodzenia epitelialnego nabycie bardziej inwazyjnego fenotypu [83,84]. EMT charakteryzuje się utratą markerów komórek nabłonkowych, w tym E-kadheryny i białek połączeń ścisłych, a także wzmożoną produkcją białek charakterystycznych dla komórek mezenchymalnych.

Przeprowadzone analizy wykazały wpływ pochodnej **5** na ograniczenie zdolności do migracji i inwazji komórek, szczególnie przy zastosowaniu wyższego stężenie związku (5 μg/ml). UA zastosowany w takich samych stężeniach nie wykazał podobnego działania. Zmiany w poziomie markerów EMT zależne były od zastosowanego stężenia badanych związków oraz linii komórkowej. Pochodna **5**, szczególnie zastosowana w wyższym stężeniu, podwyższała poziom markerów komórek epitelialnych (E-kadheryny i Klaudyny-1). Najbardziej zauważalny efekt obserwowano w przypadku poziomu Klaudyny-1, białka wchodzącego w skład połączeń ścisłych. Zmniejszenie ekspresji genu Klaudyny-1 (*CLDN1*) obserwowano w liniach komórkowych raka trzustki oraz w guzach tego narządu, co korelowało z progresją choroby i krótszym przeżyciem pacjentów z rakiem trzustki [85,86]. Podwyższenie poziomu tego białka przez pochodną **5** może być zatem kluczowe dla zachowania integralności nabłonka w przewodach trzustkowych.

Pochodna **5** obniżała poziom białek charakterystycznych dla komórek mezenchymalnych: N-kadheryny (w obu badanych liniach) i wimentyny (w komórkach linii Mia PaCa-2). Wśród testowanych czynników transkrypcyjnych zaangażowanych w EMT, poziom białka Slug był obniżony w komórkach Mia PaCa-2 i PANC-1 traktowanych pochodną **5**. W tej ostatniej linii poziom Slug jak i Snail był obniżony.

Dane literaturowe wskazują, że zwiększona liczba mitochondriów w komórkach raka trzustki, wynikająca z ich fragmentacji, wiąże się z większym potencjałem proliferacyjnym i migracyjnym komórek, a także ich opornością na leki [87]. Dlatego analizowano wpływ pochodnej **5** na morfologię tych organelli w obu badanych liniach raka trzustki. W komórkach MiaPaCa-2 traktowanych pochodną **5** przez 24 lub 48 godziny zaobserwowano zwiększenie długości, ale nie szerokości, mitochondriów w porównaniu z komórkami kontrolnymi. W przypadku linii komórkowej PANC-1 pochodna **5** także spowodowała wzrost długości mitochondriów, choć statystycznie istotne zmiany odnotowano w przypadku dłuższej ekspozycji komórek na związek (48 godzin). Zmiany wywołane przez UA nie były statystycznie istotne w porównaniu z komórkami kontrolnymi. Ponieważ zmiany w długości mitochondriów były wyraźniejsze w komórkach Mia PaCa-2, linię tę wykorzystano do dalszych badań, tj. sprawdzenia, czy zmiany w długości mitochondriów są skorelowane ze zmianami ilości ATP w komórkach. Analiza poziomu ATP pokazała, że pochodna **5** faktycznie obniża go w sposób zależny od użytego stężenia.

Obserwacje te skłoniły do postawienia hipotezy, że kombinacja pochodnej **5** z inhibitorem glikolizy może silniej wpływać na obniżenie poziomu ATP i indukcję śmierci komórek Mia PaCa-2 niż każdy ze związków zastosowany osobno. Jako inhibitor glikolizy wykorzystano 3-bromopirogronian (3-BrPA). Związek ten działa na enzymy glikolityczne, takie jak heksokinaza 2 (HK2), która jest produkowana selektywnie w komórkach nowotworowych i jest głównym czynnikiem wywołującym „efekt Warburga" oraz dehydrogenaza aldehydu 3-fosfoglicerynowego (GAPDH) i kinaza 3-fosfoglicerynianowa (3-PGK) [88–91]. Zastosowanie 3-BrPA w komórkach Mia PaCa-2 ujawniło zależne od dawki obniżenie poziomu ATP. Równoczesne traktowanie 50 μM 3-BrPA oraz pochodną **5** w stężeniach 0,1; 0,25; 0,5 lub 1 μg/ml spowodowało większą redukcję poziomu ATP niż w przypadku któregokolwiek ze związków stosowanych samodzielnie. Wyliczony

współczynnik kombinacji (CI=0.57) wskazuje na synergistyczne działanie 3-BrPA i pochodnej **5** w redukcji poziomu ATP w komórkach raka trzustki.

W kolejnym kroku oceniono wpływ skojarzonego traktowania na indukcję śmierci komórek. Procentowy udział żywych, apoptotycznych i nekrotycznych komórek Mia PaCa-2 określono za pomocą cytometrii przepływowej. Pochodna **5** zmniejszyła liczbę żywych komórek, jednocześnie zwiększając frakcję komórek apoptotycznych w sposób zależny od dawki, nie wpływając na indukcję procesu nekrozy. 3-BrPA nie indukował apoptozy, ale zwiększał udział frakcji komórek nekrotycznych. W traktowaniu skojarzonym zastosowano 50 μM 3-BrPA i niższe stężenia pochodnej **5** (0,2 lub 0,5 μg/ml), które same w sobie minimalnie indukowały śmierć komórek. 3-BrPA wzmagał redukcję poziomu żywych komórek traktowanych pochodną **5**. Odsetek martwych komórek wzrósł w komórkach traktowanych kombinacją w porównaniu z komórkami traktowanymi pojedynczymi związkami. Co ciekawe, zmiany zaszły także w sposobie śmierci komórek: zmienił się on z apoptotycznego obserwowanego dla samej pochodnej **5,** na nekrotyczny przy równoczesnym traktowaniu z inhibitorem glikolizy.

Warto zaznaczyć, że oba związki zastosowano w niskich stężeniach, które nie są cytotoksyczne przy pojedynczym zastosowaniu. Jest to spójne z przewagą terapii skojarzonej nad monoterapią, gdyż daje możliwość zmniejszenia dawek stosowanych leków, a co za tym idzie, zmniejszeniem skutków ubocznych. Terapia kombinowana pozwala także na zminimalizowanie szansy rozwoju lekooporności komórek nowotworowych przy jednoczesnym zachowaniu potencjału przeciwnowotworowego. Warto też zauważyć, że w naszym modelu kombinacja związków prowadziła do śmierci nekrotycznej komórek, a ponieważ jest to proces immunogenny, mógłby wzmacniać odpowiedź układu immunologicznego wobec komórek nowotworowych *in vivo*. Weryfikacja tej hipotezy będzie przedmiotem kolejnych badań.

10. Podsumowanie

Uzyskane w przedstawionej pracy doktorskiej wyniki wskazują, że pochodna **5** działa wielokierunkowo:

a. wykazuje potencjał antyproliferacyjny i cytotoksyczny poprzez hamowanie cyklu komórkowego w fazie G0/G1 oraz indukcję śmierci komórek (z przewagą markerów apoptozy). U podłoża tych procesów leży stres ER w komórkach nowotworowych przebiegający z uwolnieniem jonów wapnia z ER, powiększeniem objętości cystern i kanalików tego organellum, zmianami w ilości głównych regulatorów odpowiedzi na stres ER.

b. działa antynowotworowo *in vivo*. Wzrost guzów z komórek nowotworowych trzustki był hamowany u zwierząt otrzymujących pochodną **5**, a komórki guza wykazywały cechy stresu ER. Co ważne, nie zaobserwowano skutków ubocznych stosowania pirazolowej pochodnej UA u zwierząt.

c. skutecznie ogranicza migrację i inwazję komórek raka trzustki, co wskazuje na jej potencjał antymetastatyczny. Towarzyszy temu modulacja poziomu markerów EMT, zwłaszcza zwiększenie poziomu białka Klaudyny-1, co wskazuje, że związek ten może zapobiegać lub odwracać proces EMT, utrzymując integralność nabłonka i redukując tym samym potencjał przerzutowy.

d. normalizuje morfologię mitochondriów, co wiąże się ze spadkiem poziomu ATP. Zaburzenia metabolizmu energetycznego komórek nowotworowych mogą przyczyniać się do spadku ich żywotności, zdolności do migracji i inwazji.

e. połączenie pochodnej **5** z inhibitorem glikolizy, 3-BrPA, daje obiecujące wyniki w kontekście zmniejszenia żywotności komórek i obniżenia komórkowego poziomu ATP. Jednocześnie taka kombinacja wpływa na rodzaj śmierci komórek.

Poprzez wpływ na takie procesy, jak cykl podziałowy, śmierć komórek, ich migrację, inwazję, EMT i metabolizm energetyczny, pochodna **5** ogranicza wiele kluczowych etapów w progresji raka trzustki. Odkrycia te łącznie plasują pochodną **5** jako obiecującą kandydatkę do dalszych badań nad terapią tego nowotworu.

Przedstawiona praca ma także pewne ograniczenia. Wykorzystano zaledwie dwie linie komórkowe pochodzenia trzustkowego do oceny skuteczności działania związku. Warto

by było rozwinąć analizę o dodatkowe linie komórkowe raka trzustki, różniące się tłem genetycznym oraz potencjałem w tworzeniu desmoplazji. Pozwoliłoby to nie tylko na szersze zobrazowanie antyproliferacyjnych i antynowotworowych właściwości badanej pochodnej, ale także stanowiło punkt odniesienia w kolejnych etapach analiz. Do wdrożenia pochodnej **5** jako potencjalnego leku konieczne jest także zbadanie jej wpływu na komórki nowotworowe w warunkach symulujących złożone środowisko guza. Zastosowanie kultur 3D, w tym organoidów z komórek pochodzących od pacjentów lub kokultury komórek nowotworowych, fibroblastów czy komórek układu odpornościowego w obecności składników macierzy zewnątrzkomórkowej z pewnością wzbogaciłoby naszą widzę na temat skuteczności pochodnej **5** i jej wpływu na mikrośrodowisko guza.

11. Wykaz cytowanego piśmiennictwa

1. Bray, F., Laversanne, M., Weiderpass, E. & Soerjomataram, I. The ever-increasing importance of cancer as a leading cause of premature death worldwide. *Cancer* **127**, 3029–3030 (2021).
2. Bray, F. *et al.* Global cancer statistics 2022: GLOBOCAN estimates of incidence and mortality worldwide for 36 cancers in 185 countries. *CA Cancer J Clin* **74**, 229–263 (2024).
3. Siegel, R. L., Miller, K. D., Wagle, N. S. & Jemal, A. Cancer statistics, 2023. *CA Cancer J Clin* **73**, 17–48 (2023).
4. Brown, J. S. *et al.* Updating the definition of cancer. *Molecular Cancer Research* **21**, 1142–1147 (2023).
5. Cabasag, C. J. *et al.* Pancreatic cancer: an increasing global public health concern. *Gut* **71** 1686–1687 (2021).
6. Luo, G. *et al.* Global patterns and trends in pancreatic cancer incidence: age, period, and birth cohort analysis. *Pancreas* **48**, 199–208 (2019).
7. Mizrahi, J. D., Surana, R., Valle, J. W. & Shroff, R. T. Pancreatic cancer. *Lancet* **395**, 2008–2020 (2020).
8. Pereira, S. P. *et al.* Early detection of pancreatic cancer. *Lancet Gastroenterol Hepatol* **5**, 698–710 (2020).
9. Torres, C. & Grippo, P. J. Pancreatic cancer subtypes: a roadmap for precision medicine. *Ann Med* **50**, 277–287 (2018).
10. Leiphrakpam, P. D. *et al.* Trends in the global incidence of pancreatic cancer and a brief review of its histologic and molecular subtypes. *J Gastrointest Cancer* **56**, 71 (2025).
11. Grützmann, R. *et al.* Meta-analysis of microarray data on pancreatic cancer defines a set of commonly dysregulated genes. *Oncogene* **24**, 5079–5088 (2005).
12. Pon, J. R. & Marra, M. A. Driver and passenger mutations in cancer. *Annu Rev Pathol* **10**, 25–50 (2015).
13. Kamisawa, T., Wood, L. D., Itoi, T. & Takaori, K. Pancreatic cancer. *Lancet* **388**, 73–85 (2016).
14. Hu, H. feng *et al.* Mutations in key driver genes of pancreatic cancer: molecularly targeted therapies and other clinical implications. *Acta Pharmacol Sin* **42**, 1725–1741 (2021).

15. Dal Molin, M. *et al.* Clinicopathological correlates of activating GNAS mutations in intraductal papillary mucinous neoplasm (IPMN) of the pancreas. *Ann Surg Oncol* **20**, 3802–3808 (2013).

16. Zeng, G. *et al.* Aberrant Wnt/β-catenin signaling in pancreatic adenocarcinoma. *Neoplasia* **8**, 279–289 (2006).

17. Caldas, C. *et al.* Frequent somatic mutations and homozygous deletions of the p16 (MTS1) gene in pancreatic adenocarcinoma. *Nat. Genet.* **8**, 27–32 (1994).

18. Cicenas, J. *et al.* KRAS, TP53, CDKN2A, SMAD4, BRCA1, and BRCA2 mutations in pancreatic cancer. *Cancers* **9**, 42 (2017).

19. Dancer, J., Takei, H., Ro, J. Y. & Lowery-Nordberg, M. Coexpression of EGFR and HER-2 in pancreatic ductal adenocarcinoma: A comparative study using immunohistochemistry correlated with gene amplification by fluorescencent in situ hybridization. *Oncol Rep* **18**, 151–155 (2007).

20. Reshkin, S. J., Cardone, R. A. & Koltai, T. Genetic signature of human pancreatic cancer and personalized targeting. *Cells* **13**, 602 (2024).

21. Puleo, F. *et al.* Stratification of pancreatic ductal adenocarcinomas based on tumor and microenvironment features. *Gastroenterology* **155**, 1999-2013.e3 (2018).

22. Adamo, P. *et al.* Profiling tumour heterogeneity through circulating tumour DNA in patients with pancreatic cancer. *Oncotarget* **8**, 87221–87233 (2017).

23. Masugi, Y. The desmoplastic stroma of pancreatic cancer: multilayered levels of heterogeneity, clinical significance, and therapeutic opportunities. *Cancers* **14**, 3293 (2022).

24. Cannon, A. *et al.* Desmoplasia in pancreatic ductal adenocarcinoma: Insight into pathological function and therapeutic potential. *Genes Cancer* **9**, 78–86 (2018).

25. Lambert, A. *et al.* An update on treatment options for pancreatic adenocarcinoma. *Ther Adv Med Oncol* **11**, 1758835919875568 (2019).

26. Sarantis, P. *et al.* Pancreatic ductal adenocarcinoma: Treatment hurdles, tumor microenvironment and immunotherapy. *World J Gastrointest Oncol* **12**, 173–181 (2020).

27. Strobel, O. *et al.* Actual five-year survival after upfront resection for pancreatic ductal adenocarcinoma: who beats the odds? *Ann Surg* **275**, 962–971 (2022).

28. Conroy, T. *et al.* FOLFIRINOX or gemcitabine as adjuvant therapy for pancreatic cancer. *N Engl J Med* **379**, 2395–2406 (2018).

29. Nichetti, F. *et al.* NALIRIFOX, FOLFIRINOX, and gemcitabine with nab-paclitaxel as first-line chemotherapy for metastatic pancreatic cancer: a systematic review and meta-analysis. *JAMA Netw Open* **7**, e2350756–e2350756 (2024).

30. Torphy, R. J., Fujiwara, Y. & Schulick, R. D. Pancreatic cancer treatment: better, but a long way to go. *Surg Today* **50**, 1117–1125 (2020).

31. Wood, L. D., Canto, M. I., Jaffee, E. M. & Simeone, D. M. Pancreatic cancer: pathogenesis, screening, diagnosis, and treatment. *Gastroenterology* **163**, 386-402.e1 (2022).

32. Chin, V. *et al.* Chemotherapy and radiotherapy for advanced pancreatic cancer. *Cochrane Database Syst Rev* **3**, 1465-1858 (2018).

33. Rombouts, S. J. *et al.* Systematic review of resection rates and clinical outcomes after folfirinox-based treatment in patients with locally advanced pancreatic cancer. *Ann. Sur. Oncol.* **23**, 4352–4360 (2016).

34. Bjerke, J. W., Elvebakk, A., Domínguez, E. & Dahlback, A. Seasonal trends in usnic acid concentrations of Arctic, alpine and Patagonian populations of the lichen Flavocetraria nivalis. *Phytochemistry* **66**, 337–344 (2005).

35. Calcott, M. J. *et al.* Secondary metabolism in the lichen symbiosis. *Chem Soc Rev* **47**, 1730–1760 (2018).

36. Huneck, S. & Yoshimura, I. Identification of lichen substances. *Identification of Lichen Substances* 11–123 (1996).

37. Ingólfsdóttr, K. Usnic acid. *Phytochemistry* **61**, 729–736 (2002).

38. Galanty, A. *et al.* A comparative survey of anti-melanoma and anti-inflammatory potential of usnic acid enantiomers-a comprehensive in vitro approach. *Pharmaceuticals (Basel)* **14**, 945 (2021).

39. Galanty, A., Paśko, P. & Podolak, I. Enantioselective activity of usnic acid: a comprehensive review and future perspectives. *Phytochem. Rev.* **18**, 527–548 (2019).

40. Guo, L. *et al.* Review of usnic acid and Usnea barbata toxicity. *J Environ Sci Health C Environ Carcinog Ecotoxicol Rev* **26**, 317 (2008).

41. Luzina, O. A. & Salakhutdinov, N. F. Usnic acid and its derivatives for pharmaceutical use: a patent review (2000–2017). *Expert Opin Ther Pat* **28**, 477–491 (2018).

42. Wang, H., Xuan, M., Huang, C. & Wang, C. Advances in research on bioactivity, toxicity, metabolism, and pharmacokinetics of usnic acid in vitro and in vivo. *Molecules* **27**, (2022).

43. Araújo, A. A. S. *et al.* Review of the biological properties and toxicity of usnic acid. *Nat Prod Res* **29,** 2167–2180 (2015).

44. Kupchan, S. M. & Kopperman, H. L. l-Usnic acid: tumor inhibitor isolated from lichens. *Experientia* **31**, 625 (1975).

45. Bačkorová, M. *et al.* Lichen secondary metabolites are responsible for induction of apoptosis in HT-29 and A2780 human cancer cell lines. *Toxicol In Vitro* **26**, 462–468 (2012).

46. Yurdacan, B. *et al.* The role of usnic acid-induced apoptosis and autophagy in hepatocellular carcinoma. *Hum Exp Toxicol* **38**, 201–215 (2019).

47. Ebrahim, H. Y. *et al.* Usnic acid benzylidene analogues as potent mechanistic target of rapamycin inhibitors for the control of breast malignancies. *J. Nat. Prod.* **80**, 932–952 (2017).

48. Yang, Y. *et al.* Potassium usnate, a water-soluble usnic acid salt, shows enhanced bioavailability and inhibits invasion and metastasis in colorectal cancer. *Sci Rep* **8**, 1–11 (2018).

49. Yang, Y. *et al.* Inhibitory activity of (+)-usnic acid against non-small cell lung cancer cell motility. *PLoS One* **11**, (2016).

50. Galanty, A. *et al.* Usnic acid and atranorin exert selective cytostatic and anti-invasive effects on human prostate and melanoma cancer cells. *Toxicol In Vitro* **40**, 161–169 (2017).

51. Song, Y. *et al.* Usnic acid inhibits breast tumor angiogenesis and growth by suppressing VEGFR2-mediated AKT and ERK1/2 signaling pathways. *Angiogenesis* **15**, 421–432 (2012).

52. Sun, T. X. *et al.* Usnic acid suppresses cervical cancer cell proliferation by inhibiting PD-L1 expression and enhancing T-lymphocyte tumor-killing activity. *Phytother Res* **35**, 3916–3935 (2021).

53. Yildirim, M. *et al.* Anti-inflammatory effects of usnic acid in breast cancer. *Russ J Bioorg Chem* **48**, S110–S114 (2022).

54. Antonenko, Y. N. *et al.* Mechanism of action of an old antibiotic revisited: Role of calcium ions in protonophoric activity of usnic acid. *Biochim Biophys Acta Bioenerg* **1860**, 310–316 (2019).

55. Bessadottir, M. *et al.* Proton-shuttling lichen compound usnic acid affects mitochondrial and lysosomal function in cancer cells. *PLoS One* **7**, e51296 (2012).

56. Qi, W. *et al.* (+)-usnic acid induces ROS-dependent apoptosis via inhibition of mitochondria respiratory chain complexes and Nrf2 expression in lung squamous cell carcinoma. *Int J Mol Sci* **21**, 876 (2020).

57. Gimła, M. & Herman-Antosiewicz, A. Multifaceted properties of usnic acid in disrupting cancer hallmarks. *Biomedicines* **12**, 2199 (2024).

58. Chen, S., Ren, Z. & Guo, L. Hepatotoxicity of usnic acid and underlying mechanisms. *J Environ Sci Health C Toxicol Carcinog* **43**, 1–22 (2025).

59. Piska, K. *et al.* Usnic acid reactive metabolites formation in human, rat, and mice microsomes. Implication for hepatotoxicity. *Food and Chem. Toxicol.* **120**, 112–118 (2018).

60. Pramyothin, P. *et al.* Hepatotoxic effect of (+)usnic acid from Usnea siamensis Wainio in rats, isolated rat hepatocytes and isolated rat liver mitochondria. *J Ethnopharmacol* **90**, 381–387 (2004).

61. Han, D., Matsumaru, K., Rettori, D. & Kaplowitz, N. Usnic acid-induced necrosis of cultured mouse hepatocytes: Inhibition of mitochondrial function and oxidative stress. *Biochem Pharmacol* **67**, 439–451 (2004).

62. Guzow-Krzemińska, B., Guzow, K. & Herman-Antosiewicz, A. Usnic acid derivatives as cytotoxic agents against cancer cells and the mechanisms of their activity. *Curr Pharmacol Rep* **5**, 429–439 (2019).

63. Gunawan, G. A. *et al.* Divergent reactivity of usnic acid and evaluation of its derivatives for antiproliferative activity against cancer cells. *Bioorg. Med. Chem* **79**, 117157 (2023).

64. Pyrczak-Felczykowska, A. *et al.* Synthesis of usnic acid derivatives and evaluation of their antiproliferative activity against cancer cells. *J Nat Prod* **82**, 1768–1778 (2019).

65. Pyrczak-Felczykowska, A. *et al.* The isoxazole derivative of usnic acid induces an er stress response in breast cancer cells that leads to paraptosis-like cell death. *Int J Mol Sci* **23**, 1802 (2022).

66. Gimła, M. *et al.* The pyrazole derivative of usnic acid inhibits the proliferation of pancreatic cancer cells in vitro and in vivo. *Cancer Cell Int* **23**, 1–13 (2023).

67. Pyrczak-Felczykowska, A. *et al.* Natural product as a lead for impairing mitochondrial respiration in cancer cells. *J Enzyme Inhib Med Chem* **40**, 2465575 (2025).

68. Hanahan, D. & Weinberg, R. A. The hallmarks of cancer. *Cell* **100**, 57–70 (2000).

69. Hanahan, D. & Weinberg, R. A. Hallmarks of cancer: the next generation. *Cell* **144**, 646–674 (2011).

70. Hanahan, D. Hallmarks of cancer: new dimensions. *Cancer Discov* **12**, 31–46 (2022).

71. Özben, R. & Cansaran-Duman, D. The expression profiles of apoptosis-related genes induced usnic acid in SK-BR-3 breast cancer cell. *Hum Exp Toxicol* **39**, 1497–1506 (2020).

72. Nguyen, T. T. *et al.* lichen secondary metabolites in flavocetraria cucullata exhibit anti-cancer effects on human cancer cells through the induction of apoptosis and suppression of tumorigenic potentials. *PLoS One* **9**, e111575 (2014).

73. Geng, X. *et al.* Usnic acid induces cycle arrest, apoptosis, and autophagy in gastric cancer cells in vitro and in vivo. *Med Sci Monit* **24**, 556 (2018).

74. Zuo, S. T. *et al.* Usnic acid induces apoptosis via an ROS-dependent mitochondrial pathway in human breast cancer cells in vitro and in vivo. *RSC Adv* **5**, 153–162 (2014).

75. Eryilmaz, I. E. *et al.* In vitro cytotoxic and antiproliferative effects of usnic acid on hormone-dependent breast and prostate cancer cells. *J Biochem Mol Toxicol* **32**, 22208. (2018).

76. Song, Y. *et al.* Usnic acid inhibits breast tumor angiogenesis and growth by suppressing VEGFR2-mediated AKT and ERK1/2 signaling pathways. *Angiogenesis* **15**, 421–432 (2012).

77. Sun, T. X. *et al.* Usnic acid suppresses cervical cancer cell proliferation by inhibiting PD-L1 expression and enhancing T-lymphocyte tumor-killing activity. *Phytother Res* **35**, 3916–3935 (2021).

78. Varlı, M. *et al.* Usnic acid targets 14-3-3 proteins and suppresses cancer progression by blocking substrate interaction. *JACS Au* **4,** 1521-1537 (2024).

79. Kumari, M., Kamat, S. & Jayabaskaran, C. Usnic acid induced changes in biomolecules and their association with apoptosis in squamous carcinoma (A-431) cells: A flow cytometry, FTIR and DLS spectroscopic study. *Spectrochim Acta A Mol Biomol Spectrosc* **274**, 121098 (2022).

80. Su, Z. Q. *et al.* Effect-enhancing and toxicity-reducing activity of usnic acid in ascitic tumor-bearing mice treated with bleomycin. *Int Immunopharmacol* **46**, 146–155 (2017).

81. Oyadomari, S., Araki, E. & Mori, M. Endoplasmic reticulum stress-mediated apoptosis in pancreatic β-cells. *Apoptosis* **7**, 335–345 (2002).

82. Mollinedo, F. & Gajate, C. Direct endoplasmic reticulum targeting by the selective alkylphospholipid analog and antitumor ether lipid edelfosine as a therapeutic approach in pancreatic cancer. *Cancers* **13**, 4173 (2021).

83. Den Hollander, P., Maddela, J. J. & Mani, S. A. Spatial and temporal relationship between epithelial–mesenchymal transition (EMT) and stem cells in cancer. *Clin Chem* **70**, 190 (2024).

84. Youssef, K. K. *et al.* Two distinct epithelial-to-mesenchymal transition programs control invasion and inflammation in segregated tumor cell populations. *Nat Cancer* **5**, 1660–1680 (2024).

85. Liu, M. *et al.* ZIP4 promotes pancreatic cancer progression by repressing ZO-1 and claudin-1 through a ZEB1-dependent transcriptional mechanism. *Clin Cancer Res* **24**, 3186–3196 (2018).

86. Zhu, L. *et al.* Loss of Claudin-1 incurred by DNMT aberration promotes pancreatic cancer progression. *Cancer Lett* **586**, 216611 (2024).

87. Carmona-Carmona, C. A. *et al.* Divergent roles of mitochondria dynamics in pancreatic ductal adenocarcinoma. *Cancers* **14**, 2155 (2022).

88. El Sayed, S. M. *et al.* Warburg effect increases steady-state ROS condition in cancer cells through decreasing their antioxidant capacities (Anticancer effects of 3-bromopyruvate through antagonizing Warburg effect). *Med Hypotheses* **81**, 866–870 (2013).

89. Lis, P. *et al.* Screening the yeast genome for energetic metabolism pathways involved in a phenotypic response to the anti-cancer agent 3-bromopyruvate. *Oncotarget* **7**, 10153–10173 (2016).

90. Cardaci, S., Desideri, E. & Ciriolo, M. R. Targeting aerobic glycolysis: 3-bromopyruvate as a promising anticancer drug. *J Bioenerg Biomembr* **44**, 17–29 (2012).

91. Sun, Y. *et al.* Mechanisms underlying 3-bromopyruvate-induced cell death in colon cancer. *J Bioenerg Biomembr* **47**, 319–329 (2015).

12. Publikacje wchodzące w skład rozprawy doktorskiej

12.1. Publikacja nr 1

Gimła Mariola, Herman-Antosiewicz Anna

Multifaceted properties of usnic acid in disrupting cancer hallmarks

Biomedicines, 2199:10.3390

(2024)

Impact Factor = 3.9 (2024)

Punktacja MNiSW = 100

biomedicines

MDPI

Review

Multifaceted Properties of Usnic Acid in Disrupting Cancer Hallmarks

Mariola Gimła and Anna Herman-Antosiewicz *

Department of Medical Biology and Genetics, Faculty of Biology, University of Gdańsk, 80-308 Gdańsk, Poland; mariola.gimla@phdstud.ug.edu.pl

* Correspondence: anna.herman-antosiewicz@ug.edu.pl

Abstract: Cancer, a complex group of diseases marked by uncontrolled cell growth and invasive behavior, is characterized by distinct hallmarks acquired during tumor development. These hallmarks, first proposed by Douglas Hanahan and Robert Weinberg in 2000, provide a framework for understanding cancer's complexity. Targeting them is a key strategy in cancer therapy. It includes inhibiting abnormal signaling, reactivating growth suppressors, preventing invasion and metastasis, inhibiting angiogenesis, limiting replicative immortality, modulating the immune system, inducing apoptosis, addressing genome instability and regulating cellular energetics. Usnic acid (UA) is a natural compound found in lichens that has been explored as a cytotoxic agent against cancer cells of different origins. Although the exact mechanisms remain incompletely understood, UA presents a promising compound for therapeutic intervention. Understanding its impact on cancer hallmarks provides valuable insights into the potential of UA in developing targeted and multifaceted cancer therapies. This article explores UA activity in the context of disrupting hallmarks in cancer cells of different origins based on recent articles that emphasize the molecular mechanisms of this activity.

Keywords: usnic acid (UA); antiproliferative activity; cancer treatment; cancer hallmarks; lichens

Citation: Gimła, M.; Herman-Antosiewicz, A. Multifaceted Properties of Usnic Acid in Disrupting Cancer Hallmarks. *Biomedicines* **2024**, *12*, 2199. https://doi.org/10.3390/biomedicines12102199

Academic Editor: Bo-Ying Bao

Received: 29 August 2024
Revised: 18 September 2024
Accepted: 20 September 2024
Published: 26 September 2024

1. Introduction

Cancer is a complex group of diseases characterized by uncontrolled cell growth and the ability of cells to invade surrounding tissues. The hallmarks of cancer are a set of fundamental characteristics acquired by cancer cells during the development of the disease. Initially proposed by Douglas Hanahan and Robert Weinberg in 2000, these hallmarks provide an organizing principle for understanding the complexity of cancer [1]. The original six hallmarks included sustaining proliferative signaling, evading growth suppressors, resisting cell death, enabling replicative immortality, inducing angiogenesis and activating invasion and metastasis [1]. Subsequently, two emerging hallmarks were added: reprogramming of energy metabolism and evading immune destruction. These hallmarks were underpinned by two enabling characteristics: genome instability and inflammation [2]. Although some reports attempted to emphasize other aspects of cancer biology, redefine or expand the concept of cancer hallmarks, it remained instrumental in rationalizing the diverse and complex nature of cancer, providing a framework for research and potential therapeutic interventions [3–6].

By targeting the hallmark of sustained proliferative signaling, therapies aim to inhibit the abnormal growth signals that drive cancer cells to divide uncontrollably [7]. Effective cancer therapy often involves strategies to disrupt the evasion of growth suppressors by cancer cells. Inhibiting invasion and metastasis is a key focus of cancer therapies aiming to prevent the spread of cancer cells to distant tissues and organs [8]. Therapeutic interventions targeting angiogenesis, a hallmark that involves the formation of new blood vessels, seek to deprive tumors of their blood supply and impede their growth [9]. Addressing the hallmark of replicative immortality, therapies aim to limit the ability of cancer cells to divide and

escape the natural cellular aging process continuously [10]. Immune system modulation is a crucial aspect of cancer therapy, focusing on enhancing the body's ability to recognize and eliminate cancer cells, countering the hallmark of immune evasion [11]. Therapies targeting resistance to cell death mechanisms are designed to induce apoptosis or other kinds of death in cancer cells. Combating the hallmark of genome instability and mutation involves therapies to enhance DNA damage repair and prevent the accumulation of genetic alterations and chromosomal instability that drive cancer progression [12]. Therapeutic approaches targeting the ability of cancer cells to sustain chronic inflammation aim to disrupt the tumor-promoting microenvironment and hinder cancer progression [13].

Natural products are invaluable sources of bioactive agents and the discovery of leads for drugs to treat different human diseases, including cancer. This is due to high biofunctionality and molecular diversity as well as superior efficacy and safety compared with synthetic compounds. As summarized by Newman and Cragg (2020), the total number of small molecules approved as antitumor drugs over the period 1946–2019 comes to 259, of which 79% are of natural origin [14]. They include natural compounds, their derivatives (usually semisynthetically modified) or compounds inspired by natural products (made by total synthesis, but the pharmacophore is from a natural product) [14,15]. Examples of clinically effective anticancer drugs of natural origin include paclitaxel from *Taxus brevifolia* or topotecan and irinotecan from *Camptoteca acuminate*, to name a few [14]. Advances in analytical techniques, such as non-targeted metabolomics based on mass spectral networking, DNA sequencing and high-throughput screening should speed up the identification of new active compounds in natural sources [16], while computational chemistry coupled with artificial intelligence and combinatorial synthetic methodologies enhance the development of anticancer drugs based on natural compounds [17].

Usnic acid (2,6-diacetyl-7,9-dihydroxy-8,9b-dimethyldibenzo[b,d]furan-1,3(2H,9bH)-dione, UA) is one of the most investigated bioactive compounds found in lichens. It occurs in nature as (–) and (+) isomers as well as a racemic mixture [18]. These enantiomers may exhibit different biological activities and interactions due to their distinct spatial arrangements, making them important considerations in pharmaceutical and biological applications [19,20]. UA has been studied for its various biological activities such as antibacterial, antiviral, antimycotic, antiprotozoal, anti-inflammatory, analgesic, neuroprotective and anti-cancer (reviewed in [19,21–23]). The anti-cancer activity of (–)-UA was reported in 1975 when Kupchan and Kopperman isolated this compound from *Cladonia* species and treated mice harboring Lewis lung carcinoma with (–)-UA at a dose range of 20–200 mg/kg and that extended the life of animals even to 52% over the untreated control group [24].

The purpose of this article is to summarize and upgrade the knowledge of UA activity toward cancer cells in vitro and in vivo. Thus, more recent publications are presented, especially ones investigating mechanisms of UA activity in the context of targeting cancer hallmarks. This work focuses on data reported on pure UA (either purified from lichen's extracts or synthesized) and not on extracts containing this compound, its derivatives or formulations, although they are mentioned.

2. UA Inhibits Cell Proliferation and Induces Apoptosis of Cancer Cells

Cancer cells' ability to proliferate and survive harsh conditions is connected with hallmarks such as sustained proliferative signaling, which is associated with the activity of oncogenes, evading cell cycle suppressive and proapoptotic signals and replicative immortality. UA has been shown to affect these features in cancer cells.

The main pathways signaling cells' survival and proliferation encompass growth factors and their receptors, Hedgehog and Wnt signaling, to name a few. It was reported that (+)-UA reduced the transcriptional activity of β-catenin/LEF and c-jun/AP-1, the final effectors of Wnt and MAPK pathways, respectively. Thus, expression levels of c-myc, CD44 and cyclin D1, proteins crucial for cancer cell survival and proliferation, were reduced in A549, H1650, H1975 and H460 non-small-cell lung cancer cells treated with (+)-UA [25].

Numerous studies document that UA exerts antiproliferative potential inducing cell cycle arrest at either the G_0/G_1, S or G_2/M phase and/or cell death through apoptosis or necrosis.

For instance, Backorova et al. (2011) showed that UA induced cell cycle arrest in the S phase in A2780 (ovarian), HL-60 (leukemia) and HCT116 (colon cancer cells) and in some of these cells, G_2/M phase arrest took place, which was dependent on dose (50 and 100 μM) and treatment time (48 or 72 h). Interestingly, the antiproliferative activity of UA did not depend on the presence of a tumor suppressor: p53 protein. This work also revealed that UA induced apoptosis, and its extent was cell-line specific [26]. Later, when investigating mechanisms of this activity, researchers found that UA decreased mitochondrial membrane potential (MMP) and increased reactive oxygen species (ROS) or reactive nitrogen species (RNS) levels, especially after 48 and 72 h of treatment (in up to 90–100% cells) and dose-dependent changes in p53, Bcl-2 and Bax levels, which correlated with apoptosis in A2780 ovarian and HT-29 colon cancer cells [27].

G_2/M arrest may suggest that the microtubule dynamic is disturbed. However, the treatment of MCF-7 breast or H1299 lung cancer cells with UA (29 μM for 24 h) did not result in any morphological changes in microtubules or an increase in the mitotic index compared to the effects of vincristine or taxol, drugs targeting microtubules. These results suggested that the antineoplastic activity of UA is not related to alterations in the formation and/or stabilization of microtubules [28].

S phase arrest has been observed in human hepatoblastoma HepG2 treated with growing concentrations of UA (3.13, 6.25, 12.5, 25 or 50 μM). At the highest concentrations, the fractions of subG_0/G_1 cells were elevated, which were confirmed to be apoptotic cells. Lower viability was correlated with decreased levels of pro-survival proteins, such as Bcl-2 and Mcl-1 as well as Akt and p-Akt (Thr-308 and Ser-473), mTOR and p-mTOR (Ser-2448), p-S6K (Ser-371) and p-4E-BP1 (Thr-37/46). Additionally, UA elevated autophagy, which played a protective role as its inhibition by 3-methyladenine or chloroquine or downregulation of Atg7 potentiated apoptosis. Moreover, the autophagy-regulated activation of JNK played a protective role, and its inhibition increased apoptotic cell fraction [29].

Another study compared the response of HepG2 (HBV-negative) and SNU-449 (HBV-positive) hepatocellular carcinoma cell lines to UA. The lichen compound reduced viability in a dose- and time-dependent manner, and SNU-449 cells were more sensitive to UA than HepG2 cells. UA also induced cell cycle arrest at the G_0/G_1 (HepG2) or S and G2/M (SNU-449) phase and apoptotic cell death after 48 h treatment. Autophagy induction was detected after 36 h of treatment. The viability of HUVEC cells (normal endothelial cells) was not affected by UA tested in the concentration range of 6.25–100 μM, which shows the selectivity of UA toward malignant cells [30].

UA-induced decrease in pro-survival signaling pathways was also reported in other studies. Nguen et al. (2014) investigated the impact of *Flavocetraria cucullata* metabolites on a panel of noncancerous and cancer cell lines. UA at concentrations as low as 5 and 10 μM decreased p-Akt (Ser-473), p-ERK1/2 (Thr202/Tyr204 and Thr185/Tyr187) and p-c-Jun (Ser-63) in A549 lung cancer cells. UA at 10 μM modulated the epithelial–mesenchymal transition (EMT) markers: reduced mRNA for Snail, Twist and N-cadherin and elevated E-cadherin (at the transcript and protein level) in these cells, as well as reduced time-dependent migration, invasion and anchorage-independent growth of A549 and AGS gastric cancer cells. UA decreased the viability of prostate CWR22Rv-1, lung A549, colon HT29 and gastric AGS cancer cells and had no impact on the viability of four different cell lines representing normal cells. Depending on the concentration (25, 50 or 100 μM) and cell line, UA inhibited cell cycle progression after 24 h treatment in the G_0/G_1 or S phase (CWR22Rv-1 and A549) or in the G_2/M phase (AGS and HT29) and induced apoptosis of cancer cells with an elevation of a Bax:Bcl-xL ratio, procaspase-3 and PARP cleavage, especially in AGS and CWR22Rv-1 (after 48 h of exposition) [31].

Ebrahim et al. (2017) showed that UA (15 and 25 μM) induced autophagy in breast cancer cells, which was accompanied by a decrease in mTOR activity reflected by a drop in

p-Akt, p-4E-BP1, p-S6K in breast MCF-7 and MDA MB 231 cancer cells. UA also inhibited the motility and invasion of MDA MB 231 cells (at 10–30 μM and 10 μM, respectively) [32].

In gastric cancer cells, 100–400 μM UA induced G_0/G_1 arrest (in BGC823 cells) or G_2/M (in SGC7901 cells) after 24 h treatment and apoptosis with the rise of the Bax:Bcl2 ratio (also in vivo) and caspase 3 activation as well as autophagy. Additionally, in vivo, UA (100 mg/kg i.p. for 11 days) was more effective than 5-fluorouracil (5-FU, 25 mg/kg) in the retardation of BGC823 tumor growth in mice [33].

In A-431 squamous carcinoma cells, UA also induced cell cycle arrest in G_0/G_1, apoptosis and necrosis (concentration tested within a range of 25–250 μM), which was connected with a reduction in MMP and reduced glutathione level, rise in ROS production, lipid oxidation and structural changes in DNA and surface lipids and proteins [34].

Mechanisms underlying G_0/G_1 arrest induced by UA have been investigated in A549 human lung carcinoma cells. The authors observed arrest at the G_0/G_1 phase in cells treated with 25, 50 or 100 μM UA for 24 or 48 h. It was accompanied by decreased levels of CDK4 and CDK6 cyclin-dependent kinases and cyclin D1 and increased levels of p21/Cip1, CDK inhibitor. UA treatment also enhanced cell death by up to twofold (24 h treatment) and eightfold (48 h treatment). While examining the cell death-associated molecular changes, authors observed that UA induced mitochondrial membrane depolarization and cleavage of PARP [35].

UA suppressed JAK1/2-Src-STAT3 and RAS-RAF-MEK-ERK pathways in HeLa cells. It led to a drop in the production of programmed death ligand 1 (PD-L1), which not only enhanced the cytotoxic activity of T lymphocytes toward cancer cells but also resulted in a decline in viability and clonogenic potential of HeLa cells, and it correlated with reduced levels of c-myc and cyclin D1. UA inhibited mTOR, leading to MiT/TFE nuclear translocation and enhanced lysosomal biogenesis [36].

Recently, using UA-linker-Affi-Gel, 14-3-3 proteins have been identified as UA targets. Interaction between these molecules led to the degradation of 14-3-3 by proteasomal and autophagy pathways in Caco2 colon cancer cells. As 14-3-3 proteins bind to numerous phospho-proteins, their elimination affects cell proliferation, invasion, metabolism and signaling pathways regulating cell survival. Authors showed that UA (10 μM) reduced levels of different proteins overrepresented in HCT-116 colon cancer cells expressing different isoforms of 14-3-3. Among the downregulated proteins were cyclin D1, cyclin B1 and p-Cdc2 (Tyr-15), which explains UA-induced G_0/G_1 arrest. Moreover, UA reduced levels of proteins phosphorylated at positions crucial for their activity such as p-mTOR (Ser-2488), p-Akt (Ser-473), p-STAT3 (Tyr-705), p-JNK (Thr183/Tyr185) and levels of EMT markers (Snail, Twist, N-cadherin and β-catenin). UA also reduced the activity of AP-1, STAT and NF-κB transcription factors, which were elevated by the overexpression of 14-3-3 isoforms in HEK293T cells [37].

Interesting mechanisms of UA activity have been noticed in human gastric and colon cancer cells treated with potassium usnate (KU), a water-soluble form of UA. The viability of a panel of cell lines (AGS, MNK45, SNU638, Caco2, HCT116 and HT29) was dose- and time-dependently reduced by KU. Moreover, 24 h treatment with KU at IC_{50} concentrations induced cell cycle arrest in the G_0/G_1 or S phase, depending on the cell line, which was accompanied by a drop in CDK4, cyclin D2 and the transient elevation of p21 protein levels. More detailed investigations based on gastric SNU638 and colon HCT116 cancer cells revealed that KU induced endoplasmic reticulum (ER) stress with the elevation of intracellular Ca^{2+}, ROS and ER stress markers, such as BIP, PERK, IRE1α, p-EIF2a, CHOP and ATF3. ATF3 is a transcription factor controlling the expression of ER stress (such as ATF3 itself), cell cycle modulating (GADD45) and apoptotic genes (Bak, PUMA and DR5). Its activity appeared crucial for the KU cytotoxic effect. Downregulation of ATF3 by specific siRNA protected against the KU-induced elevation of Bak, p-BAD, PUMA, activation of caspase 3 and cell death. Moreover, KU (20 mg/kg i.p. injections for 16 days) applied to mice with CT26 metastatic colon cancer cells reduced the number of metastatic nodules in livers, elevating ATF3 and cancer cell apoptosis levels [38].

UA was shown to be a novel Pim-1 inhibitor (IC_{50} = 202 nM). This protein serine/threonine kinase is often overexpressed in hematopoietic malignancies and acts as an oncogene supporting myc-driven transcription, 4E-BP-1-dependent translation and inactivation of pro-apoptotic Bad. The study found that UA inhibited the proliferation of human HL-60 acute myeloid leukemia cells and K562 chronic myeloid leukemia cells (IC_{50} = 10 and 10.4 μM, respectively, after 3 days of treatment) and induced apoptosis. HL-60 cells were more responsive and after 18 h of treatment with 20 μM, the UA apoptotic fraction increased from 3% to over 30%, while such an amount of apoptotic K562 resulted from 48 h treatment with 60 μM UA. It was accompanied by the activation of caspase 3, 9 and 8, a decrease in anti-apoptotic Mcl-1, reduced p-eIF4E, p-4E-BP1 and p-Akt levels in both cell lines, as well as a decrease in c-myc, cyclin D1, p-Bad, Pim-1, MNK1 and increased p27 protein levels in K562 cells, which resulted from an inhibition of MNK1/eIF4F and Pim-1/4E-BP1 signaling pathways [39].

UA also exerted antiproliferative and pro-apoptotic effects in prostate cancer cells, hormone-independent DU-145 and PC-3 [40,41] and hormone-dependent LNCap cell lines [42]. In addition to features characteristic for apoptosis (Bax:Bcl-2 mRNA elevation, drop in MMP, caspase activation), a decrease in NFκB p50 at the protein level and *NFKB1* mRNA was reported in DU145 prostate cancer treated with 40 μM UA [41].

Another study investigated the mechanisms of the anticancer effects of (+)-UA from *Cladonia arbuscula* and (−)-UA from *Alectoria ochroleuca* on two human cell lines, T47D breast cancer cells and Capan-2 pancreatic cancer cells. The study found that both enantiomers were equally effective in inhibiting cell proliferation. (+)-UA at 10 μg/mL arrested cell cycle at G_0/G_1 after 24 h treatment and decreased MMP; however, apoptosis was not detected. Instead, necrosis was seen in Capan-2 cells treated for a longer (48 h) time [43].

The activity of UA was also investigated against OVCAR-3 and A2780 ovarian cancer cells. The study utilized real-time cell analysis and demonstrated the antiproliferative effect of UA for these cell lines with no impact on non-cancerous L929 cells. UA at a concentration of 20 μM inhibited the cell cycle at the G_0/G_1 phase and induced apoptosis of OVCAR-3 cells treated for 48 h. Evaluation of the expression of apoptosis-related genes showed that UA significantly upregulated *Casp-1*, *Casp-8*, *TRAF6*, *CHECK1*, *CHECK2*, *RIPK2*, *Bak1*, *Bag1*, *Bag4*, *BCL2A1*, *TNFRSF21*, *TP53*, *CIDEA*, *GADD45*, *BIRC3* and *5* and downregulated some genes of TNF and Bcl-2 family. It also blocked cell migration and invasion [44].

UA also modulated the expression of apoptosis-related genes of the apoptosis pathway in SKBR-3 breast cancer cells with significant elevation of mRNA for caspases 3, 4, 10, TRAF 5 and 6, numerous TNF family members, APAF1, Bik, Bak1, Bax, Bok, MCL1, p53, Chek1, Chek2, DAPK2, RIPK2, GADD45A and reduction in mRNA for Bcl2, Bcl2L11, Bag1, Bag4. Moreover, Bax, caspases 3 and 9 have also been significantly elevated at the protein levels in cells treated with 7.2 μM UA for 48 h. Notably, MCF-12A noncancerous breast epithelial cells, were resistant to UA used up to 10 μM concentration [45].

The impact of UA on breast cancer cells with attention to miRNA expression profile was investigated. MDA MB 231, MCF-7 and BT-474 cells were treated with UA (IC_{50} c.a. 13 μM) for 48 h and RNA was analyzed using microarrays. The authors identified differentially expressed miRNAs, and their number was cell-line-specific (67 in MDA MB 231, 8 in MCF-7 and 15 in BT-474). MiRNAs were almost unique to each cell line; however, their targets were discovered to play a role mainly in four pathways in all three cell lines: basal cell carcinoma, the neurotrophin signaling pathway, gap junction and the Hedgehog signaling pathway. Pathway enrichment analysis revealed that in MDA MB 231 cells, most targets of miRNA were transcripts involved in MAPK, Erb, PI3K-Akt and p53 pathways, while in BT-474, it involved Erb, mTOR signaling, focal adhesion and gap junctions. UA increased the level of has-miR-185-5p, miRNA downregulated in many cancers, which is connected with their chemoresistance [46]. This miRNA, when overexpressed in BT-474, induced G_0/G_1 cell cycle arrest and apoptosis (with no effect in MCF-12A noncancerous cells), which was connected with the upregulation of pro-apoptotic Bcl-2 members, caspases,

kinases related to cell death, death receptors and the downregulation of antiapoptotic Bcl-2 [47].

Oncogenic long noncoding RNA urothelial cancer associated 1 (*UCA1*) was identified as another target of UA. UCA1 is regarded as an oncogene due to its stimulating effects on cancer cell proliferation, migration and invasion. It was shown to be upregulated in endometrial cancer tissue compared to normal tissue and contribute to cancer development. UA inhibited the dose- and time-dependently survival of Ishikawa endometrial cancer cells (IC_{50} = 51.76 μM after 48 h treatment), which correlated with a 3-fold decrease in UCA1 level [48].

In the search for the mechanisms of antiproliferative activity of UA against breast cancer cells, Zuo et al. (2015) found that it induced ROS generation in MCF-7 cells, which triggered the mitochondrial pathway of apoptosis with the activation of c-Jun-N-terminal kinase (JNK), an increase in the Bax:Bcl-2 ratio, a drop in MMP, the release of cytochrome c and caspase cascade activation. N-acetylcysteine (NAC) protected against these effects indicating that UA-induced ROS are responsible for them. UA given intraperitoneally inhibited tumor growth in a murine xenograft model with a dose of 100 mg/kg being more effective and less toxic to animals than cyclophosphamide (25 mg/kg bw) [49].

ROS induction was also observed in H520 and Calu-1 lung squamous cell carcinoma treated with (+)-UA (10, 20 or 40 μM). Authors found that it was caused by inhibition of mitochondrial respiratory chain complexes I and III and lower stability of nuclear factor erythroid 2-related factor 2 (Nrf2). It resulted in a drop in mRNA for heme oxygenase 1 (HO1) and NAD(P)H quinone dehydrogenase 1 (NQO1), enzymes engaged in protection against ROS. Mitochondria-targeted antioxidant Mito-TEMPOL partially protected against UA-induced oxidative stress, while the Nrf2 agonist tBHQ was more effective, also protecting against UA-induced apoptosis. In the xenograft model, UA at a dose of 50 mg/kg (i.p.) reduced tumor growth, which was blocked by NAC (in drinking water) and potentiated the anticancer activity of paclitaxel (10 mg/kg) [50].

Different preparations from lichens were tested against glioma cells. Acetone extracts from *Parmelia sulcata*, *Evernia prinastri* and *Cladonia unciali* more potently reduced the viability of A172 and T89G cells than pure compounds derived from these extracts, i.e., salazinic acid, evernic acid and UA; for instance, IC_{50} values for *C. uncialis* extract were approximately 11 and 3.9 μg/mL, respectively, while IC_{50} values for (−)-UA purified from this extract were 31.5 and 13 μg/mL, respectively. Although extracts revealed weak free radical scavenging and Cu^{2+} ions reducing activities in vitro, pure compounds had no antioxidant activities. All tested extracts and compounds, including (−)-UA, inhibited superoxide dismutase (SOD) activity and (−)-UA revealed inhibitory activity against glutathione reductase (GR) and glutathione peroxidase (GPx), enzymes engaged in ROS defense [51].

UA isolated from *Usnea cornuta* extract was concentration-dependently cytotoxic to MCF-7, A-549 and HeLa cells (IC_{50} values were 89, 84 and 48.7 μM, respectively, after 24 h of treatment). More detailed studies on HeLa cells revealed that UA caused a drop in MMP and GSH levels and increased ROS production and lipid peroxidation. It also induced autophagy and chloroquine, an inhibitor of late stages of autophagy, potentiated ROS production, depletion of GSH, lipid peroxidation and apoptosis induced by UA used at 25 or 50 μM concentrations [52].

Increased ROS production may lead to DNA damage. However, data on UA-induced genotoxicity in cancer cells are inconsistent. In a study conducted by Mayer et al. (2005), UA showed antiproliferative activity against MCF-7 breast cancer cells (estrogen receptor-positive, wild type for p53) and MDA MB 231 (estrogen receptor-negative, non-functional p53) with an IC_{50} of 18.9 and 22.3 μM, respectively [53]. The authors found that the antitumor activity of UA did not involve DNA damage or p53 activation. In MCF-7 cells treated with UA, although there was an accumulation of p53 and p21 proteins, the transcriptional activity of p53 remained unaffected. They also found that there was no phosphorylation of p53 at Ser-15 after treatment of MCF-7 cells with UA, suggesting that

the oxidative stress and disruption of the normal metabolic processes of cells triggered by UA did not involve DNA damage. The property of UA as a non-genotoxic anti-cancer agent that works in a p53-independent manner was highlighted as a promising candidate for novel cancer therapy [53].

Emsen et al. (2018) found that UA, although much more toxic to U87MG glioblastoma cells than to primary rat cerebral cortex cells, PRCC (IC_{50} values by MTT after 24 h were 41.6 and 132.7 μg/mL, respectively), did not significantly elevate 8-hydroxy-2′-deoxyguanosine (marker of DNA oxidative damage) levels in cells treated with 2.5–40 μg/mL UA [54].

On the other hand, studies published in 2020 reported that UA induced DNA damage. UA (10–25 μM) applied to SNU-1 and AGS gastric cancer cells induced apoptosis, which was connected with increased Bax:Bcl-2, depolarization of the mitochondrial membrane and ROS elevation. ROS in UA-treated AGS cells were responsible for DNA double-strand breaks revealed by alkaline comet assay and an increase in γ-H2A.X, DNA-PKcs, p-ATM (Ser-1981), Chk2 and p53—markers of DNA damage response. Moreover, NAC protected against DNA damage and cell death [55].

Another study showed that UA induced DNA damage response involving ATM kinase and G_2/M cell cycle arrest in RKO colorectal cancer cells pretreated with 400 μM H_2O_2. Phosphorylation of histone H2A.X, which is the marker of DNA double-strand breaks, or ATM activation, was elevated in cells treated with H_2O_2 and UA (0.5, 1, 5, 10 μM) compared with H_2O_2 alone; however, the authors did not show how UA alone impacts DNA integrity and DNA damage response. Interestingly, low concentrations of UA (0.5 and 1 μM) reduced ROS levels in H_2O_2-treated cells, while 5 and 10 μM UA—increased ROS levels [56].

Data obtained in vivo indicate that both (+) and (−)-UA enantiomers at doses of 100 or 50 mg/kg induced DNA damage observed as increased tails in comet assays in the liver and kidneys of mice. Interestingly it was observed only 1 h after oral administration and not detected after longer times, probably due to rapid DNA repair. The authors also observed increased lipid peroxidation in cells, thus concluding that oxidative stress induced by UA might be involved in the genotoxicity of this compound [57].

DNA damage induced by UA and detected by comet assay was also reported in KB oral carcinoma cells. It was accompanied by increased ROS, reduced MMP, antioxidant enzymes and GSH levels and induction of apoptosis [58].

In addition to DNA damage due to oxidative stress, UA might be a potential inhibitor of key enzymes involved in DNA synthesis and repair. UA has been reported to be a rather weak inhibitor of PARP1 and polymerase β activity (residual activity of 73–77% after incubation with 0.5 mM UA), and some of its derivatives appeared to be much more active [59].

3. UA Inhibits Angiogenesis, Cancer Cell Motility and Invasion

Growth of tumors depends on angiogenesis; thus, the inhibition of this process can be an effective anticancer strategy. It has been demonstrated that UA inhibited angiogenesis in vivo based on a chick embryo chorioallantoic membrane assay, in a VEGF-induced mouse corneal angiogenesis model and in mice xenografted with Bcap-37 breast cancer cells [60]. Based on in vitro research, it has been shown that UA dose-dependently (1, 10, 20, 50 μM) inhibited activating phosphorylation of VEGFR2 and VEGFR2-mediated MEK/ERK1/2 and Akt/p70S6K signaling pathways in HUVEC endothelial cells, which resulted in a drop in cell proliferation, migration and tube formation and induction of apoptosis [60].

(−)-UA also inhibited HUVEC cell viability (IC_{50} after 48 h was 50 μM) and tube formation at concentrations 50 μM and higher (100 and 200 μM) [61]. It has also been shown that UA reduced VEGF and MMP-9 levels, which was partially dependent on the reduction in PD-L1 in HUVEC cells. These effects resulted in decreased tube formation, migration and the invasive potential of endothelial cells [36].

An article published in 2016 reported that (+)-UA inhibited A549, H1650 and H1975 non-small cell lung cancer cell migration and invasion at a concentration of 5 μM. The authors showed that (+)-UA decreased the level of active, GTP-bound Rac1 (by 22% compared with control) and GTP-RhoA (by 40% compared with control), which are crucial for cell motility regulation. Moreover, UA potentiated the activity of cetuximab, monoclonal antibodies against EGFR used for metastatic colon and lung cancer patients, in reducing the invasive potential of A549 cells [25]. The same team reported the antiproliferative activity of UA using a panel of colorectal cancer cell lines. At the concentration of 5 μM, UA inhibited invasion of Caco2, HCT116 and CT289 cells in vitro; however, it had no effect in the murine orthotopic liver metastasis model (applied at 5 or 10 mg/kg, 6 or 10 times within two weeks, i.p.), while its water-soluble potassium salt (UK) was more effective in vitro and in vivo. Both UA and UK decreased the mRNA levels of EMT markers, such as Twist, Snail, Slug, Zeb2 and N-cadherin in Caco2 cells [62].

SCF induces migration of c-KIT-containing colorectal cancer cells. It has been shown that (+)-UA at a concentration lower than 10 μM inhibited the SCF-induced migration of HCT116 and LS174 cells. The mechanism underlying this activity relied on the down-regulation of c-Kit gene transcription mediated by sumoylation of Transcription Factor AP-2 alpha (TFAP2A) by upregulated UBC9 and degradation of c-KIT protein due to the induction of autophagy. This, in turn, resulted from decreased ATP level and inhibition of mTOR by 8 μM (+)-UA in HCT-116 cells. Caspases 3 and 7 were not activated by (+)-UA; however, the cell's membrane was permeabilized, and LDH release after 48 h treatment increased, which suggests necrotic cell death [63].

UA inhibited the motility of prostate (DU145) and melanoma (HTB-140) cells, and it was connected with dose-dependent (at 10 or 25 μg/mL) rearrangements of the actin cytoskeleton [40].

It has been shown that the overexpression of PD-L1 in HUVEC endothelial cells led to the elevation of pro-angiogenic proteins, VEGF and MMP-9, enhanced tube formation, migration and invasion; however, UA (100 μM) protected against these processes decreasing PD-L1 level [36].

4. UA Facilitates the Immune Destruction of Cancer Cells

The programmed cell death 1 (PD-1) and its ligand PD-L1 are responsible for apoptosis and the exhaustion of T cells. PD-L1 is often elevated in cancer cells, which leads to avoidance of their destruction by immune cells. UA at 10, 30 and 100 μM concentrations has been shown to decrease PD-L1 levels in HeLa cervical cancer, A549 lung cancer, HCT116 colorectal cancer and liver cancer Hep3B cells, even if TNF stimulated production of PD-L1-α. It correlated with the enhanced cytotoxicity of co-cultured T lymphocytes toward HeLa, SiHa and CaSKi cervical cancer cells and higher production of TNF-α and ITF-γ by T cells. Authors identified mechanisms underlying diminished production of PD-L1 as reduced STAT3 and Ras signaling pathways, suppression of mTOR and subsequently increased MiT/TFE transcription factor translocation to the nucleus, enhanced biogenesis of lysosomes and proteolysis of PD-L1 [36].

It has been shown that lichen-derived extracts and compounds, including UA, possess inhibitory properties related to kynurenine pathway enzymes. (−)-UA at 100 μg/mL reduced by almost 22% indoleamine 2,3-dioxygenases 1 (IDO1), an enzyme involved in the conversion of L-tryptophan to L-kynurenine [51]. Metabolites of this pathway are crucial for the suppression of anti-tumor immune responses and IDO1 is highly expressed in multiple types of cancer [64,65].

5. UA Acts against Tumor-Promoting Inflammation

The anti-inflammatory activity of UA has been recently nicely summarized in publications by Wang et al. [23] and Pazdziora et al. [66]. However, it is worth mentioning a few studies in the context of cancer.

It has been shown that lichen-derived extracts and compounds, including UA, possess inhibitory properties related to kynurenine pathway enzymes. (−)-UA at 100 μg/mL reduced indoleamine 2,3-dioxygenases 1 (IDO1). It also strongly inhibited COX-2 (up to almost 60%), indicating its anti-inflammatory activity. Moreover, it inhibited hyaluronidase with IC_{50} = 500 μg/mL being more potent than β-escin used as a standard in this assay [51]. Hyaluronidase is responsible for generating low molecular weight hyaluronan, which displays pro-inflammatory properties, such as stimulation of macrophage activation and production of cytokines [67]. Another study by this team compared activity of (+)-UA and (−)-UA enantiomers showing that right-handed enantiomer is a slightly more potent (IC_{50} = 644.5 and 676.3 mg/mL, respectively) inhibitor of hyaluronidase [20]. This work also presented that both enantiomers (although to a different extent) decreased levels of pro-inflammatory molecules, such as Toll-like receptor 4 (TLR4), cytosolic phospholipase A2 (cPLA2), cyclooxygenases COX-1 and COX-2 in LPS-stimulated RAW 264.7 macrophages, as well as the release of nitric oxide (NO) and weakly TNF-α and IL-6 [20].

Another study investigated the anti-inflammatory effects of UA in MCF-7 breast cancer and found that it plays a crucial role in regulating the inflammatory response. UA dose-dependently decreased levels of NO, prostaglandin PGE2, cytokines IL-2, IL-6, CXCL10, CXCL8, CCL2, MCP-1 and TNF-α, as well as growth factor VEGF. Moreover, it downregulated the expression of genes coding for cyclooxygenase2 (COX-2) and inducible nitric oxide synthase (iNOS). At the same time, UA revealed pro-oxidant activity in cancer cells as it reduced glutathione and increased malondialdehyde (MDA) levels [68].

The reduction in pro-inflammatory proteins such as TNF-α, NF-κB or IL-6 was also reported in KB oral carcinoma cells treated with UA at concentrations of 10, 20 or 30 μM [58]. Moreover, the same team showed chemopreventive properties of UA as it protected against DMBA-induced oral squamous cell carcinoma in hamsters. Mechanisms underlying this activity were the suppression of inflammatory (COX-2 and iNOS) and proliferation markers (cyclin D1 and PCNA) induced by carcinogen as well as the upregulation of antioxidant levels or activity and the modulation of liver detoxification enzyme levels [69].

6. UA Deregulates Energetics in Cancer Cells

As some reports indicated that UA at high concentrations might be hepatotoxic, extensive research was performed to identify mechanisms underlying this activity. Data obtained on rodent primary hepatocytes or isolated mitochondria revealed that UA toxicity might be related to disturbed metabolism, particularly mitochondria functioning and drop in ATP level. These effects concerning normal non-cancerous cells have been beautifully presented in recent review articles [70,71]; however, it is worth mentioning a few studies.

UA is a lipophilic weak acid; thus, it can easily pass the mitochondrial membranes, and in the matrix, it releases a proton resulting in the generation of a usniate anion. It diffuses into the intermembrane space, binds a proton and UA is restored. This cycling might cause a proton leak that could dissipate the proton gradient across the membrane, changing the mitochondrial membrane potential. The protonophoric activities of UA were documented using artificial planar bilayer lipid membranes and isolated rat mitochondria [72]. The analysis of biochemical profiles of rat primary hepatocytes showed that high doses of (+)-UA (10 or 30 μM) decreased ATP levels. It was connected with the depletion of glycogen stores, a drop in glycolysis and the tricarboxylic acid (TCA) cycle. Moreover, the mechanism of UA action resembled the action of mitochondrial uncoupler, FCCP, which supported the idea that UA is a proton carrier [73]. It has also been demonstrated that UA can carry calcium ions across liposomal, mitochondrial and erythrocyte membranes, thus behaving like a calcium ionophore [74].

UA has also been shown to affect the mitochondrial function in cancer cells. Numerous studies (described in the previous paragraph) show that UA causes a drop in MMP in cancer cells, which is connected with apoptosis. However, in some models, although UA decreased the proton gradient across the mitochondrial inner membrane, no release of cytochrome c was observed. UA as a lipophilic weak acid is supposed to act as a proton

shuttle and directly dissipate mitochondrial inner membrane potential, affecting oxidative phosphorylation. Indeed, it was reported, that UA (5 and 10 µg/mL) decreased ATP level in T47D breast cancer cells after 24-h exposition. It activated AMPK, decreased mTOR/S6K signaling, upregulated p-eIF2α and induced autophagy. However, autophagy flux was impaired due to the disruption of lysosomal acidification and thus degradative processes did not occur [75]. Moreover, it was shown that UA inhibited the mitochondrial respiratory chain complexes (I and III) in lung squamous carcinoma cells, leading to a decrease in ATP production and an increase in the production of ROS [50]. Interestingly, the same team showed that UA affected lysosomal function in breast cancer cells.

Inhibition of glycolysis and mitochondrial respiration was also observed in CaCo2 and HCT116 colon cancer cells. UA at 2.5, 5 and 10 µM concentrations inhibited glycolysis (basal and compensatory) and mitochondrial functioning (basal respiration, ATP production, proton leak), which correlated with decreased expression of metabolic genes (*SLC2A1*, *SLC2A4*, *HK2*, *PFK1*, *GPI*, *ALDOA*, *PGK1*, *ENO1*, *PKM2*, *LDHA*, *CDH4*, *SRC1*, *PGC-1a*, *TFAM*, *PKM1*, *PDK1*, *ASCT2*, *SLC7A5*, *SLC7A7*, *GLS1*) and drop in SLC2A1, HK2, PKM2 and LDHA proteins, even when these processes were elevated by the surplus of an isoform of 14-3-3 [37].

Results of research investigating mechanisms of UA activity toward cancer cells in vitro and in vivo are summarized in Figure 1 and Table 1.

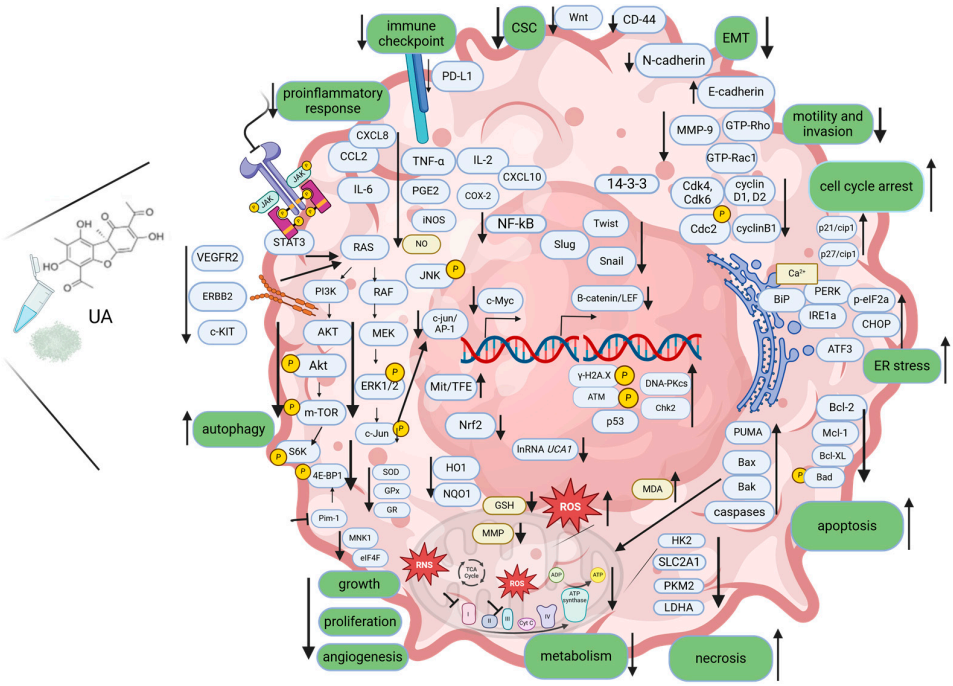

Figure 1. The mechanisms of action of UA in disrupting cancer hallmarks. UA inhibits cell proliferation, induces apoptosis of cancer cells, inhibits angiogenesis, cell motility and invasion, facilitates the immune destruction of cancer cells, acts against tumor-promoting inflammation and deregulates cellular energetics. Additionally, UA induces ER stress and autophagy and inhibits EMT and stem cell features. Created with BioRender.com.

It is worth mentioning that UA's activity was documented against cancer cells of different origins, considering both differentiation stage (epithelial, such as adenocarcinomas and squamous cell carcinomas, and nonepithelial, such as leukemia) and embryonic origin (derived from ectoderm, for instance, breast cancer; neuroectoderm such as melanoma; endoderm, for instance, liver, colon or prostate or mesoderm such as endometrial or hematopoietic cancers). However, anti-tumor potential in vivo was validated only in the case of lung, breast, gastric and colorectal tumors (Table 1).

Table 1. Mechanisms of action of UA toward cancer cells of different origin in vitro and in vivo. UA used in the research was purified from lichens (source is indicated) or synthetized (commercially available, UA).

Organ/Tissue	Cell Lines	Compound Concentrations Tested/IC_{50}	Effects In Vitro	Effects In Vivo	References
Head	human glioblastoma cell lines: A172 T98G	(−)-UA extracted from *Cladonia uncialis* IC_{50} = 91.4 ± 2.0 µM IC_{50} = 37.8 ± 3.8 µM (48 h, MTT)	UA dose-dependently decreased the viability of cancer cells. It inhibited the activities of IDO1, COX2, hyaluronidase, SOD, GR and GPx in in vitro assays. Results of the Parallel Artificial Membrane Permeability Assay indicated that UA can cross the blood–brain barrier.		[51]
	human glioblastoma cells U87MG	UA IC_{50} = 41.55 µg/mL	UA in a dose-dependent manner lowered viability and increased LDH release, especially in cancer cells. It revealed high antioxidant capacity in healthy cells (max at 10 µg/mL). UA non-significantly increased 8-OH-2′-deoxyguanosine levels in cancer cells.		[54]
	primary rat cerebral cortex cells PRCC	IC_{50} =132.69 µg/mL (48 h, MTT)			
	human oral carcinoma cells KB Normal fibroblasts HGF-1	UA IC_{50} = 30 µM (24 h, MTT)	UA in a dose-dependent manner reduced the viability of KB cancer cells, and normal fibroblasts (HGF-1) were significantly more resistant. UA at concentrations of 10, 20 or 30 µM elevated ROS level, lipid peroxidation, decreased SOD, CAT, GPx activities and reduced GSH level and MMP. It induced DNA damage, apoptosis with the downregulation of Bcl-2 and upregulation of p53, Bax, caspases 9 and 3. It decreased NF-κB, TNF-α and IL-6 levels.		[58]
Lung	non-small cell lung cancer cells A549	UA 25, 50, 100 µM (24 and 48 h trypan blue)	UA decreased viability in a dose- and time-dependent manner, induced G_0/G_1 cell cycle arrest with a drop in CDK4, CDK6, cyclin D1 and an increase in p21 levels, mitochondrial membrane depolarization (at 100 µM) and induced apoptosis.		[35]
	non-small cell lung cancer cells A549 (and a panel of other cancer and noncancerous cells)	UA isolated from *F. cucullata* 12.5, 25, 50, 100 µM	UA induced S or G_0/G_1 arrest dependent on concentration, apoptosis, decreased Bcl-xL:Bax ratio, reduced clonogenic potential (10 µM) and anchorage-independent growth, motility (5 and 10 µM) and invasion (10 µM). UA elevated E-cadherin (at mRNA ad protein level), reduced mRNA for N-cadherin, Twist and Snail (10 µM); reduced p-c-jun, p-Akt and p-ERK1/2.	Tumor-free survival of BALB/c nude mice with subcutaneously injected A549 was longer if cells were pretreated with the sublethal concentration of UA (10 µM).	[31]
	non-small cell lung cancer cells: A549 H460 H1650 H1975	(+)-UA IC_{50} = 65.3 ± 0.65 µM n/a n/a n/a	5 µM UA reduced transcriptional activity of β-catenin/LEF and AP-1; reduced mRNA for CD44, cyclin D, c-myc; decreased GTP-Rac1 and GTP-RhoA levels, inhibited motility and invasion of lung cancer cells; potentiated activity of cetuximab in inhibiting invasive potential.		[25]

Table 1. *Cont.*

Organ/Tissue	Cell Lines	Compound Concentrations Tested/IC_{50}	Effects In Vitro	Effects In Vivo	References
Lung	lung squamous carcinoma cells H520 Calu-1	(+)-UA IC_{50} = 32.51 ± 0.44 μM IC_{50} = 34.25 ± 0.05 μM (48 h, MTT)	UA induced dose-dependent ROS (10, 20 40 μM) and ROS-dependent apoptosis, inhibited mitochondria respiratory chain complexes I and III, decreased Nrf2 protein level and its transcriptional activity (drop in expression of its target genes, HO1 and NQO1), which was mediated by PI3K/Akt pathway inhibition. UA at 15 μM enhanced the cytotoxic activity of paclitaxel (at 0.1 μM) in vitro.	Tumor growth in athymic nude mice inoculated with H520 cells was significantly reduced by UA (50 mg/kg, thrice weekly i.p.) compared with controls. UA at such a dose enhanced the effect of paclitaxel (10 mg/kg, thrice weekly i.p.)	[50]
Breast	human breast cancer cell lines MCF-7 MDA MB 231	UA IC_{50} = 18.9 μM IC_{50} = 22.3 μM	The antiproliferative activity of UA did not involve DNA damage or p53 activation. Although there was an accumulation of p53 and p21 proteins in UA-treated MCF-7 cells, the transcriptional activity of p53 remained unaffected, and there was no phosphorylation of p53 at Ser15.		[53]
	human breast cancer cells T47D	(+)-UA isolated from *Cladonia arbuscula* IC_{50} = 4.2 μg/mL (−)-UA from *Alectoria ochroleuca* IC_{50} = 4.0 μg/mL (24 h, [3H] thymidine incorporation)	Both enantiomers were equally effective in inhibiting cell proliferation. (+)-UA induced G_0/G_1 cell cycle arrest and decreased MMP. There was no evidence of apoptosis of cells treated with 20 μg/mL after 24 h or necrosis of cells treated with 5 and 10 μg/mL UA for 24 or 48 h.		[43]
	human breast cancer cells T47D	(+)-UA isolated from *Cladonia arbuscula* 5 and 10 μg/mL tested	UA decreased ATP level after the 24-h exposition. It resulted in activating phosphorylation of AMPK, decreased mTOR/S6K signaling, upregulation of p-eIF2α and induction of autophagy. Autophagy flux was impaired due to the disruption of lysosomal acidification.		[75]
	human medullary breast cancer cells Bcap-37 human umbilical vascular endothelial cells HUVEC	UA 1–50 μM (48–72 h, MTS)	UA dose-dependently inhibited the proliferation of Bcap-37 cancer cells and HUVEC endothelial cells. At 1, 10, 20 μM concentrations, UA inhibited migration and capillary structure formation by HUVEC cells, induced their apoptosis and inhibited activation of VEGFR2 and Akt/p70 S6K/S6 and MEK/ERK1/2 signaling pathways.	In nude mice xenografted with Bcap-37 cancer cells and treated intralesionally with 60 mg/kg/day (22 days) of UA, tumor growth and angiogenesis were inhibited.	[60]

Table 1. *Cont.*

Organ/Tissue	Cell Lines	Compound Concentrations Tested/IC_{50}	Effects In Vitro	Effects In Vivo	References
Breast	human breast cancer cells MCF-7 MDA MB 231 SKBR-3 normal human mammary epithelial cells MCF-10A	UA IC_{50} = 34.12 ± 1.25 μM IC_{50} = 38.41 ± 1.64 μM IC_{50} = 48.07 ± 1.52 μM (24 h, MTT)	UA decreased the viability of cancer cells in a dose- and time-dependent manner, while up to 25 μM did not affect normal MCF-10A cells. UA induced apoptosis in MCF-7 cells through the mitochondrial pathway, increased the Bax:Bcl-2 ratio, reduced MMP, increased ROS (25 μM for 24 h) and activated JNK.	UA dose-dependently suppressed tumor growth in nude mice xenografted with MCF-7 cells (i.p. at 25, 50 or 100 mg/kg every 2 days for 21 days). The highest dose (100 mg/kg) was more effective for cancer cells and much less toxic than cyclophosphamide CTX (25 mg/kg).	[49]
	human breast cancer cell lines MCF-7 T47D MDA MB 231 MDA MB 468 SKBR-3 BT-474	UA IC_{50} = 11.2 μM IC_{50} = 15.9 μM IC_{50} = 13.1 μM IC_{50} = 13.7 μM IC_{50} = 14.4 μM IC_{50} = 15.1 μM (72 h, MTT)	UA at 15 and 25 μM induced autophagy in MCF-7 and MDA MB 231 cells, which correlated with a drop in p-Akt, p-4E-PB1 and p-S6K. It inhibited migration and invasion (5–30 μM) of MDA MB 231 cells. Its benzylidene derivative 52 was much more potent in vitro and in vivo.	UA benzylidene derivative 52 was tested in vivo. It inhibited MDA MB 231 and MCF-7 cells xenografted to nude mice (10 mg/kg bw, i.p. 3 times per week).	[32]
	human breast cancer cell lines MCF-7 MDA MB 231 BT-474	UA IC_{50} = 13.11 ± 0.01 μM IC_{50} = 12.84 ± 0.01 μM IC_{50} = 12.65 ± 1.00 μM (48 h, MTT)	Differentially expressed UA-responsive miRNAs were identified and they appeared almost unique to each cell line. The targets are enriched in basal cell carcinoma, MAPK and Hedgehog signaling pathways (MCF-7 cells), ErbB and mTOR signaling, focal adhesion and gap junctions (in BT474 cells), MAPK, ErbB2, PI3K-Akt and p53 signaling pathways (MDA MB 231). Among the upregulated miRNA was a tumor suppressor: has-miR-185-5p.		[46]
	human breast cancer cells SK-BR-3 normal breast epithelial cells MCF-12A	UA IC_{50} = 7.21 μM (48 h, MTT)	UA dose-dependently decreased cancer cell viability with no effect on normal cells. It modulated the expression of apoptosis-related genes, such as these coding for caspases, BCL-, TRAF- and TNF-family members and increased Bax, caspase 3 and 9 protein levels when applied at 7.21 μM for 48 h.		[45]

Table 1. *Cont.*

Organ/Tissue	Cell Lines	Compound Concentrations Tested/IC_{50}	Effects In Vitro	Effects In Vivo	References
Breast	human breast cancer cells MCF-7	UA LD_{50} = 13.11 μM	UA decreased NO, VEGF, PGE2 levels, gene expression levels of COX-2 and iNOS and cytokines (IL 2, CXCL10, CXCL8, CCL2, TNF-α, IL-6). It decreased glutathione levels and increased MDA levels in a dose-dependent manner.		[68]
	mouse mammary cancer cells 4T1	UA, HA-UA-GNPs and UA-GNPs IC_{50} = 120.04 ± 4.8 μM IC_{50} = 0.56 ± 2.8 μM IC_{50} = 92.64 ± 3.6 μM, respectively (24 h, MTT)	The cytotoxicity and cellular uptake of UA loaded into gliadin nanoparticles (GNPs) functionalized with hyaluronic acid (HA, targeting CD44 receptor) was higher than UA or UA-GNPs.	Tumor (4T1 cells) growth in BALB/C female mice was efficiently reduced by HA-UA-GNPs, compared with an equal dose (100 mg/kg of UA as an i.p. injection every two days for 21 days) of non-targeted UA-GNPs and free UA.	[76]
Liver	human hepatocellular carcinoma cells HepG-2	UA 1.56–50 μM	UA in time- and dose-dependent manner decreased cell viability, at 24 and 48 h it induced LDH release, and after 24 h induced S phase arrest and apoptosis. It decreased antiapoptotic proteins (Bcl-2, Mcl-1) and reduced activating phosphorylation of Akt, PDK1, mTOR and its substrates (S6K and 4E-BP1). UA elevated autophagy (induction and flux), which was a protective mechanism. UA elevated phosphorylation of ERK1/2, p38 and JNK. The latter kinase was involved in autophagy and apoptosis regulation.		[29]
	human hepatocellular carcinoma cells HepG-2 (HBV(-)) SNU-449 (HBV(+)) human umbilical vascular endothelial cells HUVEC	UA 6.25,12.5, 25, 50, 75 and 100 μM	UA at lower concentrations, 6.25 and 12.5 μM for HepG2 and 6.25 μM for SNU-449, increased viability measured after 24 h. Longer treatment (48 h) was connected with dose-dependent viability drop. UA induced G_0/G_1 cell cycle arrest in HepG2, S and G_2/M arrest in SNU-449, apoptosis and autophagy in both cancer cell lines with limited effect on normal control cells (HUVEC).		[30]

Table 1. *Cont.*

Organ/Tissue	Cell Lines	Compound Concentrations Tested/IC_{50}	Effects In Vitro	Effects In Vivo	References
Stomach	human gastric carcinoma cells BGC823 SGC7901	(+)-UA IC_{50} = 236.55 ± 11.12 μM IC_{50} = 618.82 ± 1.77 μM (24 h, CCK-8)	UA induced G_0/G_1 cell cycle arrest in BCG823 (100, 200, 400 μM, 24 h) and G_2/M arrest in SGC7901 (300, 600, 1200 μM), apoptosis with the rise in Bax, cleaved PARP and caspase 3 and a decrease in Bcl-2 levels. UA induced autophagy (elevated LC3-II and decreased p62 levels).	BGC823-bearing nude mice were treated with 100 mg/kg UA i.p. for 11 days (every 2 days), tumor volume and mass were 2-fold lower than control, PBS-treated mice. UA was more effective than 5-FU (25 mg/kg).	[33]
	human gastric adenocarcinoma cells AGS SNU-1	UA 10–50 μM	UA in a dose- and time-dependent manner decreased cell viability, clonogenicity and elevated apoptosis. It reduced MMP and increased Bax:Bcl-2 ratio. In AGS cells UA increased ROS generation in a time-dependent manner and DNA damage was detected by alkaline comet assay after 48 h treatment. UA (15 or 25 μM) in ROS-dependent manner upregulated p-ATM, γ-H2A.X, DNA-PKcs, p53, Chk-2 levels. NAC protected against these effects.		[55]
Pancreas	human pancreatic adenocarcinoma cells Capan-2	(+)-UA isolated from *Cladonia arbuscula* IC_{50} = 5.3 μg/mL (−)-UA from *Alectoria ochroleuca* IC_{50} = 5.0 μg/mL (24 h, [3H] thymidine incorporation)	Both enantiomers were equally effective in inhibiting cell proliferation. (+)-UA induced G_0/G_1 cell cycle arrest, decreased MMP. No evidence of apoptosis of cells treated with 20 μg/mL after 24 h, and necrosis was detected in cells treated with 5 or 10 μg/mL UA for 48 h.		[43]
Colon	human colon adenocarcinoma cells HT-29	(+) UA, IC_{50} = 99.7 ± 18.8 μM (72 h, MTT)	UA at 50 or 100 μM in a time-dependent (24, 48 and 72 h) manner decreased MMP and induced apoptosis. It was preceded by ROS elevation (observed after 1, 3 or 6 h post-treatment).		[27]
	human colorectal cancer cell lines HCT116 LS174	(+)-UA 2, 4, 8 μM tested	8 μM UA for 24 or 48 h inhibited SCF-induced cell proliferation and migration; decreased cellular ATP content and increased LDH release. It inhibited mTOR signaling (drop in p-S6K, p-4E-BP) and PKC-A. It elevated autophagy (LC3-II), which was responsible for UA-induced reduction in c-KIT receptor.		[63]

Table 1. *Cont.*

Organ/Tissue	Cell Lines	Compound Concentrations Tested/IC_{50}	Effects In Vitro	Effects In Vivo	References
Colon	human colorectal cancer cell lines HCT116 DLD1 SW480 HT29 SW620 Caco2 COLO320 Mouse colorectal cancer cells CT26	UA and potassium usnate (KU), a water-soluble usnic acid salt; 12.5–100 μM tested	UA reduced the viability of cells in a dose-dependent manner; at a 5 μM concentration, it reduced invasion in vitro. KU was more effective in the majority of tested cells. Both UA and KU decreased mRNA for N-cadherin, Snail, Twist, Slug and ZEB2 and protein levels of Twist, Snail and Slug EMT markers in Caco2 cells. KU decreased expression of genes related to motility (*CAPN1*, *CDC42*, *CFL1*, *IGF1*, *WASF1*, *WASL*) in Caco2 cells (UA only affected *CFL1* and *IGF1*).	Firefly luciferase-expressing CT26 cells were inoculated via splenic injection to form multiple tumor foci in the livers of male BALB/c mice. UA at 5 or 10 mg/mL i.p. (6 or 10 times for 2 weeks) or KU at a dose of 5, 10 or 20 mg/kg/mouse i.p. (6 times for 2 weeks) were applied. KU exhibited more potent anticancer effects (PARP cleavage, caspase 3 activation, reduction in EMT markers) and at 20 mg/kg inhibited liver metastasis in an orthotopic murine colorectal cancer model.	[62]
	human colorectal cancer cell lines Caco2, HCTT116 HT29 human gastric cancer cells AGS, MNK45, SNU638	KU-potassium usnate IC_{50} = 38.9 ± 1.76 μM IC_{50} = 56.5 ± 1.49 μM IC_{50} = 103.5 ± 0.76 μM IC_{50} = 41.3 ± 1.61 μM IC_{50} = 120.8 ± 0.51 μM IC_{50} = 46.4 ± 1,63 μM (24 h, MTT)	The viability of a panel of cell lines was dose- and time-dependently reduced by KU. The 24 h treatment with KU at IC50 concentrations induced cell cycle arrest in the G_0/G_1 or S phase, depending on the cell line, reduced CDK4, cyclin D2 and transiently elevated p21 protein levels. It induced apoptosis by the mitochondrial pathway. In SNU638 and HCT116 cells KU induced ER stress with the elevation of intracellular Ca^{2+}, ROS and ER stress markers, such as BIP, PERK, IRE1α, p-eIF2a, CHOP and ATF3 proteins as well as ATF3-regulated genes. Downregulation of ATF3 by specific siRNA protected against KU-induced elevation of Bak, p-BAD, PUMA, activation of caspase 3 and cell death.	KU applied (20 mg/kg i.p. injections for 16 days) to mice with CT26 metastatic colon cancer cells reduced the number of metastatic nodules in livers, elevated ATF3 and cancer cell apoptosis levels.	[38]

Table 1. *Cont.*

Organ/Tissue	Cell Lines	Compound Concentrations Tested/IC_{50}	Effects In Vitro	Effects In Vivo	References
Colon	human colon carcinoma cells RKO	UA 0.5, 1, 5, 10 μM tested	UA at 5 or 10 μM potentiated the inhibitory effect of H_2O_2 (400 mM) on the proliferation and migration of RKO cells. Combined treatment enhanced DNA damage, ATM, p-ATM and γ-H2AX elevation, G_2/M cell cycle arrest, apoptosis and autophagy and elevated ROS. ATM level was controlled by UA-upregulated mir18a-5p.		[56]
	human colorectal cancer cells Caco2 HCT116	UA 2.5, 5, 10, 20 μM tested	UA time- and dose-dependently reduced 14-3-3 proteins, which depended on proteasome and autophagy. It correlated with decreased p-cdc2 level and G_0/G_1 arrest. UA at 5 μM decreased invasion in cells expressing different isoforms of 14-3-3 as well as EMT markers, Snail, Twist, N-cadherin, β-catenin (at 10 μM). Among other downregulated proteins were cyclin D1, cyclin B1, p-mTOR, p-Akt, p-STAT3 and p-JNK. UA also reduced the activity of AP-1, STAT and NF-kB transcription factors, which were elevated by overexpression on 14-3-3 isoforms in HEK293T cells. UA inhibited glycolysis and mitochondrial respiration in CaCo2 and HCT116, which correlated with decreased expression of metabolic genes and drop in SLC2A1, HK2, PKM2 and LDHA proteins, even when these processes were elevated by the surplus of an isoform of 14-3-3.		[37]
Prostate	human prostate cancer cell lines PC-3 DU-145 normal prostate epithelial cells PNT2 Skin fibroblasts HSF	UA isolated from *Cladonia arbuscula* (Wallr.) EC_{50} = 2.67 μg/mL EC_{50} = 8.6 μg/mL EC_{50} = 18.2 μg/mL EC_{50} = 20.5 μg/mL (48 h, cell number)	UA inhibited the proliferation of both prostate cancer cells and induced apoptosis of PC-3 cells (cleavage PARP, caspase 7 and 9 elevations). UA induced actin cytoskeleton rearrangements in a dose-dependent manner in both cancer cell lines and reduced DU-145 cell motility.		[40]
Prostate	human prostate cancer cells DU-145	UA IC_{50} = 42.15 ± 3.76 μM (48 h, MTT)	UA decreased cell viability in a dose- and time-dependent manner, reduced MMP, elevated Bax:Bcl-2 mRNA, activated apoptosis and downregulated NF-κB p50.		[41]

Table 1. *Cont.*

Organ/Tissue	Cell Lines	Compound Concentrations Tested/IC_{50}	Effects In Vitro	Effects In Vivo	References
Ovaries	human ovarian adenocarcinoma cells A2780	(+)-UA IC_{50} = 75.9 ± 2 µM (72 h, MTT)	At 50 or 100 µM in a time-dependently (48 and 72 h) increased S phase cell cycle arrest, UA decreased MMP and induced apoptosis. It was preceded by RNS elevation (observed after 3 or 6 h post-treatment).		[26,27]
	human ovarian adenocarcinoma cells lines OVCAR-3 A2780 mouse fibroblasts L929	(+)-UA IC_{50} = 20 µM xCELLingence system and MTT	UA in a dose- and time-dependent manner reduced the viability of cancer cells while normal fibroblasts were more resistant (24 h). 20 µM UA induced G_0/G_1 cell cycle arrest and apoptosis, inhibited migration and invasion of OVCAR-3 cells. UA modulated transcriptome, particularly elevated expression of some genes connected with apoptosis (caspase 1 and 8, for instance).		[44]
Uterus	human cervical cancer cell lines HeLa SiHa CaSKi (and other types of cancer cells) normal human cervical epithelial cells HcerEpic human umbilical vascular endothelial cells HUVEC	UA 3, 10, 30 and 100 µM tested (24 h, MTT)	UA dose-dependently reduced PD-L1 levels in a panel of cancer cells, including HeLa. It inhibited PD-L1 protein synthesis and enhanced its degradation in HeLa cells, which correlated with its lower level at the cell surface and enhanced T-lymphocyte killing activity toward cervical cancer cells. It inhibited mTOR, which induced autophagy and autophagic degradation of PD-L1. UA inhibited Jak1/2-Src-STAT3 and Ras-MEK-ERK pathways leading to reduced PD-L1 expression, a drop in c-myc and cyclin D1 levels and reduced clonogenic potential. UA diminished the PD-L1-mediated angiogenic potential of HUVEC cells.		[36]
	human cervical cancer cells HeLa	UA isolated from *Usnea cornuta* IC_{50} = 48.65 µM (24 h, MTT)	UA at 25 and 50 µM increased ROS levels, lipid peroxidation, decreased MMP and GSH levels and increased caspase3/7 activity and cell death. UA induced protective autophagy—its inhibition by chloroquine increased UA cytotoxicity.		[52]
Uterus	endometrial cancer cells Ishikawa	UA IC_{50} = 51.76 µM (48 h, XTT)	UA inhibited cell proliferation and downregulated the expression of oncogenic lncRNA UCA1.		[48]
Blood	human acute myeloid leukemia cells HL-60 human chronic myelogenous leukemia cells K562	UA IC_{50} = 10.00 ± 1.03 µM IC_{50} = 10.39 ± 0.60 µM (3 days, cell number)	UA induced apoptosis in human leukemia cells with HL-60 cells being more responsive. It correlated with caspase 3, 9 and 8 activation, PARP cleavage and drop in Mcl-1. UA inhibited Mnk1/eIF4E and Pim1/4E-BP1 signaling, increased p27 and decreased cyclin D1, p-Bad, c-myc, Pim-1 levels. UA inhibited Pim-1 activity in vitro.		[39]

Table 1. *Cont.*

Organ/Tissue	Cell Lines	Compound Concentrations Tested/IC_{50}	Effects In Vitro	Effects In Vivo	References
Skin	human melanoma cells HBT-140 Skin fibroblasts HSF	UA isolated from *Cladonia arbuscula* (Wallr.) EC_{50} = 13.7 µg/mL EC_{50} = 19.3 µg/mL (72 h, cell number)	UA exerted weak cytostatic effects and apoptosis induction. At 10 and 25 µg/mL, it induced rearrangements of the actin cytoskeleton in a dose-dependent manner, 10 µg/mL UA inhibited cell motility.		[40]
Skin	human melanoma cell lines HTB140 A375 WM793 Murine macrophages RAW264.7	(+)-UA and (−)-UA IC_{50} = 14.7 and 20.6 µg/mL IC_{50} = 11.8 and 22.2 µg/mL IC_{50} = 30.1 and 52.1 µg/mL respectively (48 h, LDH)	Both enantiomers decreased the viability and proliferation of cells in a dose- and time-dependent manner, but their potency was enantiomers and cell-line specific. They inhibited cell migration (at 10 µg/mL) and acted synergistically with doxorubicin in A375 cells. They weakly decreased the release of pro-inflammatory TNF-a, IL-6 and NO and significantly reduced the synthesis of TLR4, cPLA2, COX-1 and COX-2 in LPS-stimulated macrophages (10 or 25 µg/mL concentrations tested).		[20]
Skin	squamous cell carcinoma A-431 normal human embryonic kidney cells HEK293T	UA IC50 = 98.9 ± 6 µM (48 h, MTT)	UA induced dose-dependent cytotoxicity (within the range 25–250 µM) in cancer but not in normal cells. It induced LDH release and PI accumulation by cancer cells. It correlated with ROS elevation, lipid peroxidation, changes in surface lipids and proteins, drop in GSH level and MMP. UA induced G_0/G_1 cell cycle arrest and apoptosis.		[34]

7. Combination Therapies Using UA

Increasing knowledge on mechanisms underlying the anticancer activity of UA is inclined toward combination therapies using UA and clinically approved drugs. Such combinations aim to enhance the anticancer effect and reduce the toxicity of a drug.

The synergistic effect was observed when UA (at 12.5 or 50 µM concentration) was combined with low concentrations of tamoxifen, the selective estrogen receptor modulator), or enzalutamide (a second-generation androgen receptor inhibitor) for treating hormone-dependent breast MCF-7 or prostate LNCaP cancer cells, respectively. UA potentiated cell cycle perturbations and apoptosis induced by drugs. These effects were also observed in non-cancerous cells, however, at different extents than in cancer cells. Mechanisms of synergistic activity were not explored [77]. The same team reported that the combination of UA with sorafenib, a drug used in systemic chemotherapy of hepatocellular carcinoma, acted synergistically toward HepG2 and SNU-449 cells. Sorafenib at lower concentrations was not toxic to normal cells but when combined with UA more effectively arrested the cell cycle and induced apoptosis than any compound used alone and at the same time was less toxic to the HUVEC cell line [78].

It has also been shown that 5 µM UA and an anti-EGFR antibody, cetuximab, more effectively inhibited the invasive potential of A549 lung cancer cells than any of the compounds alone [25]. UA at a concentration of 15 µM enhanced the activity of paclitaxel

at 0.1 μM toward H520 and Calu-1 lung cancer cells in vitro. Moreover, UA at a dose of 50 mg/kg (i.p.) reduced H520 xenograft tumor growth in vivo and potentiated the anticancer activity of paclitaxel (10 mg/kg) [50].

Another in vivo study investigated the efficacy of (+)-UA and bleomycin combination on hepatoma H22-bearing mice. Bleomycin is widely used to treat malignant ascites; however, it causes pulmonary fibrosis, which is connected with excessive inflammatory response and oxidative stress in lung tissue. UA (25, 50, 100 mg/kg, p.o.) combined with bleomycin (15 mg/kg, i.p.) revealed significantly better effectiveness than bleomycin alone in reducing ascites fluid, inhibiting ascites cell viability, arresting the cell cycle at G_0/G_1 phase and promoting apoptosis. It was associated with the transcriptional upregulation of p53/p21 and downregulation of cyclins E1 and D1. Moreover, UA reduced the side effects of bleomycin, including lung tissue damage. It was connected with a reduction in MDA, hydroxyproline (HYP), TNF-α, IL-1β, IL-6, TGF-β1 and p–Smad2/3 and an increase in SOD and Smad7 levels in lung tissues of H22-bearing mice treated with bleomycin [79].

More recently, the combination of (+)-UA or (−)-UA with doxorubicin was tested on HTB140, A375 and WM793 melanoma cells. The synergistic, additive or antagonistic effects were observed depending on the cell line, doses used and treatment time. Interestingly, UA (especially (−)-UA) sensitized to the drug WM793 cells, which are quite resistant to doxorubicin [20].

8. Bioavailability and Pharmacokinetics

The absorption, distribution, metabolism and excretion (ADME) are important factors in understanding the pharmacokinetics and potential toxicity of the new drug, and in the case of UA such data are limited. The available literature provides some insights into the dosage and administration of UA, particularly in the context of its pharmacokinetics and toxicity. For instance, studies conducted on rabbits indicate that plasma D(+)-UA levels following intravenous (5 mg/kg) administration showed a triexponential elimination with a mean terminal half-life of 10.7 ± 4.6 h. Following oral administration at a dose of 20 mg/kg the UA peak plasma concentration of 32.5 ± 6.8 g/mL was reached after 12.2 ± 3.8 h, and a mean terminal half-life was 18.9 ± 2.9 h. The mean absolute bioavailability of UA administrated orally was 77.8% [80].

Studies in rats administered intraperitoneally with 25 mg/kg of D(+)-UA have demonstrated that the molecule is distributed in different tissues, with a higher concentration found in lungs and liver, followed by blood (an average tissue-to-plasma concentration ratio was 1.777, 1.503 and 1.192, respectively). Moreover, approximately 99.2% of UA was bound to plasma proteins and showed albumin concentration-dependent binding (up to 6.5 g/L of albumin) [81], which was similar to results obtained by others showing that more than 99% of UA is bound in human or rat plasma [82].

UA metabolism has been studied in vitro using human plasma, hepatocytes and liver subcellular fractions. Three monohydroxylated metabolites and two glucuronide conjugates of UA were identified after incubation with human liver S9 fraction using liquid chromatography/mass spectrometry (LC/MS). Hepatic clearance of UA was estimated as 13.9 mL/min/kg and it was shown that UA is primarily metabolized by CYP1A2 while conjugation of UA with glycuronic acid depends on UGT1A1 and UGT1A3. Moreover, the study revealed that UA is a potent inhibitor of CYP2C19 and CYP2C9 and a less potent inhibitor of CYP2C8 and CYP2C19 [82].

The trapping assay with glutathione and UPLC-MS/MS analysis was used to elucidate reactive metabolites of UA in human, rat and mice liver microsomes. Authors found dehydrogenated and hydroxylated UA metabolic adducts with glutathione. These reactive adducts and/or depletion of GSH by UA might be related to UA hepatotoxicity. Interestingly, differences in metabolites were identified between human and rodent models and between (+) and (−)-UA enantiomers in human microsomes [83].

A more recent study investigated the metabolism of UA and its relationship to toxicity based on in vitro experiments using human liver microsomes, rat liver microsomes and

S9 fraction combined with UPLC-Q-TOF-MS for metabolite identification. The authors identified 14 phase I metabolites and 4 phase II metabolites of UA and found that the key UA metabolizing enzymes are CYP2C9, CYP3A4, CYP2C8 and UGT1A1. UA was not toxic to human primary hepatocytes when applied at 0.01–25 μM concentrations for 48 h; however, it was toxic to mouse 3T3 fibroblasts (IC_{50} = 7.4 μM). Using a model of coincubation of human liver microsomes with 3T3 cells, authors found that UA (1–50 μM) or its metabolites were not toxic to 3T3 cells, at least after a short 4 h exposition; thus, they concluded that UA cytotoxicity might be related to chronic exposure [84].

Data on in vivo toxicology are scarce. Acute toxicity has been only determined for mice and rabbits, and 50% lethal dose (LD_{50}) values in the case of oral applications were 838 mg/kg and > 500 mg/kg, respectively [85]. Intraperitoneal injections of UA suspension at a dose of 15 mg/kg/day for 15 days in male Swiss mice caused a hepatic dysfunction as revealed by a high level of serum transaminase and histological observation of necrotic areas in the livers.

Data in humans are limited to reports on cases of severe hepatotoxicity (hepatonecrosis, fulminant hepatic failure and other complications) after taking dietary supplements containing UA, such as Lipokinetix, a weight loss formula [86].

9. Perspectives for the Use of UA as an Anticancer Drug

As shown in previous paragraphs, UA is effective in targeting cancer hallmarks; however, data from in vitro and in vivo models indicate that rather high concentrations of UA have to be applied, which might be toxic to healthy cells, especially hepatocytes. Another problem with the use of UA is its low water solubility. Thus, extensive research efforts are aimed in at least two directions: to obtain knowledge on structure–activity correlations and receive UA derivatives with enhanced activity and better selectivity toward cancer cells and to improve UA bioavailability by enhancing its solubility in water or delivery into the cells [87].

Numerous modifications to the UA structure have been reported and screened for antiproliferative activity (rev. in [87]). Some UA derivatives reveal much better activity than the parent compound, and molecular mechanisms of their action, as well as toxicological and pharmacokinetic studies, are important for their further clinical development. For instance, our results with a pyrazole derivative of UA, referred to as compound 5, have demonstrated superior anticancer activity compared to the parent compound. This derivative has shown significant inhibitory effects on the growth and proliferation of pancreatic cancer cells both in vitro (IC_{50} = 0.90–1.35 μg/mL after 48 h treatment) and in animal models. The compound induced the release of calcium ions from the ER, leading to ER stress in cancer cells. It also causes G_0/G_1 cell cycle arrest and cell death. When tested in nude mice with xenografted pancreatic cancer cells, the UA derivative 5 successfully inhibited tumor growth without causing apparent toxicity to the kidneys or liver [88].

The hydrophilic potassium salt of UA (KU) shows more favorable characteristics than the parent compound, which was comprehensively presented in the review article by de Araujo et al. [89]. Results by Yang et al. clearly indicate that the bioavailability of KU, measured as the amounts in tumor, liver and plasma of CT26 syngeneic tumor xenograft-bearing mice after oral administration (30 mg/kg), was higher than that of UA. Moreover, KU was more potent than UA in the inhibition of invasiveness of the majority of colorectal cell lines in vitro, and at a dose of 20 mg/kg (i.p.), it significantly decreased liver metastasis in an orthotopic murine colorectal cancer model [62]. In the KU acute oral toxicity tests in Swiss Webster mice, LD_{50} was evaluated as >200 mg/kg indicating much lower toxicity than UA [90].

Another way to improve the therapeutic index of UA is to develop drug delivery systems. Data on UA encapsulated into lipid-based nanocarriers (liposomes, nanoemulsions), polymeric nanocarriers or microparticles (of different structures and compositions) and nonorganic nanoparticles (magnetic or diamond) are comprehensively presented and discussed in a recent review by Zugic et al. [91]. For instance, Farzan et. al. developed a novel

UA delivery system, where UA was encapsulated within nanoparticles of biodegradable gliadin (GNP) functionalized with hyaluronic acid (HA), which targets CD44 receptors overexpressed on breast cancer cells. This approach allowed for the targeted delivery of UA specifically to breast cancer cells, increasing efficacy and reducing side effects (UA IC_{50} = 120.04 μM, while UA-loaded nanoparticles HA-UA-GNPs IC_{50} = 0.56 μM and UA-GNPs IC_{50} = 92.64 μM). Tumor growth in mice treated with HA-UA-GNPs was significantly reduced compared with tumors in UA-GNPs or free UA-treated animals. The study demonstrated successful in vitro and translational research, bridging laboratory findings with potential clinical applications [76].

10. Overall Conclusions and Future Directions

Presented data indicate the versatility of UA in targeting different cancer hallmarks, including the inhibition of abnormal growth signals that drive uncontrolled cell division; induction of apoptosis or other cell death programs; disruption of cancer cell metabolism; inhibition of the new blood vessels formation which are crucial for the sustained growth of tumors; inhibition of migratory and invasive potential of cancer cells; the immunomodulatory potential in mobilizing body's immune response against malignant cells; and anti-inflammatory properties, which can be beneficial in addressing a tumor-promoting inflammatory microenvironment (Figure 1).

Although the promising antiproliferative potential of UA toward cancer cell lines is well documented, particularly in vitro (Table 1), further research is necessary to reveal the full potential of this compound. Firstly, not all researchers incorporate matched normal cell lines to assess cancer-specific effects. Moreover, the application of a panel of cancer cell lines from different tumor types, such as the NCI-60 Human Tumor Cell Lines Screen panel or cell lines from the Cancer Cell Line Encyclopedia (CCLE) should allow testing UA across diverse cancer types in a high-throughput way or for initial efficacy screening and biomarker discovery. Secondly, the efficacy of UA in vivo, or at least in conditions resembling complex in vivo environments is limited, thus more relevant models should be used. The simplest way to investigate cancer–noncancerous interaction simulating in vivo conditions is a coculture system where the response of cancer cells to a drug is recorded in the presence of additional components of ECM, for instance, fibroblasts or macrophages. Additionally, 3D spheroid cultures are more physiologically relevant models than 2D cultures, and organoids either patient-derived or based on organoid cell lines better recapitulate tumor heterogeneity and microenvironment. Finally, exploration of UA action should be based on animal models, including cell line-derived xenografts (CDX) in which well-characterized cancer cells are implanted in immunodeficient mice or patient-derived xenografts (PDX) where patient tumor fragments are implanted into immunodeficient mice. It is also possible to use genetically engineered mouse models that spontaneously develop tumors, particularly for studies on the chemopreventive activity of UA or its derivatives.

Overall, the multifaceted actions of UA underscore its potential as a promising therapeutic agent in the fight against various types of cancer, offering a range of mechanisms to disrupt cancer hallmarks and inhibit tumor progression. Further research is needed, not only on the mechanistic aspects of activity and toxicity of UA or UA derivatives and formulations but most of all on biopharmaceutical properties, efficacy and safety in vivo to reconcile the promising great potential of UA with the current lack of its therapeutic use in cancer patients.

Author Contributions: Conceptualization, M.G. and A.H.-A.; Methodology, M.G. and A.H.-A.; Writing—Original Draft Preparation, M.G. and A.H.-A.; Writing—Review and Editing, M.G. and A.H.-A.; Visualization, M.G. and A.H.-A.; Supervision, A.H.-A.; Project Administration, A.H.-A.; Funding Acquisition, A.H.-A. All authors have read and agreed to the published version of the manuscript.

Funding: This research was funded by the National Science Centre, Poland (project no. 2017/26/M/NZ7/00668).

Conflicts of Interest: The authors declare no conflicts of interest.

References

1. Hanahan, D.; Weinberg, R.A. The hallmarks of cancer. *Cell* **2000**, *100*, 57–70. [CrossRef] [PubMed]
2. Hanahan, D.; Weinberg, R.A. Hallmarks of cancer: The next generation. *Cell* **2011**, *144*, 646–674. [CrossRef]
3. Hanahan, D. Hallmarks of cancer: New dimensions. *Cancer Discov.* **2022**, *12*, 31–46. [CrossRef] [PubMed]
4. Fouad, J.A.; Aanei, C. Revisiting the hallmarks of cancer. *Am. J. Cancer Res.* **2017**, *7*, 1016–1036.
5. Blagosklonny, M.V. Hallmarks of cancer and hallmarks of aging. *Aging* **2022**, *14*, 4176–4187. [CrossRef] [PubMed]
6. Ravi, S.; Alencar, A.M., Jr.; Arakelyan, J.; Xu, W.; Stauber, R.; Wang, C.I.; Papyan, R.; Ghazaryan, N.; Pereira, R.M. An update to hallmarks of cancer. *Cureus* **2022**, *14*, e24803. [CrossRef]
7. Feitelson, M.A.; Arzumanyan, A.; Kulathinal, R.J.; Blain, S.W.; Holcombe, R.F.; Mahajna, J.; Marino, M.; Martinez-Chantar, M.L.; Nawroth, R.; Sanchez-Garcia, I.; et al. Sustained proliferation in cancer: Mechanisms and novel therapeutic targets. *Semin. Cancer Biol.* **2015**, *35*, S25–S54. [CrossRef]
8. Pickup, M.W.; Mouw, J.K.; Weaver, V.M. The extracellular matrix modulates the hallmarks of cancer. *EMBO Rep.* **2014**, *15*, 1243–1253. [CrossRef]
9. Liu, Z.L.; Chen, H.H.; Zheng, L.L.; Sun, L.P.; Shi, L. Angiogenic signaling pathways and anti-angiogenic therapy for cancer. *Signal Transduct. Target. Ther.* **2023**, *8*, 198. [CrossRef]
10. Yaswen, P.; MacKenzie, K.L.; Keith, W.N.; Hentosh, P.; Rodier, F.; Zhu, J.; Firestone, G.L.; Matheu, A.; Carnero, A.; Bilsland, A.; et al. Therapeutic targeting of replicative immortality. *Semin. Cancer Biol.* **2015**, *35*, S104–S128. [CrossRef]
11. Kim, S.K.; Cho, S.W. The evasion mechanisms of cancer immunity and drug intervention in the tumor microenvironment. *Front. Pharmacol.* **2022**, *13*, 868695. [CrossRef] [PubMed]
12. Al-Rawi, D.H.; Lettera, E.; Li, J.; DiBona, M.; Bakhoum, S.F. Targeting chromosomal instability in patients with cancer. *Nat. Rev. Clin. Oncol.* **2024**, *21*, 645–659. [CrossRef] [PubMed]
13. Wang, M.; Chen, S.; He, X.; Yuan, Y.; Wei, X. Targeting inflammation as cancer therapy. *J. Hematol. Oncol.* **2024**, *17*, 13. [CrossRef] [PubMed]
14. Newman, D.J.; Cragg, G.M. Natural products as sources of new drugs over the nearly four decades from 01/1981 to 09/2019. *J. Nat. Prod.* **2020**, *83*, 770–803. [CrossRef] [PubMed]
15. Li, J.; Gu, A.; Nong, X.M.; Zhai, S.; Yue, Z.Y.; Li, M.Y.; Liu, Y. Six-membered aromatic nitrogen heterocyclic anti-tumor agents: Synthesis and applications. *Chem. Rec.* **2023**, *23*, e202300293. [CrossRef]
16. Zhang, M.; Otsuki, K.; Li, W. Molecular networking as a natural products discovery strategy. *Acta Mater. Medica* **2023**, *2*, 126–141. [CrossRef]
17. Chunarkar-Patil, P.; Kaleem, M.; Mishra, R.; Ray, S.; Ahmad, A.; Verma, D.; Bhayye, S.; Dubey, R.; Singh, H.N.; Kumar, S. Anticancer drug discovery based on natural products: From computational approaches to clinical studies. *Biomedicines* **2024**, *12*, 201. [CrossRef]
18. Huneck, S.; Yoshimura, Y. *Identification of Lichen Substances*, 1st ed.; Springer: Berlin/Heidelberg, Germany, 1996.
19. Galanty, A.; Paśko, P.; Podolak, I. Enantioselective activity of usnic acid: A comprehensive review and future perspectives. *Phytochem. Rev.* **2019**, *18*, 527–548. [CrossRef]
20. Galanty, A.; Zagrodzki, P.; Gdula-Argasinska, J.; Grabowska, K.; Koczurkiewicz-Adamczyk, P.; Wrobel-Biedrawa, D.; Podolak, I.; Pekala, E.; Pasko, P. A Comparative survey of anti-melanoma and anti-inflammatory potential of usnic acid enantiomers-a comprehensive in vitro approach. *Pharmaceuticals* **2021**, *14*, 945. [CrossRef]
21. Guo, L.; Shi, Q.; Fang, J.L.; Mei, N.; Ali, A.A.; Lewis, S.M.; Leakey, J.E.; Frankos, V.H. Review of usnic acid and Usnea barbata toxicity. *J. Environ. Sci. Health. C Environ. Carcinog. Ecotoxicol. Rev.* **2008**, *26*, 317–338. [CrossRef]
22. Luzina, O.A.; Salakhutdinov, N.F. Usnic acid and its derivatives for pharmaceutical use: A patent review (2000–2017). *Expert Opin. Ther. Pat.* **2018**, *28*, 477–491. [CrossRef] [PubMed]
23. Wang, H.; Xuan, M.; Huang, C.; Wang, C. Advances in research on bioactivity, toxicity, metabolism, and pharmacokinetics of usnic acid in vitro and in vivo. *Molecules* **2022**, *27*, 7469. [CrossRef]
24. Kupchan, S.M.; Kopperman, H.L. l-usnic acid: Tumor inhibitor isolated from lichens. *Experientia* **1975**, *31*, 625. [CrossRef] [PubMed]
25. Yang, Y.; Nguyen, T.T.; Jeong, M.H.; Crisan, F.; Yu, Y.H.; Ha, H.H.; Choi, K.H.; Jeong, H.G.; Jeong, T.C.; Lee, K.Y.; et al. Inhibitory activity of (+)-usnic acid against non-small cell lung cancer cell motility. *PLoS ONE* **2016**, *11*, e0146575. [CrossRef] [PubMed]
26. Backorova, M.; Backor, M.; Mikes, J.; Jendzelovsky, R.; Fedorocko, P. Variable responses of different human cancer cells to the lichen compounds parietin, atranorin, usnic acid and gyrophoric acid. *Toxicol. In Vitro* **2011**, *25*, 37–44. [CrossRef]
27. Backorova, M.; Jendzelovsky, R.; Kello, M.; Backor, M.; Mikes, J.; Fedorocko, P. Lichen secondary metabolites are responsible for induction of apoptosis in HT-29 and A2780 human cancer cell lines. *Toxicol. In Vitro* **2012**, *26*, 462–468. [CrossRef]
28. O'Neill, M.A.; Mayer, M.; Murray, K.E.; Rolim-Santos, H.M.; Santos-Magalhaes, N.S.; Thompson, A.M.; Appleyard, V.C. Does usnic acid affect microtubules in human cancer cells? *Braz. J. Biol.* **2010**, *70*, 659–664. [CrossRef]
29. Chen, S.; Dobrovolsky, V.N.; Liu, F.; Wu, Y.; Zhang, Z.; Mei, N.; Guo, L. The role of autophagy in usnic acid-induced toxicity in hepatic cells. *Toxicol. Sci.* **2014**, *142*, 33–44. [CrossRef]
30. Yurdacan, B.; Egeli, U.; Eskiler, G.G.; Eryilmaz, I.E.; Cecener, G.; Tunca, B. The role of usnic acid-induced apoptosis and autophagy in hepatocellular carcinoma. *Hum. Exp. Toxicol.* **2019**, *38*, 201–215. [CrossRef]

31. Nguyen, T.T.; Yoon, S.; Yang, Y.; Lee, H.-B.; OH, S.; Jeong, M.-H.; Kim, J.-J.; Yee, S.-T.; Cris¸an, F.; Moon, C.; et al. Lichen secondary metabolites in Flavocetraria cucullata exhibit anti-cancer effects on human cancer cells through the induction of apoptosis and suppression of tumorigenic potentials. *PLoS ONE* **2014**, *9*, e111575. [CrossRef]
32. Ebrahim, H.Y.; Akl, M.R.; Elsayed, H.E.; Hill, R.A.; El Sayed, K.A. Usnic acid benzylidene analogues as potent mechanistic target of rapamycin inhibitors for the control of breast malignancies. *J. Nat. Prod.* **2017**, *80*, 932–952. [CrossRef] [PubMed]
33. Geng, X.; Zhang, X.; Zhou, B.; Zhang, C.; Tu, J.; Chen, X.; Wang, J.; Gao, H.; Qin, G.; Pan, W. Usnic acid induces cycle arrest, apoptosis, and autophagy in gastric cancer cells in vitro and in vivo. *Med. Sci. Monit.* **2018**, *24*, 556–566. [CrossRef] [PubMed]
34. Kumari, M.; Kamat, S.; Jayabaskaran, C. Usnic acid induced changes in biomolecules and their association with apoptosis in squamous carcinoma (A-431) cells: A flow cytometry, FTIR and DLS spectroscopic study. *Spectrochim. Acta A Mol. Biomol. Spectrosc.* **2022**, *274*, 121098. [CrossRef] [PubMed]
35. Singh, N.; Nambiar, D.; Kale, R.K.; Singh, R.P. Usnic acid inhibits growth and induces cell cycle arrest and apoptosis in human lung carcinoma A549 cells. *Nutr. Cancer* **2013**, *65* (Suppl. S1), 36–43. [CrossRef]
36. Sun, T.X.; Li, M.Y.; Zhang, Z.H.; Wang, J.Y.; Xing, Y.; Ri, M.; Jin, C.H.; Xu, G.H.; Piao, L.X.; Jin, H.L.; et al. Usnic acid suppresses cervical cancer cell proliferation by inhibiting PD-L1 expression and enhancing T-lymphocyte tumor-killing activity. *Phytother. Res.* **2021**, *35*, 3916–3935. [CrossRef]
37. Varli, M.; Bhosle, S.R.; Kim, E.; Yang, Y.; Tas, I.; Zhou, R.; Pulat, S.; Gamage, C.D.B.; Park, S.Y.; Ha, H.H.; et al. Usnic acid targets 14-3-3 proteins and suppresses cancer progression by blocking substrate interaction. *JACS Au* **2024**, *4*, 1521–1537. [CrossRef]
38. Yoo, K.H.; Kim, D.H.; Oh, S.; Park, M.S.; Kim, H.; Ha, H.H.; Cho, S.H.; Chung, I.J.; Bae, W.K. Transcriptome analysis upon potassium usnate exposure reveals ATF3-induced apoptosis in human gastric and colon cancer cells. *Phytomedicine* **2021**, *91*, 153655. [CrossRef]
39. Fan, Y.-B.; Huang, M.; Cao, Y.; Gong, P.; Liu, W.-B.; Jin, S.-Y.; Wen, J.-C.; Jing, Y.-K.; Liu, D.; Zhao, L.-X. Usnic acid is a novel Pim-1 inhibitor with the abilities of inhibiting growth and inducing apoptosis in human myeloid leukemia cells. *RSC Adv.* **2016**, *6*, 24091–24096. [CrossRef]
40. Galanty, A.; Koczurkiewicz, P.; Wnuk, D.; Paw, M.; Karnas, E.; Podolak, I.; Wegrzyn, M.; Borusiewicz, M.; Madeja, Z.; Czyz, J.; et al. Usnic acid and atranorin exert selective cytostatic and anti-invasive effects on human prostate and melanoma cancer cells. *Toxicol. In Vitro* **2017**, *40*, 161–169. [CrossRef]
41. Erdoğan, Ö.; Abas, B.I.; Çevik, Ö. Usnic acid exerts antiproliferative and apoptotic effects by suppressing NF-κB p50 in DU145 cells. *Eur. J. Biol.* **2023**, *82*, 251–257.
42. Eryilmaz, I.E.; Guney Eskiler, G.; Egeli, U.; Yurdacan, B.; Cecener, G.; Tunca, B. In vitro cytotoxic and antiproliferative effects of usnic acid on hormone-dependent breast and prostate cancer cells. *J. Biochem. Mol. Toxicol.* **2018**, *32*, e22208. [CrossRef] [PubMed]
43. Einarsdottir, E.; Groeneweg, J.; Bjornsdottir, G.G.; Harethardottir, G.; Omarsdottir, S.; Ingolfsdottir, K.; Ogmundsdottir, H.M. Cellular mechanisms of the anticancer effects of the lichen compound usnic acid. *Planta Med.* **2010**, *76*, 969–974. [CrossRef] [PubMed]
44. Çolak, B.; Cansaran-Duman, D.; Guney Eskiler, G.; Földes, K.; Yangın, S. Usnic acid-induced programmed cell death in ovarian cancer cells. *Rendiconti Lincei Sci. Fis. Nat.* **2022**, *33*, 143–152. [CrossRef]
45. Ozben, R.S.; Cansaran-Duman, D. The expression profiles of apoptosis-related genes induced usnic acid in SK-BR-3 breast cancer cell. *Hum. Exp. Toxicol.* **2020**, *39*, 1497–1506. [CrossRef] [PubMed]
46. Kilic, N.; Islakoglu, Y.O.; Buyuk, I.; Gur-Dedeoglu, B.; Cansaran-Duman, D. Determination of usnic acid responsive miRNAs in breast cancer cell lines. *Anticancer Agents Med. Chem.* **2019**, *19*, 1463–1472. [CrossRef]
47. Degerli, E.; Torun, V.; Cansaran-Duman, D. miR-185-5p response to usnic acid suppresses proliferation and regulating apoptosis in breast cancer cell by targeting Bcl2. *Biol. Res.* **2020**, *53*, 19. [CrossRef]
48. Seçme, M.; Dodurga, Y. Usnic acid inhibits cell proliferation and downregulates lncRNA UCA1 expression in Ishikawa endometrial cancer cells. *Nat. Prod. Biotech.* **2021**, *1*, 28–37.
49. Zuo, S.-T.; Wang, L.-P.; Zhang, Y.; Zhao, D.-N.; Li, Q.-S.; Shao, D.; Fang, X.-D. Usnic acid induces apoptosis via an ROS-dependent mitochondrial pathway in human breast cancer cells in vitro and in vivo. *RSC Adv.* **2015**, *5*, 153–162. [CrossRef]
50. Qi, W.; Lu, C.; Huang, H.; Zhang, W.; Song, S.; Liu, B. (+)-Usnic acid induces ROS-dependent apoptosis via inhibition of mitochondria respiratory chain complexes and Nrf2 expression in lung squamous cell carcinoma. *Int. J. Mol. Sci.* **2020**, *21*, 876. [CrossRef]
51. Studzinska-Sroka, E.; Majchrzak-Celinska, A.; Zalewski, P.; Szwajgier, D.; Baranowska-Wojcik, E.; Kapron, B.; Plech, T.; Zarowski, M.; Cielecka-Piontek, J. Lichen-derived compounds and extracts as biologically active substances with anticancer and neuroprotective properties. *Pharmaceuticals* **2021**, *14*, 1293. [CrossRef]
52. Kumari, M.; Kamat, S.; Singh, S.K.; Kumar, A.; Jayabaskaran, C. Inhibition of autophagy increases cell death in HeLa cells through usnic acid isolated from lichens. *Plants* **2023**, *12*, 519. [CrossRef] [PubMed]
53. Mayer, M.; O'Neill, M.A.; Murray, K.E.; Santos-Magalhaes, N.S.; Carneiro-Leao, A.M.; Thompson, A.M.; Appleyard, V.C. Usnic acid: A non-genotoxic compound with anti-cancer properties. *Anticancer Drugs* **2005**, *16*, 805–809. [CrossRef] [PubMed]
54. Emsen, B.; Aslan, A.; Turkez, H.; Joughi, A.; Kaya, A. The anti-cancer efficacies of diffractaic, lobaric, and usnic acid: In vitro inhibition of glioma. *J. Cancer Res. Ther.* **2018**, *14*, 941–951. [CrossRef] [PubMed]

55. Kumar, K.; Mishra, J.P.N.; Singh, R.P. Usnic acid induces apoptosis in human gastric cancer cells through ROS generation and DNA damage and causes up-regulation of DNA-PKcs and gamma-H2A.X phosphorylation. *Chem. Biol. Interact.* **2020**, *315*, 108898. [CrossRef]
56. Wu, W.; Gou, H.; Dong, J.; Yang, X.; Zhao, Y.; Peng, H.; Chen, D.; Geng, R.; Chen, L.; Liu, J. Usnic acid inhibits proliferation and migration through ATM mediated DNA damage response in RKO colorectal cancer cell. *Curr. Pharm. Biotechnol.* **2021**, *22*, 1129–1138. [CrossRef]
57. Prokopiev, I.; Filippova, G.; Filippov, E.; Voronov, I.; Sleptsov, I.; Zhanataev, A. Genotoxicity of (+)- and (-)-usnic acid in mice. *Mutat. Res. Genet. Toxicol. Environ. Mutagen.* **2019**, *839*, 36–39. [CrossRef]
58. Azhamuthu, T.; Kathiresan, S.; Senkuttuvan, I.; Asath, N.A.A.; Ravichandran, P.; Vasu, R. Usnic acid alleviates inflammatory responses and induces apoptotic signaling through inhibiting NF-kB expressions in human oral carcinoma cells. *Cell Biochem. Funct.* **2024**, *42*, e4074. [CrossRef]
59. Zakharenko, A.; Sokolov, D.; Luzina, O.; Sukhanova, M.; Khodyreva, S.; Zakharova, O.; Salakhutdinov, N.; Lavrik, O. Influence of usnic acid and its derivatives on the activity of mammalian poly(ADP-ribose)polymerase 1 and DNA polymerase beta. *Med. Chem.* **2012**, *8*, 883–893. [CrossRef]
60. Song, Y.; Dai, F.; Zhai, D.; Dong, Y.; Zhang, J.; Lu, B.; Luo, J.; Liu, M.; Yi, Z. Usnic acid inhibits breast tumor angiogenesis and growth by suppressing VEGFR2-mediated AKT and ERK1/2 signaling pathways. *Angiogenesis* **2012**, *15*, 421–432. [CrossRef]
61. Koparal, A.T. Anti-angiogenic and antiproliferative properties of the lichen substances (-)-usnic acid and vulpinic acid. *Z. Naturforsch. C J. Biosci.* **2015**, *70*, 159–164. [CrossRef]
62. Yang, Y.; Bae, W.K.; Lee, J.Y.; Choi, Y.J.; Lee, K.H.; Park, M.S.; Yu, Y.H.; Park, S.Y.; Zhou, R.; Tas, I.; et al. Potassium usnate, a water-soluble usnic acid salt, shows enhanced bioavailability and inhibits invasion and metastasis in colorectal cancer. *Sci. Rep.* **2018**, *8*, 16234. [CrossRef] [PubMed]
63. Wu, W.; Hou, B.; Tang, C.; Liu, F.; Yang, J.; Pan, T.; Si, K.; Lu, D.; Wang, X.; Wang, J.; et al. (+)-Usnic acid inhibits migration of c-KIT positive cells in human colorectal cancer. *Evid. Based Complement. Alternat. Med.* **2018**, *2018*, 5149436. [CrossRef] [PubMed]
64. Zhai, L.; Ladomersky, E.; Lenzen, A.; Nguyen, B.; Patel, R.; Lauing, K.L.; Wu, M.; Wainwright, D.A. IDO1 in cancer: A Gemini of immune checkpoints. *Cell. Mol. Immunol.* **2018**, *15*, 447–457. [CrossRef] [PubMed]
65. Meireson, A.; Devos, M.; Brochez, L. IDO expression in cancer: Different compartment, different functionality? *Front. Immunol.* **2020**, *11*, 531491. [CrossRef] [PubMed]
66. Pazdziora, W.; Podolak, I.; Grudzinska, M.; Pasko, P.; Grabowska, K.; Galanty, A. Critical assessment of the anti-Inflammatory potential of usnic acid and its derivatives—A review. *Life* **2023**, *13*, 1046. [CrossRef]
67. Donelan, W.; Dominguez-Gutierrez, P.R.; Kusmartsev, S. Deregulated hyaluronan metabolism in the tumor microenvironment drives cancer inflammation and tumor-associated immune suppression. *Front. Immunol.* **2022**, *13*, 971278. [CrossRef]
68. Yildirim, M.; Degirmenci, U.; Akkapulu, M.; Gungor, M.; Oztornacı, R.O.; Berkoz, M.; Comelekoglu, U.; Yalın, A.E.; Yalın, S. Anti-inflammatory effects of usnic acid in breast cancer. *Russ. J. Bioorg. Chem.* **2022**, *48*, S110–S114. [CrossRef]
69. Azhamuthu, T.; Kathiresan, S.; Senkuttuvan, I.; Abulkalam Asath, N.A.; Ravichandran, P. Usnic acid attenuates 7,12-dimethylbenz[a] anthracene (DMBA) induced oral carcinogenesis through inhibiting oxidative stress, inflammation, and cell proliferation in male golden Syrian hamster model. *J. Biochem. Mol. Toxicol.* **2024**, *38*, e23553. [CrossRef]
70. Kwong, S.P.; Wang, C. Review: Usnic acid-induced hepatotoxicity and cell death. *Environ. Toxicol. Pharmacol.* **2020**, *80*, 103493. [CrossRef]
71. Croce, N.; Pitaro, M.; Gallo, V.; Antonini, G. Toxicity of usnic acid: A narrative review. *J. Toxicol.* **2022**, *2022*, 8244340. [CrossRef]
72. Antonenko, Y.N.; Khailova, L.S.; Rokitskaya, T.I.; Nosikova, E.S.; Nazarov, P.A.; Luzina, O.A.; Salakhutdinov, N.F.; Kotova, E.A. Mechanism of action of an old antibiotic revisited: Role of calcium ions in protonophoric activity of usnic acid. *Biochim. Biophys. Acta Bioenerg.* **2019**, *1860*, 310–316. [CrossRef] [PubMed]
73. Fujimoto, K.; Kishino, H.; Hashimoto, K.; Watanabe, K.; Yamoto, T.; Mori, K. Biochemical profiles of rat primary cultured hepatocytes following treatment with rotenone, FCCP, or (+)-usnic acid. *J. Toxicol. Sci.* **2020**, *45*, 339–347. [CrossRef] [PubMed]
74. Chelombitko, M.A.; Firsov, A.M.; Kotova, E.A.; Rokitskaya, T.I.; Khailova, L.S.; Popova, L.B.; Chernyak, B.V.; Antonenko, Y.N. Usnic acid as calcium ionophore and mast cells stimulator. *Biochim. Biophys. Acta Biomembr.* **2020**, *1862*, 183303. [CrossRef] [PubMed]
75. Bessadottir, M.; Egilsson, M.; Einarsdottir, E.; Magnusdottir, I.H.; Ogmundsdottir, M.H.; Omarsdottir, S.; Ogmundsdottir, H.M. Proton-shuttling lichen compound usnic acid affects mitochondrial and lysosomal function in cancer cells. *PLoS ONE* **2012**, *7*, e51296. [CrossRef]
76. Farzan, M.; Varshosaz, J.; Mirian, M.; Minaiyan, M.; Pezeshki, A. Hyaluronic acid-conjugated gliadin nanoparticles for targeted delivery of usnic acid in breast cancer: An in vitro/in vivo translational study. *J. Drug Deliv. Sci. Technol.* **2023**, *84*, 104459. [CrossRef]
77. Eskiler, G.G.; Eryilmaz, I.E.; Yurdacan, B.; Egeli, U.; Cecener, G.; Tunca, B. Synergistic effects of hormone therapy drugs and usnic acid on hormone receptor-positive breast and prostate cancer cells. *J. Biochem. Mol. Toxicol.* **2019**, *33*, e22338. [CrossRef]
78. Yurdacan, B.; Egeli, U.; Guney Eskiler, G.; Eryilmaz, I.E.; Cecener, G.; Tunca, B. Investigation of new treatment option for hepatocellular carcinoma: A combination of sorafenib with usnic acid. *J Pharm. Pharmacol.* **2019**, *71*, 1119–1132. [CrossRef]

79. Su, Z.Q.; Liu, Y.H.; Guo, H.Z.; Sun, C.Y.; Xie, J.H.; Li, Y.C.; Chen, J.N.; Lai, X.P.; Su, Z.R.; Chen, H.M. Effect-enhancing and toxicity-reducing activity of usnic acid in ascitic tumor-bearing mice treated with bleomycin. *Int. Immunopharmacol.* **2017**, *46*, 146–155. [CrossRef]
80. Krishna, D.R.; Venkataramana, D. Pharmacokinetics of D(+)-usnic acid in rabbits after intravenous and oral administration. *Drug Metab. Dispos.* **1992**, *20*, 909–911.
81. Krishna, D.R.; Ramana, D.V.; Mamidi, N.V. In vitro protein binding and tissue distribution of D(+) usnic acid. *Drug Metabol. Drug Interact.* **1995**, *12*, 53–63. [CrossRef]
82. Foti, R.S.; Dickmann, L.J.; Davis, J.A.; Greene, R.J.; Hill, J.J.; Howard, M.L.; Pearson, J.T.; Rock, D.A.; Tay, J.C.; Wahlstrom, J.L.; et al. Metabolism and related human risk factors for hepatic damage by usnic acid containing nutritional supplements. *Xenobiotica* **2008**, *38*, 264–280. [CrossRef] [PubMed]
83. Piska, K.; Galanty, A.; Koczurkiewicz, P.; Zmudzki, P.; Potaczek, J.; Podolak, I.; Pekala, E. Usnic acid reactive metabolites formation in human, rat, and mice microsomes. Implication for hepatotoxicity. *Food Chem. Toxicol.* **2018**, *120*, 112–118. [CrossRef] [PubMed]
84. Wang, H.; Xuan, M.; Diao, J.; Xu, N.; Li, M.; Huang, C.; Wang, C. Metabolism and toxicity of usnic acid and barbatic acid based on microsomes, S9 fraction, and 3T3 fibroblasts in vitro combined with a UPLC-Q-TOF-MS method. *Front. Pharmacol.* **2023**, *14*, 1207928. [CrossRef] [PubMed]
85. Francos, V. NTP Nomiation for Usnic Acid and Usnea Barbata Herb. Available online: https://ntp.niehs.nih.gov/ntp/htdocs/st_rpts/tox105_508.pdf (accessed on 21 August 2024).
86. Sanchez, W.; Maple, J.T.; Burgart, L.J.; Kamath, P.S. Severe hepatotoxicity associated with use of a dietary supplement containing usnic acid. *Mayo Clin. Proc.* **2006**, *81*, 541–544. [CrossRef] [PubMed]
87. Guzow-Krzemińska, B.; Guzow, K.; Herman-Antosiewicz, A. Usnic acid derivatives as cytotoxic agents against cancer cells and the mechanisms of their activity. *Curr. Pharm. Rep.* **2019**, *5*, 429–439. [CrossRef]
88. Gimla, M.; Pyrczak-Felczykowska, A.; Malinowska, M.; Hac, A.; Narajczyk, M.; Bylinska, I.; Reekie, T.A.; Herman-Antosiewicz, A. The pyrazole derivative of usnic acid inhibits the proliferation of pancreatic cancer cells in vitro and in vivo. *Cancer Cell Int.* **2023**, *23*, 210. [CrossRef]
89. Araujo, H.D.A.; Silva, H.; Silva Junior, J.G.D.; Albuquerque, M.; Coelho, L.; Aires, A.L. The natural compound hydrophobic usnic acid and hydrophilic potassium usnate derivative: Applications and comparisons. *Molecules* **2021**, *26*, 5995. [CrossRef]
90. Araújo, H.D.A.; Silva Júnior, J.G.; Saturnino Oliveira, J.R.; Ribeiro, H.M.L.; Barroso Martins, M.C.; Cavalcanti Bezerra, M.A.; Lima Aires, A.; Azevedo Albuquerque, C.P.; Melo-Júnior, M.R.; Pontes Filho, N.T.; et al. Usnic acid potassium salt: Evaluation of the acute Toxicity and antinociceptive effect in murine model. *Molecules* **2019**, *24*, 2042. [CrossRef]
91. Zugic, A.; Tadic, V.; Savic, S. Nano- and microcarriers as drug delivery systems for usnic acid: Review of literature. *Pharmaceutics* **2020**, *12*, 156. [CrossRef]

12.1.1. Oświadczenia autorów

Gdańsk, 06.03.2025 r.

mgr Mariola Gimła
Katedra Biologii i Genetyki Medycznej
Wydział Biologii
Uniwersytet Gdański

Oświadczenie o wkładzie w publikację

Oświadczam, że mój wkład w publikacje:

Gimła, M.; Herman-Antosiewicz, A. Multifaceted Properties of Usnic Acid in Disrupting Cancer Hallmarks. Biomedicines 2024, 12, 2199. https://doi.org/10.3390/biomedicines12102199. PMID: 39457512

Polegał na:

- Zaplanowaniu koncepcji pracy przegladowej
- Napisaniu wstępnej wersji pracy przegladowej
- Przygotowaniu grafik
- Przeglądzie literatury
- Poprawieniu ostatecznej wersji manuskryptu
- Udziale w dyskusji z recenzentami

Mariola Gimła

Gdańsk, 06.03.2025 r.

prof. dr hab. Anna Herman-Antosiewicz
Katedra Biologii i Genetyki Medycznej
Wydział Biologii
Uniwersytet Gdański

Oświadczenie o wkładzie w publikację

Oświadczam, że mój wkład w publikację:

Gimła, M.; Herman-Antosiewicz, A. Multifaceted Properties of Usnic Acid in Disrupting Cancer Hallmarks. Biomedicines 12, 2199 (2024). https://doi.org/10.3390/biomedicines12102199. PMID: 39457512

polegał na:

- zaplanowaniu koncepcji pracy przegladowej
- udziale w napisaniu wstępnej wersji pracy
- korekcie grafik
- poprawieniu ostatecznej wersji manuskryptu
- przeglądzie literatury
- udziale w dyskusji z recenzentami
- opiece merytorycznej nad mgr Mariolą Gimłą
- kierowaniu projektem Harmonia

Wydział Biologii
KATEDRA BIOLOGII I GENETYKI MEDYCZNEJ
Anna Herman-Antosiewicz
prof. dr hab. Anna Herman-Antosiewicz

12.2. Publikacja nr 2

Gimła Mariola, Pyrczak-Felczykowska Agnieszka, Malinowska Marcelina, Hać Aleksandra, Narajczyk Magdalena, Bylińska Irena, Reekie Tristan, Herman-Antosiewicz Anna

The pyrazole derivative of usnic acid inhibits the proliferation of pancreatic cancer cells in vitro and in vivo

Cancer Cell International, 210:10.1186

(2023)

Impact Factor = 5.3 (2023)

Punktacja MNiSW = 100

Cancer Cell International

RESEARCH

Open Access

The pyrazole derivative of usnic acid inhibits the proliferation of pancreatic cancer cells in vitro and in vivo

Mariola Gimła[1], Agnieszka Pyrczak-Felczykowska[2], Marcelina Malinowska[1], Aleksandra Hać[1], Magdalena Narajczyk[3], Irena Bylińska[4], Tristan A. Reekie[5] and Anna Herman-Antosiewicz[1*]

Abstract

Background Pancreatic cancer is one of the leading causes of cancer death in Western societies. Its late diagnosis and resistance to chemotherapies result in a high mortality rate; thus, the development of more effective therapies for the treatment of pancreatic cancer is strongly warranted. Usnic acid (UA) is a secondary metabolite of lichens that shows modest antiproliferative activity toward cancer cells. Recently, we reported the synthesis of a UA pyrazole derivative, named **5**, which was more active than the parent compound toward cervical cancer cells. Here, its anticancer potential has been evaluated in detail in other cancer cells, particularly pancreatic cancer cells.

Methods The impact of UA and derivative **5** on cell viability, morphology, cell cycle, and death was assessed using the MTT test, electron microscopy, flow cytometry, and immunoblotting, respectively. The calcium ions level was detected fluorometrically. In vivo, the anticancer activity of **5** was evaluated in a murine xenograft model.

Results Derivative **5** inhibited the viability of different cancer cells. Noncancerous cells were less sensitive. It induced the release of calcium ions from the endoplasmic reticulum (ER) and ER stress, which was manifested by cell vacuolization. It was accompanied by G0/G1 cell cycle arrest and cell death of pancreatic cancer cells. When applied to nude mice with xenografted pancreatic cancer cells, **5** inhibited tumor growth, with no signs of kidney or liver toxicity.

Conclusions UA derivative **5** is superior to UA inhibiting the growth and proliferation of pancreatic cancer cells. ER stress exaggeration is a mechanism underlying the activity of derivative **5**.

Keywords Cancer, Usnic acid, Endoplasmic reticulum stress, Cell death, Lichens, Vacuolization

Introduction

Pancreatic cancer is the seventh leading cause of cancer deaths in both sexes. In 2020, it accounted for almost as many deaths (446.000) as cases (496.000). Incidence and mortality rates are fourfold and fivefold higher in highly developed countries, and the highest incidence rates are detected in Europe, North America, Australia and New Zealand [1]. Survival rates for pancreatic cancer remain low, despite improvements in overall 5-year survival from < 5% in the 1990s to 9% in the USA and Europe in 2019. Low survival rates are, in part, due to the advanced stage at diagnosis in most cases, with only ~ 20% of

*Correspondence:
Anna Herman-Antosiewicz
anna.herman-antosiewicz@ug.edu.pl
[1] Department of Medical Biology and Genetics, Faculty of Biology, University of Gdańsk, Wita Stwosza 59, 80-308 Gdańsk, Poland
[2] Department of Physiology, Medical University of Gdańsk, 80-211 Gdańsk, Poland
[3] Electron Microscopy Section, Faculty of Biology, University of Gdańsk, 80-308 Gdańsk, Poland
[4] Department of Biomedical Chemistry, Faculty of Chemistry, University of Gdańsk, 80-308 Gdańsk, Poland
[5] School of Science, University of New South Wales Canberra, Australian Capital Territory, Canberra 2600, Australia

patients with early-stage, surgically resectable disease [2]. The majority of cancers in the pancreas (> 90%) are pancreatic ductal adenocarcinomas [3].

Therapies used to treat pancreatic cancer (surgery, radiotherapy and conventional chemotherapies) have only modest effects on survival length. For example, only 5.4% of patients are sensitive to gemcitabine, a first-line chemotherapy agent. Thus, effective novel therapies are urgently needed to treat this disease.

Usnic acid ($C_{18}H_{16}O_7$) [2,6-diacetyl-7,9-dihydroxy-8,9b-dimethyldibenzofuran-1,3(2*H*,9b*H*)-dione; UA] is a secondary metabolite found in lichens and has been shown to possess a broad spectrum of biological activities, including antiproliferative, anti-metastatic and anti-angiogenic activities, that might protect against cancer development or progression (reviewed in [4–8]). UA has been shown to display cytotoxicity against a wide panel of murine and human cancer cells in vitro, albeit at rather high concentrations (reviewed in [6]). For instance, the IC_{50} of (+)-UA in lung squamous cell carcinoma (H520 and Calu-1) was 32–34 µM after 48 h of treatment [9], in colon (HCT116 and HT-29) and ovarian cancer cells (A2780) after 72 h of treatment was 100–157 µM and 76 µM, respectively [10], and the IC_{50} of (-)-UA in glioblastoma cells (T89G and A-172) was 38 µM (13 µg/mL) or 91 µM (31.5 µg/mL) after 48 h of treatment [11]. More recently, UA activity against gastric cancer cells was evaluated, and IC_{50} values after 24 h of treatment were calculated as approximately 237 µM for BGC823 cells and 619 µM for SGC7901 cells [12].

Importantly, quite controversial results related to UA safety have been reported. When used as a supplement to induce human weight loss, UA revealed unwanted hepatotoxic effects. Depending on the supplement used, the daily intake of UA could reach 300—1350 mg and was used from a few weeks to 3 months [13, 14]. In primary cultured murine hepatocytes, 5 µM UA induced necrosis in 98% of cells within 16 h, and it was associated with inhibition and uncoupling of the electron transport chain in mitochondria, leading to a reduction in ATP levels in hepatocytes [15]. Intraperitoneal injections of UA suspension at a dose of 15 mg/kg/day for 15 days in male Swiss mice caused hepatic dysfunction, as revealed by a high level of serum transaminase and histological observation of necrotic areas in livers [16]. Therefore, research efforts concentrate on the modification of the UA structure to obtain derivatives with higher potency against cancer cells and lower side effects toward healthy cells.

Recently, we reported the synthesis of UA derivatives that are more cytotoxic toward cancer cells than the parent compound [17, 18]. Moreover, the isoxazole derivative of UA induced massive vacuolization of MCF-7 breast cancer cells, which resulted from endoplasmic reticulum (ER) stress and led to paraptosis-like cell death [18, 19].

In this study, we tested a new pyrazole UA derivative, named **5** ((*R*)-8-acetyl-5,7-dihydroxy-3,4a,6-trimethyl-1,4a-dihydro-4*H*-benzofuro[3,2-*f*]indazol-4-one), that is superior to recently described **2** and **3a** toward HeLa cancer cells (the IC_{50} values determined after 24 h of treatment were approximately four- and ninefold lower, respectively) [17]. We show that similar to isoxazole derivative **2**, pyrazole derivative **5** induced ER stress in breast MCF-7 cells and also in pancreatic cancer cells. As pancreatic cells exhibit high secretory functions and therefore are characterized by highly developed ER, exacerbation of ER stress has been proposed as a promising target for pancreatic cancer therapy [20, 21]. Thus, we further concentrated on the activity of compound **5** toward pancreatic cancer cells in in vitro and in vivo models.

Materials and methods

Reagents used in the study

Procedures for the synthesis of UA pyrazole derivative **5** have been described in [17]. Fetal bovine serum, DMEM, penicillin/streptomycin antibiotic mixture and Matrigel were purchased from Corning (USA). (+)-UA, DMSO, and thiazolyl blue tetrazolium bromide (MTT) were purchased from Sigma–Aldrich (St. Louis, MO, USA).

Antibodies against GRP78/BiP, and anti-rabbit, anti-mouse, and anti-β-actin antibodies conjugated with horseradish peroxidase were purchased from Sigma–Aldrich. Antibodies against IRE1α and GADD153/CHOP were from Santa Cruz Biotechnology (Santa Cruz, CA, USA), and an antibody against PARP was purchased from Cell Signaling Technology (Danvers, MA, USA). The inhibitors: 2-aminoethoxydiphenylborane (2-APB); 1,2-bis(2-aminophenoxy)ethane-*N*,*N*,*N*′,*N*′-tetraacetic acid (BAPTA) were purchased from Sigma–Aldrich.

Cell culture conditions

The human breast adenocarcinoma cell line MCF-7 was obtained from CLS Cell Lines Service GmbH (Eppelheim, Germany), human dermal fibroblasts HDFa were obtained from Thermo Fisher Scientific (Product

(See figure on next page.)

Fig. 1. 5, but not UA, decreases the viability of cancer cells, and noncancerous cells are less sensitive. **A** Chemical structures of compound **5** and UA. **B**-**E** Viability of MCF-7, PANC-1, Mia PACa-2 (cancer cells) and HDFa (noncancerous cells). Viability was measured using an MTT test after 24 or 48 h of treatment with **5** or UA at the indicated concentrations. Statistical significance between control and **5**-treated cells was determined by ANOVA followed by Dunnett's post hoc test: a—$P < 0.0001$, b—$P < 0.001$, c—$P < 0.05$. Experiments were performed 3–6 times in triplicate

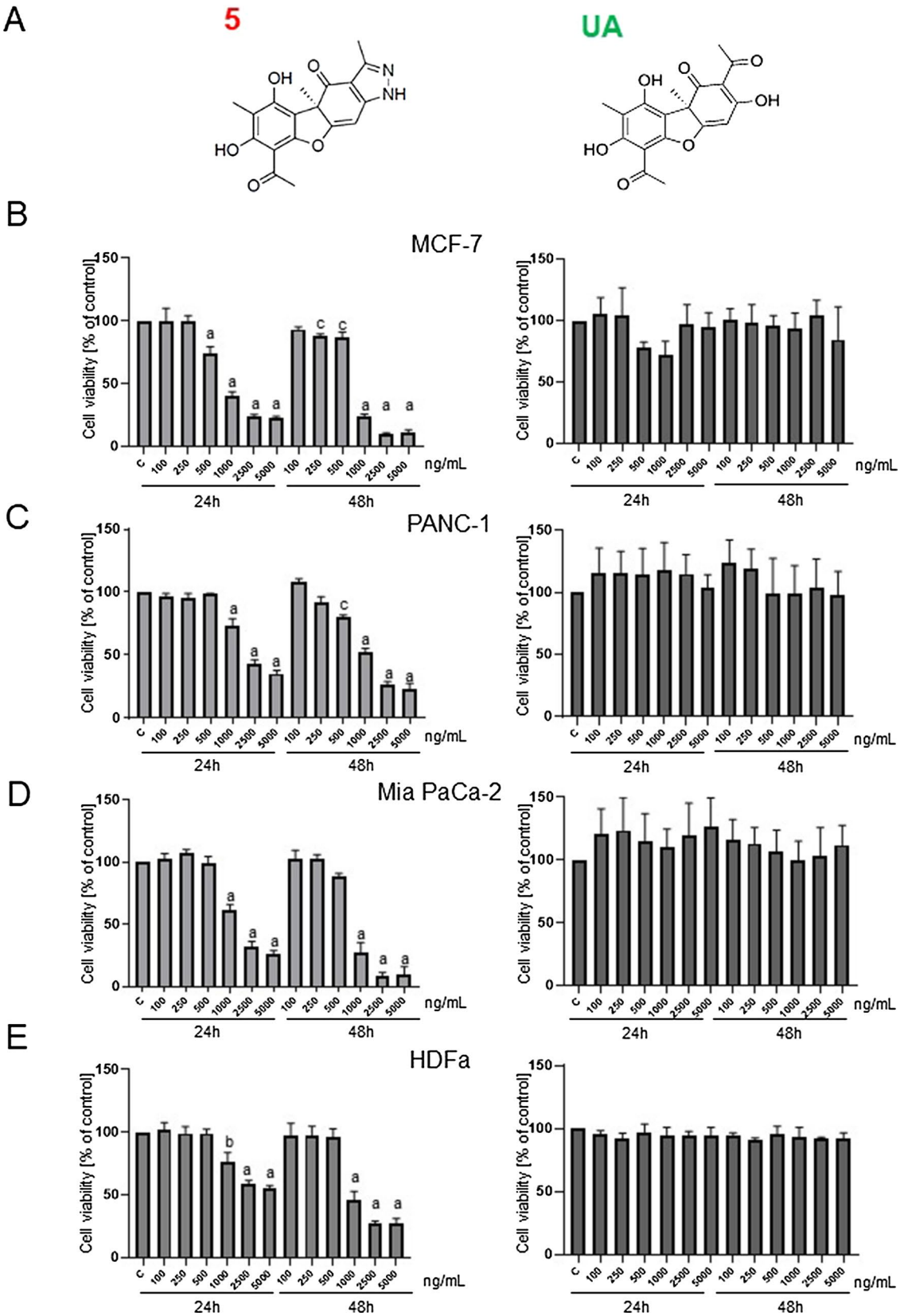

Fig. 1 (See legend on previous page.)

Table 1 Sensitivity ($IC_{50,}$ μg/mL) of different cancer and noncancerous cell lines to usnic acid derivative **5** after 24 or 48 h of drug treatment

Origin	Cell line	IC_{50} (24 h)	IC_{50} (48 h)
breast	MCF-7	1.10	0.82
cervix	HeLa	0.66	0.29
lung	A549	0.71	0.46
liver	HepG2	0.80	0.36
colon	HCT15	2.09	1.38
pancreas	PANC-1	2.71	1.35
pancreas	Mia PaCa-2	1.96	0.90
skin fibroblasts	HDFa	4.78	1.68

Each value is the mean of at least three experiments

Line Cascade Biologics™), and the human pancreatic cancer cell lines MIA PaCa-2 and PANC-1, were provided by Dr. I. Inkielewicz-Stępniak from the Medical University of Gdansk, Poland. All cell lines were tested for mycoplasma contamination before their use.

Monolayer cultures of MCF-7 cells were maintained in RPMI 1640; HDFa, Mia PaCa-2 and PANC-1 cells were maintained in DMEM (4 mM L-glutamine and 4500 mg/L of glucose). Basic media were supplemented with 10% (v/v) fetal bovine serum and a 1% penicillin–streptomycin mixture. Each cell line was maintained at 37 °C in a humidified atmosphere with 5% CO_2.

Cell viability assay

Cell viability was determined by the MTT method. Cells were seeded at a density of 4×10^3 (for 24 h tests) or 2×10^3 (for 48 h tests) per well of a 96-well plate and allowed to attach overnight. The medium was replaced with fresh medium supplemented with desired concentrations of **5** for 24 h or 48 h. In some experiments, cells were pretreated with 2-APB (30 μM) or BAPTA (10 μM) for one hour. Before the end of treatment, 25 μl of MTT solution (4 mg/mL) was added to each well. After 3 h of incubation, the medium was removed, and formazan crystals were dissolved in 100 μl of DMSO. Absorbance was measured at 570 nm (with a reference wavelength of 660 nm) in a Victor^3 microplate reader. Data were obtained from at least three independent experiments performed in triplicate. IC_{50} values were calculated using GraphPad Prism software. The selectivity index was calculated as the IC_{50} value in the normal cell line divided by the IC_{50} value in the cancer cell line.

Measurement of Ca^{2+} level

Cells were seeded at a density of 2×10^4 per well in a 96-well plate and allowed to attach overnight. The medium was replaced with fresh medium supplemented with desired concentrations of **5** for 6 h (MCF-7) and 12 h (Mia PaCa-2, PANC-1). In some experiments, cells were pretreated with 2-APB (30 μM) or BAPTA (10 μM). The Ca^{2+} level was evaluated using a Fluo-4 Direct Assay Kit (Invitrogen) according to the manufacturer's instructions.

Cell cycle and cell death determination

The effect of the investigated compounds on cell cycle distribution and cell death was determined by Muse™ Cell Analyzer (Millipore). Cells were seeded in 6-well plates at a density of 2×10^5 per well. After 24 h, the cells were treated with 1 or 5 μg/mL derivative **5**, UA, or an equivalent amount of DMSO. After 24 h (cell cycle) or 48 h (cell death), both medium and trypsinized cells were collected, centrifuged for 10 min at 300 × g, stained using the Muse™ Cell Cycle Kit or Muse ™ Annexin-V & Dead Cell Assay Kit and counted by flow cytometry.

Transmission electron microscopy (TEM)

Transmission electron microscopy was performed essentially as described previously [18]. Briefly, cells (2×10^5) were plated in 12-well plates and allowed to attach overnight. Next, the cells were treated with either DMSO (control), 1 or 5 μg/mL **5** for 24 or 48 h at 37 °C. For TEM, cells were fixed in ice-cold 2.5% electron microscopy grade glutaraldehyde (Polysciences) in PBS (pH 7.4). The samples were rinsed with PBS, postfixed in 1% osmium tetroxide with 0.1% potassium ferricyanide, dehydrated through a graded series of ethanol washes (30–100%), and embedded in Epon (Fluka). Semithin (300 nm) sections were cut using an RMC Power Tome XL ultramicrotome, stained with 0.5% toluidine blue and examined under a light microscope. Ultrathin sections (65 nm) were cut using a Leica UC7 ultramicrotome, stained with Uranyless (Delta Microscopies) and Reynold's lead citrate (Delta Microscopies), and examined on a Tecnai G2 Spirit BioTWIN transmission electron microscope at 120 kV.

Immunoblotting

Cells were treated with **5** or UA (1 or 5 μg/mL for 6 or 24 h) and lysed using a solution containing 50 mM Tris (pH 7.5), 1% Triton X-100, 150 mM NaCl, 0.5 mM EDTA, and protease and phosphatase inhibitor cocktails (Roche Diagnostics). The lysates were cleared by centrifugation. Proteins were separated by SDS–PAGE and transferred onto a PVDF membrane. The membrane was blocked with 5% nonfat dry milk in phosphate-buffered saline and incubated with the desired primary antibody overnight at 4 °C. The membrane was then treated with the appropriate secondary antibody for 1 h at room temperature. Immunoreactive bands were detected with an enhanced chemiluminescence reagent (Thermo Scientific). Blots were stripped and reprobed with anti-β-actin antibodies to normalize for differences in protein loading. Each

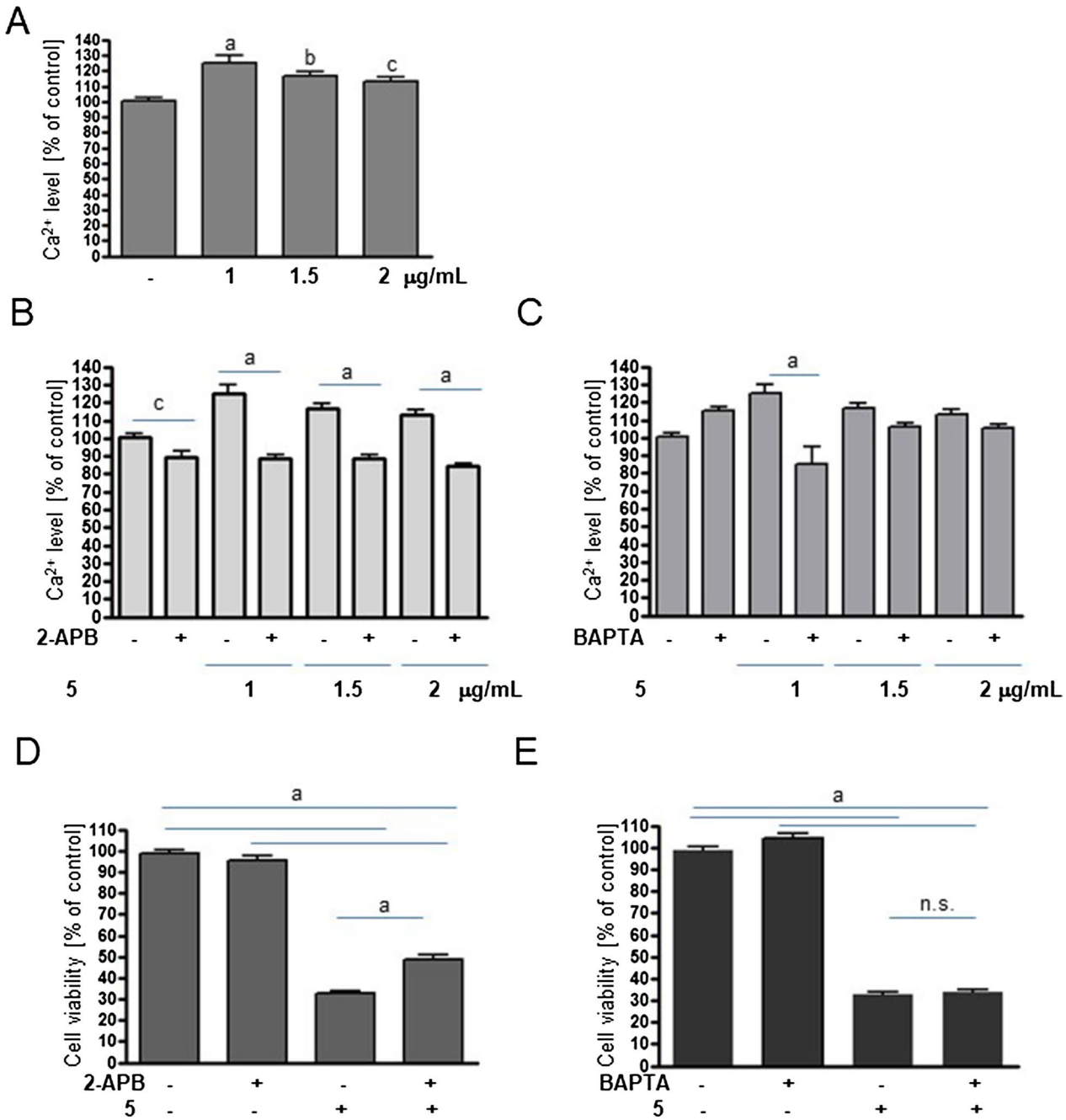

Fig. 2 UA derivative **5** elevates cytosolic Ca^{2+} levels in breast cancer cells. **A** Relative level of Ca^{2+} in MCF-7 cells treated with vehicle (DMSO, 100%) or **5** at the indicated concentrations for 6 h. **B**-**C** Effect of 2-APB (30 µM, **B**) or 2- BAPTA (10 µM, **C**) 1-h pretreatment on Ca^{2+} levels in MCF-7 cells treated or not with compound **5**. **D**-**E**: Effect of 2-APB (**D**) or BAPTA (**E**) pretreatment on the viability of MCF-7 cells treated or not with **5** for 24 h. The data are shown as the mean ± SE (n = 7–11). Statistical significance was determined by ANOVA followed by Dunnett's (**A**) or Sidak's (**B**-**E**) post hoc tests: a—$P < 0.0001$, b—$P < 0.001$, c—$P < 0.05$, n.s.—not significant

protein was detected three times in independently prepared lysates. Densitometry analysis was carried out using Quantity One 1-D Analysis software (Bio-Rad).

Animal studies

The experiments on mice were conducted at the Tri-City Academic Laboratory Animal Centre (Gdańsk). The

animal protocol was approved by the Local Ethics Committee for Animal Experimentation in Bydgoszcz (permit No. 20/2019). Animal experimentation was performed in accordance with EU directive 2010/63/EU. Female BALB/c-Nude mice (CAnN. Cg-Foxn1nu/Crl, 5 weeks old) were purchased from AnimaLab (Poznań, Poland). Animals were housed in IVC cages under 12 h light and dark cycles with food and water ad libitum. Animals were adapted to the experimental conditions for one week before the start of the experiment. To generate tumor xenografts 5×10^6 Mia PaCa-2 cells in Matrigel were injected subcutaneously into the flanks of each mouse. When the tumor volume reached approximately 80 mm^3, the mice were randomly divided into groups (n = 9 in each group). Animals were treated for 4 weeks, 3 times a week by oral gavage with corn oil (control group) or **5** suspended in corn oil (400 mg/kg). Tumor growth and body weight were recorded every 2–3 days. At the end of the experiment, the mice were sacrificed, and the tumors, livers and kidneys were excised, measured, and stored for further analysis.

Histopathology

Dissected tumors, livers and kidneys were fixed with 4% paraformaldehyde in PBS and paraffin-embedded. Five-micrometer-thick sections were mounted on Superfrost Plus adhesive slides (Thermo Scientific, USA). All samples were stained with hematoxylin and eosin (H&E, Eosin Y, Harris Hematoxylin Shandon, Thermo Scientific) to determine the tissue structure and degree of vacuolization. Slides were mounted with DPX (Fluka, Switzerland). All comparative sections were performed at the same time using identical conditions. Images were taken using an Olympus light microscope IX51 with a CCD camera and CellSens Software.

Statistical analysis

All data are shown as the means ± standard errors (SE) of at least three independent experiments. The significance of differences between the control and treated cells in viability tests was analyzed with ANOVA and Dunnett's or Sidak's multiple comparison post hoc tests using GraphPad Prism (version 8). Differences were considered significant at $P < 0.05$.

Results

UA pyrazole derivative is active against cancer cells of different origins

The UA pyrazole derivative, (*R*)-8-acetyl-5,7-dihydroxy-3,4a,6-trimethyl-1,4a-dihydro-4*H*-benzofuro[3,2-*f*]indazol-4-one, named **5** (Fig. 1A), was synthesized as described in [17] and revealed potent activity against HeLa cervical cancer cells [17]. Here, its anticancer potential was evaluated against a panel of human cancer cells derived from different organs as well as normal cells using the MTT viability assay. As Table 1 shows, derivative **5** more efficiently decreased the viability of cancer cells than healthy fibroblasts (selectivity index ranged from 1.8 for PANC-1 to 7.2 for HeLa cells after 24 h of treatment). It was more potent than previously investigated derivatives **2** (isoxazole) or **3** (pyrazole) against MCF-7 (the IC_{50} determined after 24 h of treatment was threefold lower than that for derivative **2**) and HeLa cells (the IC_{50} values were approximately fourfold- and ninefold lower than for **2** and **3**, respectively) [17, 18]. Mia PaCa-2 and PANC-1 pancreatic cancer cells appeared to be less sensitive to derivative **5** than MCF-7 cells; however, the IC_{50} values after 48 h of treatment were still close to 1 µg/mL, and **5** reduced the viability of cells in a dose- and time-dependent manner, contrary to parental UA (Fig. 1B-D). Skin fibroblasts were more resistant to derivative **5** than cancer cells (Fig. 1E).

Recently, it has been shown that UA isoxazole derivative **2** elevates cytosolic Ca^{2+} levels in MCF-7 cells, leading to ER stress [19]. To elucidate whether derivative **5** acts in a similar way, MCF-7 cells were treated with **5**, and cytosolic Ca^{2+} levels were evaluated. As shown in Fig. 2A, derivative **5** increased the level of Ca^{2+}. This effect resulted from Ca^{2+} release from the ER as an inhibitor of IP3 receptors, 2-APB, blocked this process, in contrast to BAPTA, a nonpermeable extracellular calcium chelator, which did not (Fig. 2B-C). Moreover, inhibition of Ca^{2+} leakage from the ER by 2-APB partially protected against a **5**-induced drop in MCF-7 viability, while BAPTA had no effect (Fig. 2D-E).

(See figure on next page.)

Fig. 3 Derivative **5** induces vacuolization and ER stress. **A**: Morphology of MCF-7, PANC-1 and Mia PaCa-2 cells examined under light microscopy (magnification 200x). Cells were treated with DMSO (control) or 1 µg/mL of derivative **5** for 48 h. Enlarged sections of samples treated with **5** are shown in the insets. **B**: Immunoblots for ER stress markers, BIP, IRE1, and GADD153 in pancreatic cancer cells treated with DMSO or **5** (1 or 5 µg/mL) for 6 or 24 h. The blots were stripped and reprobed with the anti-β-actin antibody to ensure equal protein loading. Densitometric scanning data after correction for loading control (mean of 3 repetitions) are above the immunoreactive bands. **C**: Relative level of Ca^{2+} in pancreatic cancer cells (PANC-1 and Mia PaCa-2) treated with vehicle (DMSO, 100%) or **5** at the indicated concentrations for 12 h. The data are shown as the mean ± SE (n = 7–11). Statistical significance was determined by ANOVA followed by Dunnett's post hoc test: **b**—$P < 0.001$, **c**—$P < 0.05$

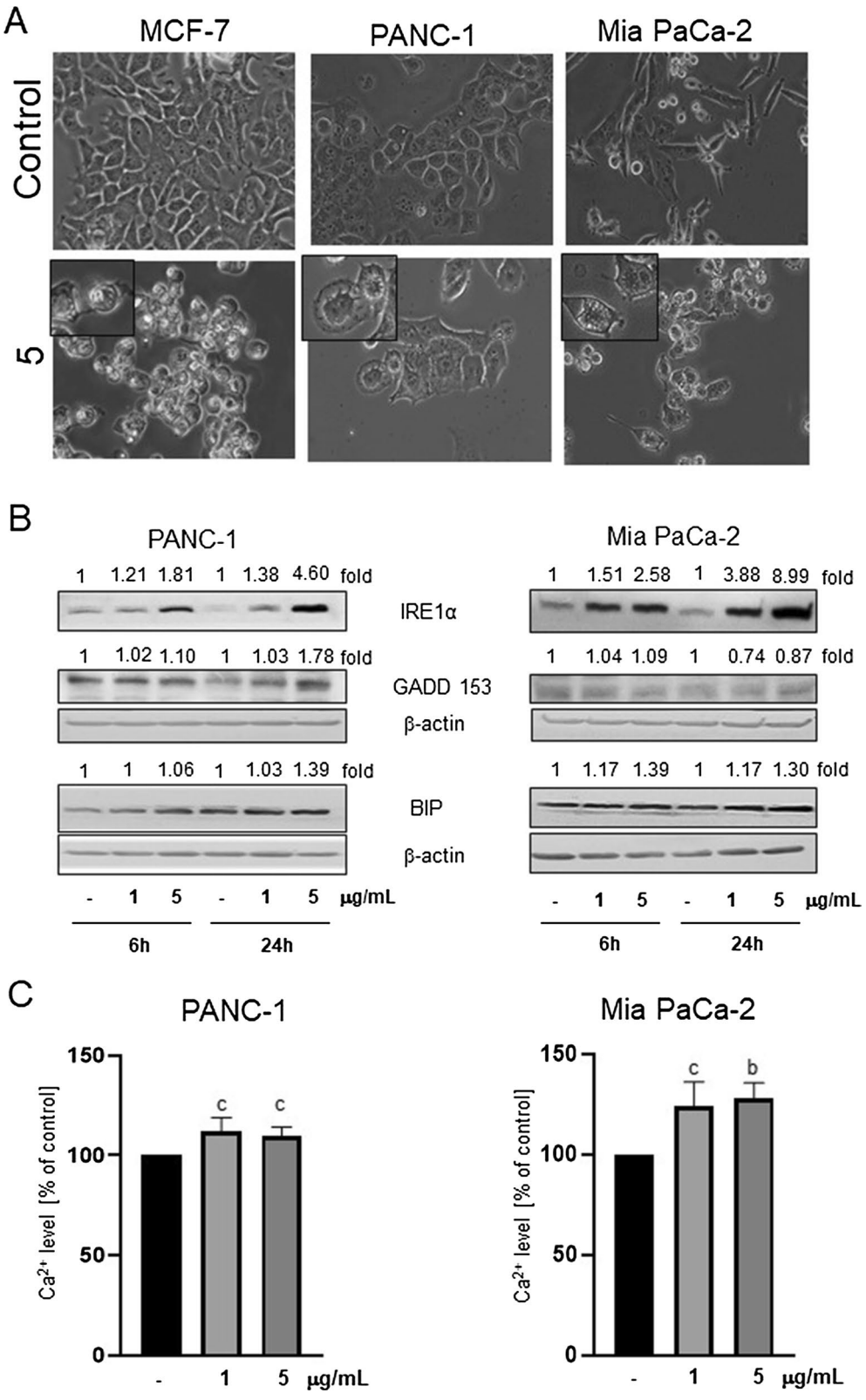

Fig. 3 (See legend on previous page.)

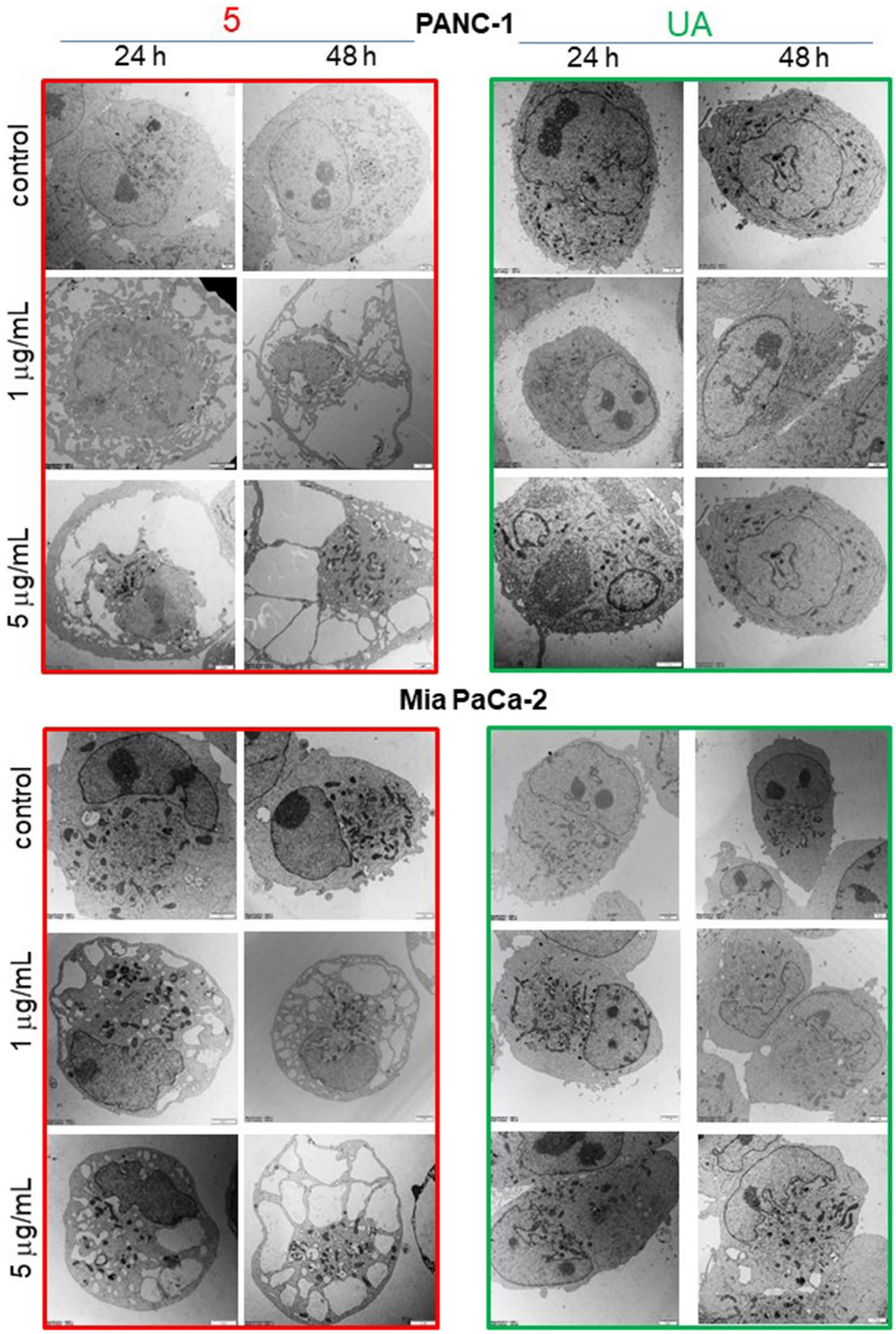

Fig. 4 Derivative **5** but not parental UA induces massive vacuolization of pancreatic cancer cells. Morphology of PANC-1 and Mia PaCa-2 cells examined under TEM. Cells were treated with DMSO (control), **5** or UA at 1 or 5 µg/mL for 24 or 48 h. Representative pictures of cells at magnifications of 2900x, 4800 × or 6800 × are shown

Table 2 Derivative **5** blocks pancreatic cancer cell cycle progression in G0/G1 phase in a time-dependent manner

Name	Concentration [μg/mL]	Cell cycle phase [%]		
		G0/G1	S	G2/M
PANC-1				
Control		43.8 ± 1.3	20.4 ± 0.9	34.5 ± 1.7
(+) usnic acid	1	44.3 ± 2.6^{ns}	20.5 ± 0.8^{ns}	33.8 ± 3.4^{ns}
	5	42.7 ± 1.1^{ns}	18.9 ± 1.2^{ns}	36.3 ± 1.9^{ns}
5	1	47.8 ± 2.3^{ns}	18.8 ± 2.1^{ns}	31.9 ± 1.2^{ns}
	5	61.9 ± 4.3^{a}	8.1 ± 2.2^{b}	28.4 ± 2.3^{ns}
Mia PaCa-2				
Control		42.3 ± 1.1	29.9 ± 1.7	33.5 ± 1.2
(+) usnic acid	1	39.8 ± 1.4^{ns}	24.3 ± 3.6^{ns}	33.2 ± 2.4^{ns}
	5	41.2 ± 2.7^{ns}	24.9 ± 3.6^{ns}	31.4 ± 2.1^{ns}
5	1	48.0 ± 1.5^{ns}	19.2 ± 1.7^{ns}	29.5 ± 2.6^{ns}
	5	54.5 ± 0.8^{a}	15.7 ± 0.9^{ns}	26.9 ± 1.7^{c}

Cells were treated with 1 or 5 μ g/mL UA or derivative **5** for 24 h. Each value is the mean (± SE) of three experiments. Statistical significance was determined with ANOVA and Sidak's multiple comparison test and a – $P < 0.0001$, b – $P < 0.001$, c – $P < 0.05$, ns – not significant

It was reported that some cancers, such as pancreatic cancer, are characterized by constant ER stress, and its elevation might be an efficient way to eradicate them [21, 22]; thus, Mia PaCa-2 and PANC-1 pancreatic cancer cells were used to elucidate whether derivative **5** impacts their ER homeostasis. As shown in Fig. 3A, **5** induced vacuolization of pancreatic cancer cells, similar to MCF-7 cells. Markers of ER stress, such as BIP, IRE1α, GADD153, were elevated, as revealed by immunoblotting (Fig. 3B). Moreover, derivative **5** increased Ca^{2+} levels in the cytoplasm of pancreatic cancer cells (Fig. 3C), which was inhibited by 2-APB but not by BAPTA (Additional file 1: Fig. S1). Emptyfication of Ca^{2+} stores might be the cause of ER stress induction, as in the case of MCF-7 cells.

A more detailed investigation of the ultrastructure of pancreatic cancer cells revealed dose- and time-dependent vacuolization upon treatment with **5,** and no such features were observed in cells treated with UA at the same concentrations (Fig. 4). Analysis of electron microscopy images indicated that large vacuoles that appear in pancreatic cancer cells are of ER origin, which supports ER stress induction. In the case of PANC-1, cells with damaged plasmalemma have also been found, which is a feature of necrotic death. In contrast, UA used at similar concentrations had minimal effect on pancreatic cancer cell morphology (Fig. 4).

UA derivative 5 inhibits cell cycle progression and induces cell death in pancreatic cancer cells

To further elucidate the mechanisms of the antiproliferative activity of derivative **5** in pancreatic cancer cells, its effect on the cell cycle and cell death was investigated. As shown in Table 2, treatment with derivative **5** for 24 h increased the percentage of G0/G1 cells in a dose-dependent manner, and at the same time, the number of cells in the S and G2/M phases decreased. UA at the same concentrations had minimal effects on the cell cycle.

Analysis of cancer cell death using the detection of phosphatidylserine by Annexin V and membrane permeabilization by the accumulation of 7-aminoactinomycin D (7-AAD) dye indicated that derivative **5** decreased the number of viable cells and increased the number of apoptotic cells, particularly in the case of the Mia PaCa-2 cell line: derivative **5** at a 5 μg/mL concentration elevated the total fraction of apoptotic cells from 20% to over 70% after 48 h of treatment (Fig. 5B). In the case of PANC-1, viable cells dropped from 80 to 60%, and there were 30% and 10% apoptotic and necrotic cells, respectively, upon treatment with 5 μg/mL derivative **5** (Fig. 5A). UA was less effective in the induction of cell death than derivative **5** (Fig. 5C-D). Immunoblotting for caspase-cleaved PARP confirmed that **5** is more active than UA in apoptosis induction, particularly in Mia PaCa-2 cells (Fig. 5E-F).

Orally administered derivative 5 retards Mia PaCa-2 xenograft growth in mice

The results presented in this work indicate that **5** is more potent than UA as an antiproliferative agent against cancer cells, including pancreatic cancer cells. To elucidate whether **5** is active in vivo as well, we tested it in murine models. The acute toxicology tests based on the oral administration of **5** to laboratory strain BALB/c mice allowed for the determination of the Maximum Tolerated Dose as 400 mg/kg (data not shown). Next, the effect of **5** on the growth of Mia PaCa-2 xenografts in nude mice was tested. As shown in Fig. 6A, orally administered **5** inhibited tumor growth, which was evident after 6 doses. The tested derivative did not affect body mass (Fig. 6B).

Histopathological analysis showed that derivative **5** changed the structure of the tumor, which might be connected with cancer cell death induction (Fig. 6C). Vacuolization of tumor cells can be noticed in **5**-treated animals. Importantly, such changes were not observed in the livers and kidneys of either control or **5**-treated animals (Fig. 6D-E).

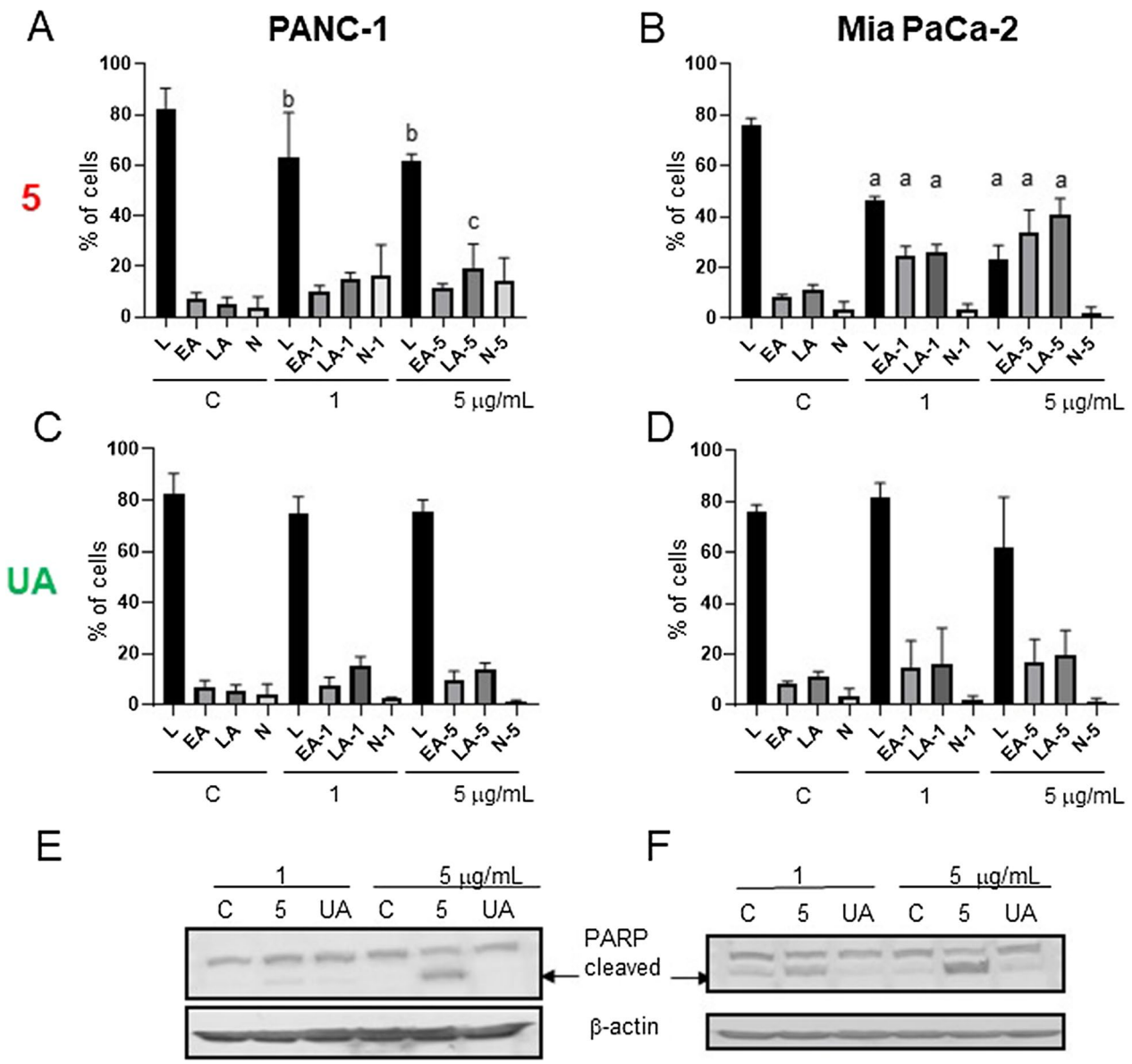

Fig. 5 Derivative **5** induces the death of pancreatic cancer cells. **A**-**D**: PANC-1 (**A**, **C**) or Mia PaCa-2 (**B**, **D**) cells were treated with DMSO (control, **C**), **5** (upper graphs—**A**, **B**) or UA (lower graphs—**C**, **D**) at 1 or 5 μg/mL for 48 h. The amounts of live (L), early apoptotic (EA), late apoptotic (LA), and necrotic (N) cells were determined by flow cytometry after staining with Muse™ Annexin V and Dead Cell Kit. The results are presented as the mean ± SE of 3–6 independent experiments. Statistical significance between the respective control and **5**-treated fractions was determined with ANOVA and Sidak's post hoc test and is marked with a ($P < 0.0001$), b ($P < 0.001$), and c ($P < 0.05$). **E**: PANC-1 and **F**: Mia PaCa-2 immunoblots for caspase-cleaved PARP. The blots were stripped and reprobed with an anti-β -actin antibody to ensure equal protein loading

Discussion

This work shows that the new pyrazole UA derivative **5** induces cell cycle arrest and death of pancreatic cancer cells and is connected with ER stress induction. The tested compound is much more active than parental UA, which, when used at the same concentrations, has almost no effect on cancer cells.

There are only a few reports investigating the activity of UA or its derivatives in pancreatic cancer cells. Previously, the activity of (+)-UA from *Cladonia arbuscula* and (−)-UA from *Alectoria ochroleuca* was tested in T47D breast and Capan-2 pancreatic cancer cells. Both enantiomers revealed similar anti-proliferative effects against tested cell lines (the IC_{50} was 4.2 μg/mL and 4.0

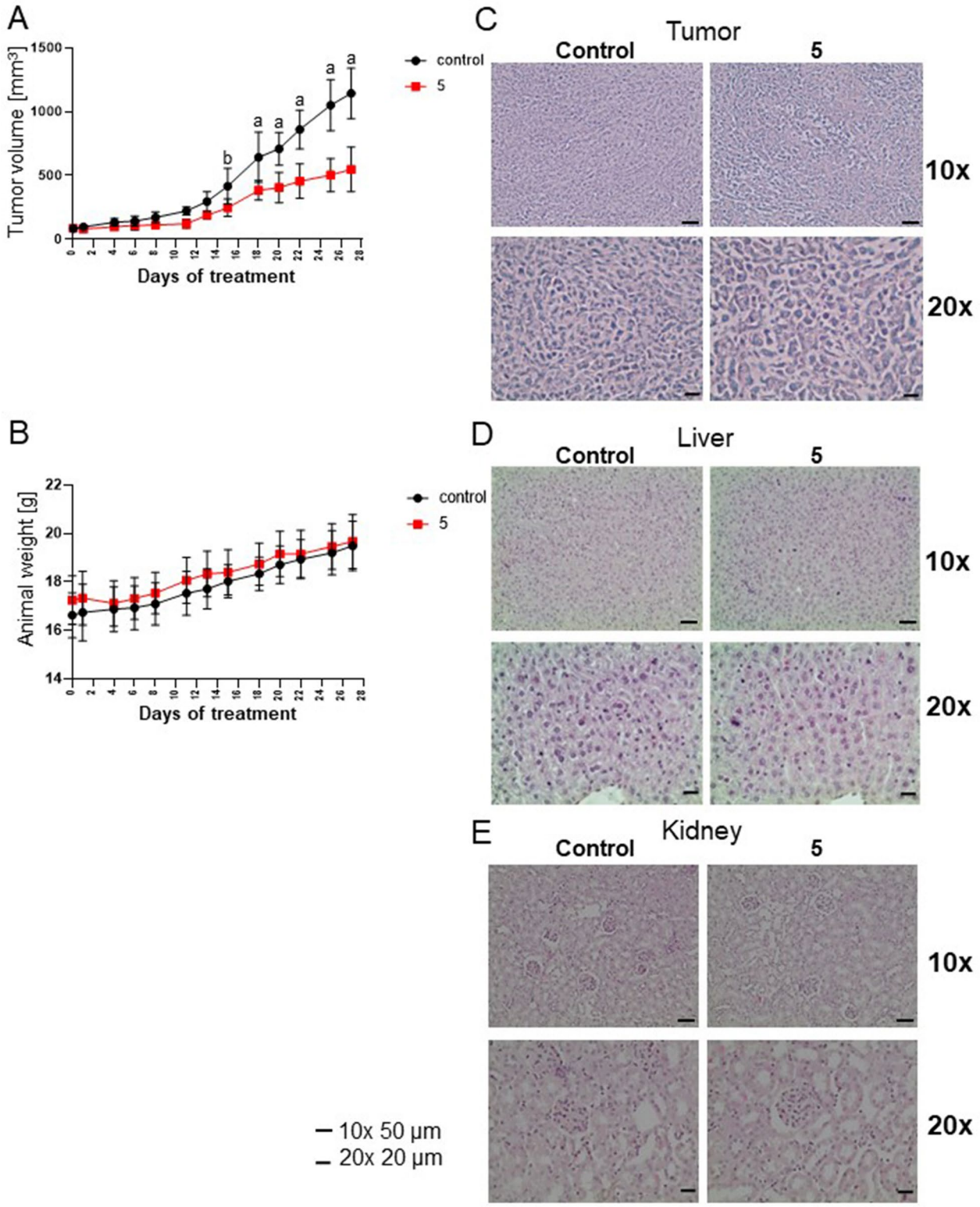

Fig. 6 Derivative **5** inhibits the growth of Mia PaCa-2 cell xenografts in nude mice. Effect of **5** (400 mg/mL) or vehicle (corn oil) treatment on the tumor volumes (**A**) and body weights of animals (n = 9) (**B**). Statistical significance between the control and **5**-treated groups was determined by ANOVA followed by Sidak's post hoc test: a—$P < 0.0001$, b—$P < 0.001$. **C**-**E**: Histology of tumor (**C**), liver (**D**) or kidney (**E**) sections in control and **5**-treated mice. Images were taken under a 10 × or 20 × objective, and representative results are shown. Tissue sections were fixed, embedded in paraffin, sectioned, and processed for H & E staining

μg/mL for (+) and (−)-usnic acid against T47D, and 5.3 μg/mL and 5.0 μg/mL against Capan-2, respectively) measured by ^{3}H thymidine incorporation into DNA. UA reduced cancer cell size and at 10 μg/mL, induced G0/G1 cell cycle arrest and mitochondrial membrane depolarization. It also caused necrosis but only in Capan-2 pancreatic cancer cells exposed for 48 h to 5 or 10 μg/mL UA [23]. Later, the same authors confirmed that 10 μg/mL UA caused necrosis but not apoptosis in tested cell lines [24]. Modifications of the UA structure revealed that some derivatives show enhanced activity compared to the parent compound. UA enamine with an imidazole substituent (2e (R, *E*)-6-acetyl-2-[1-(3-(1*H*-imidazol-1-yl) propylamino)ethylidene]-7,9-dihydroxy-8,9b-dimethyldibenzofuran-1,3(2*H*,9b*H*)-dione) and UA pyrazole (4a, (R)-8-acetyl-5,7-dihydroxy-3,4a,6-trimethyl-1-phenyl-1*H*-benzofuro[3,2-f]indazol-4(4a*H*)-one) revealed potent antiproliferative activity against cervix (HeLa), breast (MDA-MB-231), lung (A549) and pancreas (Mia PaCa-2) cancer cells with IC_{50} values of approximately 4–6 and 6–7.5 μM, respectively, in an SRB viability assay [25]. A more detailed examination in HeLa cells showed that both derivatives used at a 10 μM concentration for 24 h destabilized microtubules, which led to G2/M block in the cell cycle [25].

Here, we showed that pyrazole derivative **5** inhibited pancreatic cancer cell viability, inducing cell cycle arrest in the G0/G1 phase and cell death. Mia PaCa-2 cells were slightly more sensitive to **5,** which at 1 or 5 μg/mL concentration induced mainly apoptosis after 48 h of treatment (51 and 74% apoptotic cells, respectively, compared to 20% in controls). In PANC-1 cells, derivative **5** at 1 or 5 μg/mL moderately induced apoptosis (24 and 27 vs. 14%), but necrotic cells were also detected in flow cytometry experiments (13 and 11 vs. 5%) and TEM images. PANC-1 cell cycle arrest was higher than that in Mia PaCa-2 cells treated for 24 h with 5 μg/mL derivative **5** (62% and 55%, respectively, compared to 43% in controls). Such differences in response to derivative **5** might be related to the genetic background of these cell lines. Nevertheless, **5** induced massive vacuolization in both pancreatic cancer cell lines, similar to breast cancer cells. Vacuolization resulted from ER stress accompanied by the release of ER-stored Ca^{2+} to the cytosol, which was observed in breast and pancreatic cancer cells.

Solid tumors often suffer from hypoxia, oxidative stress and deprivation of nutrients, including glucose. All these processes are well-known inducers of ER stress. This accumulation of misfolded proteins in the lumen of the ER triggers the unfolded protein response (UPR) which restores homeostasis in this organelle. It relies on changes in gene expression to produce enzymes engaged in protein folding or degradation and in the inhibition of global translation to reduce translational load. This is accompanied by the expansion of ER size [26, 27]. In the majority of cases, the UPR plays an adaptive pro-survival role. However, persistent and unresolved ER stress leads to cell death [28]. Pancreatic cells exhibit a high level of synthesis and secretion of hormones and digestive enzymes; therefore, they possess a highly developed ER, which makes them especially sensitive to ER stress-induced apoptosis [20, 29]. Highly developed ER is also observed in pancreatic cancer cells. Moreover, pancreatic tumors show a high basal level of ER stress [30]. Therefore, ER targeting is regarded as a promising approach to the therapy of pancreatic cancer [21, 22].

Conclusions

The results presented in this work indicate that the antiproliferative activity of UA derivative **5** relies on ER stress induction in cancer cells, including pancreatic cancer cells, both growing in vitro and in an animal model. Importantly, the treatment of animals with **5** neither had adverse effects nor affected the morphology of healthy organs. These features make derivative **5** a promising candidate for future research on its use for the treatment of pancreatic cancer patients.

Abbreviations

2-APB	Aminoethoxydiphenylborane
BAPTA	1,2-Bis(2-aminophenoxy)ethane-*N*,*N*,*N*′,*N*′-tetraacetic acid
BiP	Binding immunoglobin protein
ER	Endoplasmic reticulum
IRE1α	Inositol requiring enzyme 1 alpha
DMSO	Dimethyl sulfoxide
GADD153	Growth arrest DNA damage 153
PARP	Poly(ADP-ribose) polymerase
PBS	Phosphate-buffered saline
SE	Standard error
UA	(+)-Usnic acid
UPR	Unfolded protein response
vs.	Versus

Supplementary Information

The online version contains supplementary material available at https://doi.org/10.1186/s12935-023-03054-x.

Additional file 1. Figure S1. Elevation of cytosolic Ca^{2+} levels in pancreatic cancer cells results from its release from ER. The relative level of Ca^{2+} in PANC-1 (**A**) and Mia PaCa-2 (**B**) cells treated with vehicle (DMSO, 100%), **5** at indicated concentrations with or without inhibitor of IP3 receptors (2-APB at 30 μM, left panels) or extracellular calcium chelator (BAPTA, 10 μM, right panels) for 12 h. The data are shown as the mean ± SE (n=6-9). Statistical significance was determined by ANOVA followed by Sidak's post-hoc tests: a - $P < 0.0001$, b - $P < 0.001$, c - $P < 0.05$, n.s. - not significant.

Acknowledgements

We acknowledge Dr Anna Żyłko and other staff from the Tri-City Academic Laboratory Animal Centre, the Medical University of Gdańsk, for their support in animal handling and the performance of in vivo experiments.

Author contributions
M.G, and A.H.-A conceived the experiments; T.A.R. synthesized **5**; M.G., A.P.-F., M.M., A.H., M.N., I.B., A. H.-A. designed and performed the experiments as well as analyzed the data. A.H.-A. coordinated the study and wrote the original draft of the manuscript. M.G., A.P.-F., M.M., A.H., M.N., I.B., and T.A.R. reviewed and edited the manuscript. All authors read and approved the final manuscript.

Funding
This research was funded by National Science Centre, Poland (project no. 2017/26/M/NZ7/00668).

Availability of data and materials
The data supporting the findings of this study are available from the corresponding author upon reasonable request.

Declarations

Ethics approval and consent to participate
The study with the use of animals was conducted according to the guidelines of the Declaration of Helsinki, and approved by the Local Ethics Committee for Animal Experimentation in Bydgoszcz (permit No. 20/2019, dated 23.04.2019).

Consent for publication
Not applicable.

Competing interests
The authors declare that they have no competing interests.

Received: 11 May 2023 Accepted: 3 September 2023
Published online: 24 September 2023

References

1. Sung H, Ferlay J, Siegel RL, Laversanne M, Soerjomataram I, Jemal A, Bray F. Global cancer statistics 2020: GLOBOCAN estimates of incidence and mortality worldwide for 36 cancers in 185 countries. CA Cancer J Clin. 2021;71(3):209–49.
2. Klein AP. Pancreatic cancer epidemiology: understanding the role of lifestyle and inherited risk factors. Nat Rev Gastroenterol Hepatol. 2021;18(7):493–502.
3. Wood LD, Hruban RH. Pathology and molecular genetics of pancreatic neoplasms. Cancer J. 2012;18(6):492–501.
4. Ingolfsdottir K. Usnic acid. Phytochemistry. 2002;61(7):729–36.
5. Araujo AA, de Melo MG, Rabelo TK, Nunes PS, Santos SL, Serafini MR, Santos MR, Quintans-Junior LJ, Gelain DP. Review of the biological properties and toxicity of usnic acid. Nat Prod Res. 2015;29(23):2167–80.
6. Luzina OA, Salakhutdinov NF. Biological activity of usnic acid and its derivatives: Part 2. Effects on higher organisms molecular and physicochemical aspects. Russ J Bioorg Chem. 2016;42:249–68.
7. Galanty A, Pasko P, Podolak I. Enantioselective activity of usnic acid: a comprehensive review and future perspectives. Phytochem Rev. 2019;18:527–48.
8. Solarova Z, Liskova A, Samec M, Kubatka P, Busselberg D, Solar P. Anticancer potential of lichens' secondary metabolites. Biomolecules. 2020;10(1):87.
9. Qi W, Lu C, Huang H, Zhang W, Song S, Liu B. (+)-Usnic acid induces ROS-dependent apoptosis via inhibition of mitochondria respiratory chain complexes and Nrf2 expression in lung squamous cell carcinoma. Int J Mol Sci. 2020;21(3):876.
10. Backorova M, Backor M, Mikes J, Jendzelovsky R, Fedorocko P. Variable responses of different human cancer cells to the lichen compounds parietin, atranorin, usnic acid and gyrophoric acid. Toxicol In Vitro. 2011;25(1):37–44.
11. Studzinska-Sroka E, Majchrzak-Celinska A, Zalewski P, Szwajgier D, Baranowska-Wojcik E, Kapron B, Plech T, Zarowski M, Cielecka-Piontek J. Lichen-derived compounds and extracts as biologically active substances with anticancer and neuroprotective properties. Pharmaceuticals (Basel). 2021;14(12):1293.
12. Geng X, Zhang X, Zhou B, Zhang C, Tu J, Chen X, Wang J, Gao H, Qin G, Pan W. Usnic acid induces cycle arrest, apoptosis, and autophagy in gastric cancer cells in vitro and in vivo. Med Sci Monit. 2018;24:556–66.
13. Sanchez W, Maple JT, Burgart LJ, Kamath PS. Severe hepatotoxicity associated with use of a dietary supplement containing usnic acid. Mayo Clin Proc. 2006;81(4):541–4.
14. Guo L, Shi Q, Fang JL, Mei N, Ali AA, Lewis SM, Leakey JEA, Frankos VH. Review of usnic acid and *Usnea barbata* toxicity. J Environ Sci Health C Environ Carcinog Ecotoxicol Rev. 2008;26(4):317–38.
15. Han D, Matsumaru K, Rettori D, Kaplowitz N. Usnic acid-induced necrosis of cultured mouse hepatocytes: inhibition of mitochondrial function and oxidative stress. Biochem Pharmacol. 2004;67(3):439–51.
16. da Silva Santos NP, Nascimento SC, Wanderley MS, Pontes-Filho NT, da Silva JF, de Castro CM, Pereira EC, da Silva NH, Honda NK, Santos-Magalhaes NS. Nanoencapsulation of usnic acid: an attempt to improve antitumour activity and reduce hepatotoxicity. Eur J Pharm Biopharm. 2006;64(2):154–60.
17. Gunawan GA, Gimla M, Gardiner MG, Herman-Antosiewicz A, Reekie TA. Divergent reactivity of usnic acid and evaluation of its derivatives for antiproliferative activity against cancer cells. Bioorg Med Chem. 2023;79:117157.
18. Pyrczak-Felczykowska A, Narlawar R, Pawlik A, Guzow-Krzeminska B, Artymiuk D, Hac A, Rys K, Rendina LM, Reekie TA, Herman-Antosiewicz A. Synthesis of usnic acid derivatives and evaluation of their antiproliferative activity against cancer cells. J Nat Prod. 2019;82(7):1768–78.
19. Pyrczak-Felczykowska A, Reekie TA, Jakalski M, Hac A, Malinowska M, Pawlik A, Rys K, Guzow-Krzeminska B, Herman-Antosiewicz A. The isoxazole derivative of usnic acid induces an ER stress response in breast cancer cells that leads to paraptosis-like cell death. Int J Mol Sci. 2022;23(3):1802.
20. Oyadomari S, Araki E, Mori M. Endoplasmic reticulum stress-mediated apoptosis in pancreatic beta-cells. Apoptosis. 2002;7(4):335–45.
21. Mollinedo F, Gajate C. Direct endoplasmic reticulum targeting by the selective alkylphospholipid analog and antitumor ether lipid edelfosine as a therapeutic approach in pancreatic cancer. Cancers (Basel). 2021;13(16):4173.
22. Botrus G, Miller RM, Uson Junior PLS, Kannan G, Han H, Von Hoff DD. Increasing stress to induce apoptosis in pancreatic cancer via the Unfolded Protein Response (UPR). Int J Mol Sci. 2022;24(1):577.
23. Einarsdottir E, Groeneweg J, Bjornsdottir GG, Harethardottir G, Omarsdottir S, Ingolfsdottir K, Ogmundsdottir HM. Cellular mechanisms of the anticancer effects of the lichen compound usnic acid. Planta Med. 2010;76(10):969–74.
24. Bessadottir M, Egilsson M, Einarsdottir E, Magnusdottir IH, Ogmundsdottir MH, Omarsdottir S, Ogmundsdottir HM. Proton-shuttling lichen compound usnic acid affects mitochondrial and lysosomal function in cancer cells. PLoS ONE. 2012;7(12): e51296.
25. Mallavadhani UV, Vanga NR, Balabhaskara R, Jain N. Synthesis and antiproliferative activity of novel (+)-usnic acid analogues. J Asian Nat Prod Res. 2020;22(3):562–77.
26. Marciniak SJ, Ron D. Endoplasmic reticulum stress signaling in disease. Physiol Rev. 2006;86(4):1133–49.
27. Schroder M, Kaufman RJ. ER stress and the unfolded protein response. Mutat Res. 2005;569(1–2):29–63.
28. Corazzari M, Gagliardi M, Fimia GM, Piacentini M. Endoplasmic reticulum stress, unfolded protein response, and cancer cell fate. Front Oncol. 2017;7:78.
29. Fonseca SG, Gromada J, Urano F. Endoplasmic reticulum stress and pancreatic beta-cell death. Trends Endocrinol Metab. 2011;22(7):266–74.
30. Robinson CM, Talty A, Logue SE, Mnich K, Gorman AM, Samali A. An emerging role for the unfolded protein response in pancreatic cancer. Cancers (Basel). 2021;13(2):261.

Publisher's Note

12.2.1. Materiały dodatkowe do publikacji nr 2

Gimła Mariola, Pyrczak-Felczykowska Agnieszka, Malinowska Marcelina, Hać Aleksandra, Narajczyk Magdalena, Bylińska Irena, Reekie Tristan, Herman-Antosiewicz Anna

The pyrazole derivative of usnic acid inhibits the proliferation of pancreatic cancer cells in vitro and in vivo

Cancer Cell International, 210:10.1186

(2023)

Fig. S1

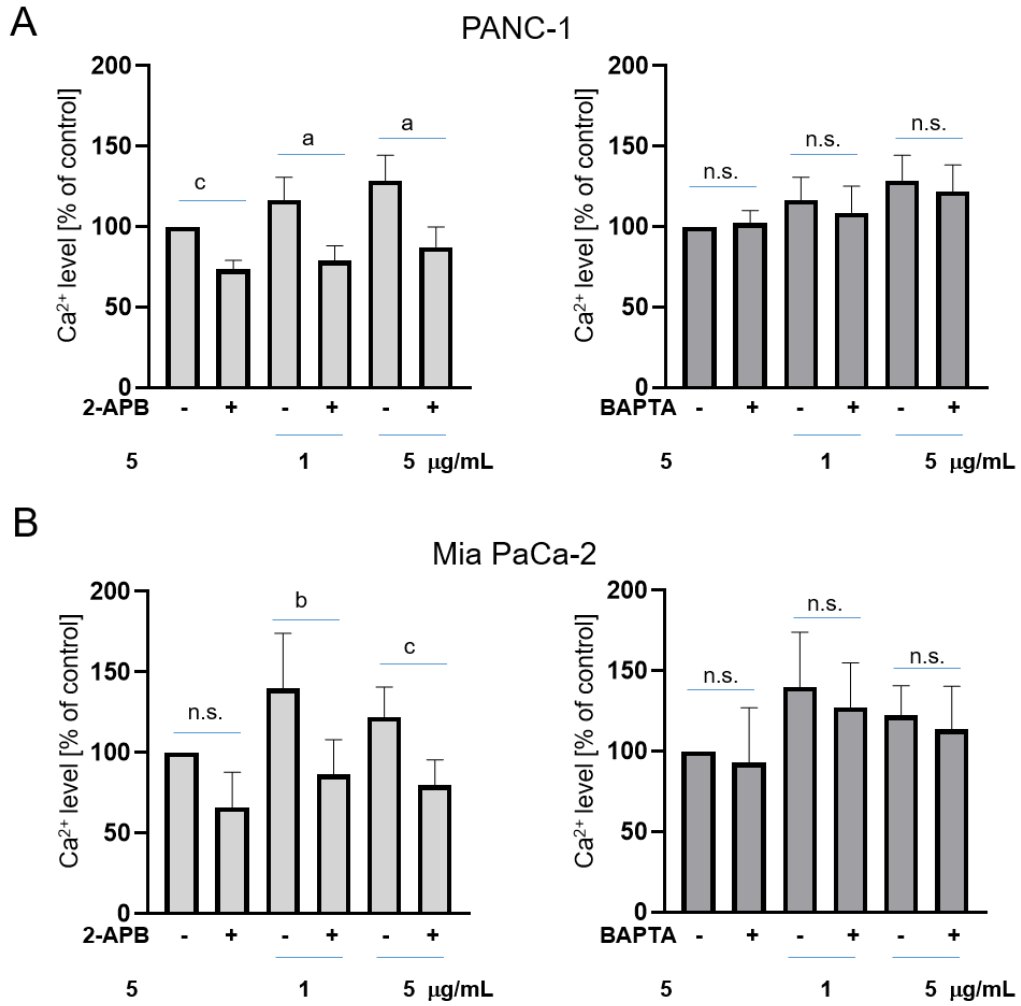

Elevation of cytosolic Ca^{2+} levels in pancreatic cancer cells results from its release from ER. The relative level of Ca^{2+} in PANC-1 (**A**) and Mia PaCa-2 (**B**) cells treated with vehicle (DMSO, 100%), **5** at indicated concentrations with or without inhibitor of IP3 receptors (2-APB at 30 μM, left panels) or extracellular calcium chelator (BAPTA, 10 μM, right panels) for 12 h. The data are shown as the mean ± SE (n=6-9). Statistical significance was determined by ANOVA followed by Sidak's post-hoc tests: a - $P < 0.0001$, b - $P < 0.001$, c - $P < 0.05$, n.s. - not significant.

12.2.2. Oświadczenia autorów

Gdańsk, 06.03.2025 r.

Mariola Gimła
Katedra Biologii i Genetyki Medycznej
Wydział Biologii
Uniwersytet Gdański

Oświadczenie o wkładzie w publikację

Oświadczam, że mój wkład w publikację:

Gimła, M., Pyrczak-Felczykowska, A., Malinowska, M., Hac, A., Narajczyk, M., Bylinska, I., Reekie, T., A., Herman-Antosiewicz, A. The pyrazole derivative of usnic acid inhibits the proliferation of pancreatic cancer cells in vitro and in vivo. Cancer Cell Int 23, 210 (2023). https://doi.org/10.1186/s12935-023-03054-x. PMID: 37743482

polegał na:

- Zaplanowniu i przeprowadzeniu eksperymentów na liniach komórkowych
- Przygotowaniu materiału do mikroskopii elektronowej
- Przygotowaniu linii komórkowej do ksenoprzeszczepów
- Analizie i interpretacji otrzymanych danych
- Udziale w przygotowaniu manuskryptu publikacji
- Korekcie grafik
- Poprawieniu ostatecznej wersji manuskryptu

Mariola Gimła

Gdańsk, 06.03.2025 r.

dr Agnieszka Pyrczak-Felczykowska
Katedra Fizjologii
Gdański Uniwersytet Medyczny

Oświadczenie o wkładzie w publikację

Oświadczam, że mój wkład w publikację:

Gimła, M., Pyrczak-Felczykowska, A., Malinowska, M., Hac, A., Narajczyk, M., Bylinska, I., Reekie, T., A., Herman-Antosiewicz, A. The pyrazole derivative of usnic acid inhibits the proliferation of pancreatic cancer cells in vitro and in vivo. Cancer Cell Int 23, 210 (2023). https://doi.org/10.1186/s12935-023-03054-x. PMID: 37743482

polegał na:

- Przeprowadzeniu eksperymentu dotyczacego zbadania poziomu wapnia w komórkach linii MCF-7
- Udziale w przygotowaniu manuskryptu publikacji

Agnieszka Pyrczak-Felczykowska

Gdańsk, 06.03.2025 r.

dr Marcelina Malinowska
Katedra Biologii i Genetyki Medycznej
Wydział Biologii
Uniwersytet Gdański

Oświadczenie o wkładzie w publikację

Oświadczam, że mój wkład w publikację:

Gimła, M., Pyrczak-Felczykowska, A., Malinowska, M., Hac, A., Narajczyk, M., Bylinska, I., Reekie, T., A., Herman-Antosiewicz, A. The pyrazole derivative of usnic acid inhibits the proliferation of pancreatic cancer cells in vitro and in vivo. Cancer Cell Int 23, 210 (2023). https://doi.org/10.1186/s12935-023-03054-x. PMID: 37743482

polegał na:

- Zaplanowanie i przeprowadzenie doświadczeń *in vivo* oraz analiza uzyskanych danych
- Wykonanie i analiza danych histopatologicznych
- Udział w przygotowaniu manuskryptu publikacji

Gdańsk, 06.03.2025 r.

dr Aleksandra Hać
Katedra Biologii i Genetyki Medycznej
Wydział Biologii
Uniwersytet Gdański

Oświadczenie o wkładzie w publikację

Oświadczam, że mój wkład w publikację:

Gimła, M., Pyrczak-Felczykowska, A., Malinowska, M., Hac, A., Narajczyk, M., Bylinska, I., Reekie, T., A., Herman-Antosiewicz, A. The pyrazole derivative of usnic acid inhibits the proliferation of pancreatic cancer cells in vitro and in vivo. Cancer Cell Int 23, 210 (2023). https://doi.org/10.1186/s12935-023-03054-x. PMID: 37743482

polegał na:

- Przeprowadzeniu eksperymentu dotyczacego zbadania poziomu wapnia w komórkach linii Mia PaCa-2 i Panc-1 po zastosowaniu inhibitorów 2-ABP i BAPTA (wyniki zamieszczone w suplemencie pracy)
- Udziale w przygotowaniu manuskryptu publikacji

Wydział Biologii
KATEDRA BIOLOGII i GENETYKI MEDYCZNEJ
dr Aleksandra Hać

Gdańsk, 06.03.2025 r.

dr hab. Magdalena Narajczyk
Laboratorium Bioobrazowania
Wydział Biologii
Uniwersytet Gdański

Oświadczenie o wkładzie w publikację

Oświadczam, ze mój wkład w publikację:

Gimła, M., Pyrczak-Felczykowska, A., Malinowska, M., Hac, A., Narajczyk, M., Bylinska, I., Reekie, T., A., Herman-Antosiewicz, A. The pyrazole derivative of usnic acid inhibits the proliferation of pancreatic cancer cells in vitro and in vivo. Cancer Cell Int 23, 210 (2023). https://doi.org/10.1186/s12935-023-03054-x. PMID: 37743482

polegał na:

- Przygotowaniu preparatów i zdjęć wykorzystanych w mikroskopii elektronowej
- Udziale w przygotowaniu manuskryptu publikacji

Magdalena Narajczyk

Gdańsk, 06.03.2025 r.

dr inż. Irena Bylińska
Katedra Chemii Biomedycznej
Wydział Chemii
Uniwersytet Gdański

Oświadczenie o wkładzie w publikację

Oświadczam, że mój wkład w publikację:

Gimła, M., Pyrczak-Felczykowska, A., Malinowska, M., Hac, A., Narajczyk, M., Bylinska, I., Reekie, T., A., Herman-Antosiewicz, A. The pyrazole derivative of usnic acid inhibits the proliferation of pancreatic cancer cells in vitro and in vivo. Cancer Cell Int 23, 210 (2023). https://doi.org/10.1186/s12935-023-03054-x. PMID: 37743482

polegał na:

- Analizie i interpretacji danych dot. zależności struktura- funkcja pochodnej kwasu usninowego
- Udziale w przygotowaniu manuskryptu publikacji

Irena Bylińska

March 14, 2025

Tristan A. Reekie
School of Science
University of New South Wales Canberra
Australian Capital Territory
Canberra, 2600, Australia

Author contributions

I hereby declare that my contribution in the article:

Gimła, M., Pyrczak-Felczykowska, A., Malinowska, M., Hac, A., Narajczyk, M., Bylinska, I., Reekie, T., A., Herman-Antosiewicz, A. The pyrazole derivative of usnic acid inhibits the proliferation of pancreatic cancer cells in vitro and in vivo. Cancer Cell Int 23, 210 (2023). https://doi.org/10.1186/s12935-023-03054-x. PMID: 37743482

included:

- synthesized derivative 5
- reviewed and edited the manuscript

signature

Gdańsk, 06.03.2025 r.

prof. dr hab. Anna Herman-Antosiewicz
Katedra Biologii i Genetyki Medycznej
Wydział Biologii
Uniwersytet Gdański

Oświadczenie o wkładzie w publikację

Oświadczam, że mój wkład w publikację:

Gimła, M., Pyrczak-Felczykowska, A., Malinowska, M., Hac, A., Narajczyk, M., Bylinska, I., Reekie, T., A., Herman-Antosiewicz, A. The pyrazole derivative of usnic acid inhibits the proliferation of pancreatic cancer cells in vitro and in vivo. Cancer Cell International 23, 210 (2023). https://doi.org/10.1186/s12935-023-03054-x. PMID: 37743482

polegał na:

- udziale w planowaniu eksperymentów
- udziale w analizie i interpretacji wyników
- przygotowaniu manuskryptu publikacji
- opiece merytorycznej nad mgr Mariolą Gimłą
- kierowaniu projektem Harmonia

Wydział Biologii
KATEDRA BIOLOGII i GENETYKI MEDYCZNEJ
Anna Herman-Antosiewicz
prof. dr hab. Anna Herman-Antosiewicz

12.3. Publikacja nr 3

Gimła Mariola, Hać Aleksandra, Reekie Tristan, Herman-Antosiewicz Anna

Impact of usnic acid pyrazole derivative on the metastatic potential and mitochondria of pancreatic cancer cells

Manuskrypt złożony do redakcji *BMC Cancer* 19.03.2025,
w procesie recenzji

Impact of usnic acid pyrazole derivative on the metastatic potential and mitochondria of pancreatic cancer cells

Mariola Gimła[1], Aleksandra Hać[1], Tristan A. Reekie[2] and Anna Herman-Antosiewicz[1*]

[1] Department of Medical Biology and Genetics, Faculty of Biology, University of Gdańsk, Gdańsk, Poland

[2] School of Science, University of New South Wales Canberra, Australian Capital Territory, Canberra, Australia

**Correspondence to:*

Anna Herman-Antosiewicz

Department of Medical Biology and Genetics

University of Gdańsk

Wita Stwosza 59

80-308 Gdańsk

Poland

Phone: +48 58 523 6304;

e-mail: anna.herman-antosiewicz@ug.edu.pl

Orcid: 0000-0003-0526-2168

Abstract

Background Pancreatic cancer is characterized by the highest mortality rate among cancer patients worldwide. Thus, the design of more effective therapies affecting different stages of pancreatic cancer development is strongly warranted. Recently, we reported the synthesis of a UA pyrazole derivative, named **5**, which was more active than the parent compound toward different cancer cells, including pancreatic cancer cells. It induced endoplasmic reticulum stress, cell cycle arrest and death of these cells, both growing *in vitro* and as xenografts in mice.
Methods The impact of UA and derivative **5** on cell motility and invasion was investigated using the scratch test and transwell invasion assay, respectively. The morphology of mitochondria was analyzed using electron microscopy. Epithelial-mesenchymal transition (EMT) markers and cell death were analyzed by immunoblotting and flow cytometry, respectively. Combination index (CI) analysis was used to assess the interaction of drugs.
Results The present work demonstrates that derivative **5** significantly inhibited migration and invasion of Mia PaCa-2 and PANC-1 human pancreatic cancer cells, while also modulating EMT markers. Additionally, it affected mitochondrial morphology and function, increasing mitochondrial length and decreasing ATP levels. The glycolysis inhibitor, 3-bromopyruvate (3BrPA), enhanced the **5**-induced decrease in ATP synergistically (CI=0.57). The combination of derivative **5** with 3BrPA increased cell death, shifting it from an apoptotic to a necrotic mode.
Conclusions These findings suggest that derivative **5** holds promise as a potential therapeutic agent for pancreatic cancer, targeting multiple cellular processes including migration, invasion, EMT, and energy metabolism.

Keywords Pancreatic cancer, metastasis, mitochondria, metabolism, cell death, usnic acid, 3-bromopyruvate

Background

Pancreatic cancer is the 12th leading cancer, however, it has the highest mortality rate. According to the latest Globocan report, 510,566 new cases and 467,005 deaths of pancreatic cancer patients were recorded in 2022. This disease ranks as the sixth leading cause of cancer mortality in both sexes combined and is responsible for almost 5% of all cancer deaths worldwide [1]. The incidence is rising and a two-fold increase is expected by 2030 [2].

Pancreatic ductal adenocarcinoma (PDAC), the most common type of PC, is highly heterogeneous at molecular and cellular levels, contributing to treatment resistance and low survival rates [3]. The disease's genetic complexity involves oncogenic activation of KRAS and mutations in tumor suppressor genes such as *TP53*, *SMAD4*, and *CDKN2A* [4-6]. The hyperaggressive disease evolves from non-invasive precursor lesions, making early detection challenging. Metastatic pancreatic cancer has significant challenges due to its aggressive nature, late diagnosis, and resistance to treatments [7]. Molecular mechanisms of metastasis in pancreatic cancer involve processes such as epithelial-mesenchymal transition (EMT), as well as NF-κB and KRAS signaling [3, 6-9]. Understanding the molecular mechanisms of metastasis and utilizing advanced imaging techniques and biomarkers are crucial in improving outcomes for patients with this devastating disease [9, 10]. The only effective treatment of PDAC is the surgical removal of the tumor, however, only 15-20% of patients are eligible for this at the time of diagnosis as they are required to have no metastases to lymph nodes or other organs [11]. Thus, the majority of patients must be treated with systemic chemotherapy. Despite substantial progress in recent years, chemotherapy remains largely ineffective in producing meaningful clinical responses or improving PDAC patient survival [12]. Adjuvant therapies with gemcitabine, FOLFRINOX and nab-paclitaxel only slightly improve survival rates and are highly toxic. For example, in the case of patients treated with gemcitabine, the first-line drug, only 5.4% show a response after using this chemotherapy agent [13, 14]. Data published in

2020 showed that the actual 5-year survival for patients diagnosed with pancreatic cancers of all stages between 2004 and 2011 was 4.2%. Surgically resected patients saw an actual 5-year survival of 17.4% while some 0.9% of non-resected patients passed the 5-year mark [15].

The limited efficacy of PDAC treatment prompts the search for new therapeutic options, also among compounds of natural origin and targeting specific pathways or organelles that are crucial for a given tumor. PDACs rely on ATP produced by oxidative phosphorylation (OXPHOS) from the mitochondria to grow and metastasize [16]. It has been shown that constitutively active oncogene KRAS (present in up to 90% of PDAC cases) is responsible, among others, for changes in mitochondrial morphology toward their fragmentation, which increases OXPHOS and allows for tumor progression [17, 18]. Thus, targeting mitochondria is a promising strategy, especially since pancreatic cancer stem cells, which are responsible for the failure of therapies and relapse of disease, are extremely sensitive to inhibition of mitochondria function as they are unable to increase compensatory glycolytic flux [19].

Derivatives of compounds that exist in nature are potential new chemotherapeutics. Usnic acid (UA, 2,6-diacetyl-7,9-dihydroxy-8,9b-dimethyldibenzo[b,d]furan-1,3(2H,9bH)-dione, 1) is a secondary metabolite found in lichens. It has been shown to inhibit cancer cell proliferation but might also be toxic to healthy cells, especially hepatocytes [20-22]. Thus, derivatives of UA are designed and tested to provide compounds that are more active and selective to cancer than noncancerous cells [23]. We recently reported the synthesis and antiproliferative activity of UA pyrazole derivative **5,** (*R*)-8-acetyl-5,7-dihydroxy-3,4a,6-trimethyl-1,4a-dihydro-4*H*-benzofuro[3,2-*f*] indazol-4-one [24, 25]. It inhibited the viability of different cancer cells at lower than UA concentrations and more importantly, noncancerous cells were less sensitive. Derivative **5** induced the release of calcium ions from the endoplasmic reticulum (ER) and ER stress, manifested by cell vacuolization. It was accompanied by G_0/G_1 cell cycle arrest and death of pancreatic cancer cells *in vitro* and tumor growth reduction *in vivo*

[25]. Recently, it was reported that another isoxazole derivative of UA (ISOXUS) targeted mitochondrial complex II, which reduced mitochondrial electron flow and oxygen consumption rate and translated into reduced viability of MCF-7 breast cancer cells [26].

In the present work, we focused on the ability of derivative **5** to inhibit other stages of cancer progression which led to metastasis. We investigated the impact of derivative **5** on pancreatic cancer cell migration and invasion, as well as the expression of epithelial-mesenchymal transition (EMT) markers. Moreover, as derivative **5** affected mitochondrial morphology and ATP level in the cells, we tested whether treatment of pancreatic cancer cells with the combination of derivative **5** and glycolysis inhibitor, 3-bromopyruvate (3BrPA), would be more effective in cancer cell eradication.

Methods

Reagents

The procedure of synthesizing UA pyrazole derivative **5** has been described in [24]. Fetal bovine serum (FBS), DMEM, penicillin/streptomycin antibiotic mixture and Matrigel were purchased from Corning (USA). (+)-UA, DMSO, and 3BrPA were purchased from Sigma–Aldrich (St. Louis, MO, USA). Antibodies for E-cadherin (cat. no. 3195), N-cadherin (cat. no. 13116), Vimentin (cat. no. 5741), Claudin-1 (cat. no.13255), Snail (cat. no. 3879), Slug (cat no. 9585) were purchased from Cell Signaling Technology (Danvers, MA, USA). Anti-β-actin antibodies conjugated with horseradish peroxidase (cat. no, A3854) were purchased from Sigma–Aldrich.

Cell culture conditions

The human pancreatic cancer cell lines, Mia PaCa-2 and PANC-1 were provided by Dr. I. Inkielewicz-Stępniak from the Medical University of Gdansk, Poland. Both cell lines were

tested for mycoplasma contamination before their use. Cells were maintained in DMEM containing 4 mM L-glutamine and 4500 mg/L of glucose. The basic medium was supplemented with 10% (v/v) FBS and a 1% penicillin-streptomycin mixture. Cells were maintained at 37 °C in a humidified atmosphere with 5% CO_2.

Migration assay

Cells were seeded into 12-well plates at a density of 3×10^5 cells per well and incubated for 24 h under standard conditions. Then, using a pipette tip, a scratch was made through the center of the well. The cell medium was removed, the wells were rinsed with PBS buffer and a new medium containing the tested compounds at appropriate concentrations was added. Photographic documentation was made using an Olympus IX 73 microscope (Olympus, Japan), immediately after the scratches were made and after 48 h. The images obtained were analyzed using the ImageJ program and the MR Wound Healing Tool.

Invasion assay

The effect of the investigated compounds on cell invasion was determined by invasion chambers coated with Corning Matrigel following the manufacturer`s instructions. Cells were seeded in 24-well invasion chambers at a density of 5×10^5 per well. The cells were treated with 1 or 5 μg/mL derivative **5** (which corresponds to 2.93 and 14.65 μM, respectively), UA (which corresponds to 2.90 and 14.5 μM, respectively) or an equivalent amount of DMSO. After 16 h non-invading cells were removed. Invaded cells were stained and counted using an Olympus IX 73 microscope (Olympus, Japan) at 40x magnification.

Cell death determination

The effect of the investigated compounds on cell death was determined by Muse™ Cell Analyzer (Millipore). Cells were seeded in 6-well plates at a density of 2×10^5 per well. After 24 h, the cells were treated with derivative **5** alone or with 3BrPA, or an equivalent amount of DMSO. After 48 h, both medium and trypsinized cells were collected, centrifuged for 10 min at 300 × g, stained using the Muse ™ Annexin-V & Dead Cell Assay Kit, and counted by flow cytometry.

ATP level measurement

Cells were seeded at a density of 4×10^3 per well of a 96-well plate and allowed to attach overnight. The medium was replaced with the fresh medium supplemented with desired concentrations of derivative **5**, 3BrPA, or a combination of both for 48 h. ATP level was determined by ATPlite Luminescence ATP Assay System (PerkinElmer, Waltham, MA, USA), following the manufacturer's protocol. The combination index (CI) was calculated by: $CI = CD5/(IC50)_{D5} + CBr/(IC50)_{Br}$, wherein CD5 and CBr are the concentrations of the derivative **5** and 3BrPA that in combination cause a 50% drop in ATP; $(IC50)_{D5}$ and $(IC50)_{Br}$ are the concentrations of derivative **5** and 3BrPA that individually reduce ATP to 50% of that in control cells. CI value <1 indicates synergism [27, 28].

Transmission electron microscopy (TEM)

Transmission electron microscopy was performed as described previously [29]. Briefly, cells (2×10^5) were plated in 12-well plates and allowed to attach overnight. Next, the cells were treated with either DMSO (control), 1 or 5 μg/mL derivative **5** for 24 or 48 h at 37 °C. For TEM, cells were fixed in ice-cold 2.5% electron microscopy grade glutaraldehyde (Polysciences) in PBS (pH 7.4). The samples were rinsed with PBS, postfixed in 1% osmium tetroxide with 0.1%

potassium ferricyanide, dehydrated through a graded series of ethanol washes (30–100%), and embedded in Epon (Fluka). Semithin (300 nm) sections were cut using an RMC Power Tome XL ultramicrotome, stained with 0.5% toluidine blue and examined under a light microscope. Ultrathin sections (65 nm) were cut using a Leica UC7 ultramicrotome, stained with Uranyless (Delta Microscopies) and Reynold's lead citrate (Delta Microscopies), and examined on a Tecnai G2 Spirit BioTWIN transmission electron microscope at 120 kV. The size of mitochondria was determined using ImageJ Software.

Immunoblotting

Cells were treated with 5 μg/mL derivative **5** or UA (2.93 and 2.90, respectively) for 48 h and lysed using a solution containing 50 mM Tris (pH 7.5), 1% Triton X-100, 150 mM NaCl, 0.5 mM EDTA, protease and phosphatase inhibitor cocktails (Roche Diagnostics). The lysates were cleared by centrifugation. Proteins were separated by SDS–PAGE and transferred onto a PVDF membrane. The membrane was blocked with 5% nonfat dry milk in phosphate-buffered saline and incubated overnight with the desired primary antibody at 4 °C. The membrane was then treated with the appropriate secondary antibody for 1 h at room temperature. Immunoreactive bands were detected with an enhanced chemiluminescence reagent (Thermo Scientific). Blots were stripped and reprobed with anti-β-actin antibodies to normalize for differences in protein loading. Each protein was detected three times in independently prepared lysates. Densitometry analysis was performed using Quantity One 1-D Analysis software (Bio-Rad).

Statistical analysis

All data are shown as the means ± standard error of measurement (SEM) of at least three independent experiments. The significance of differences between the control and treated cells

ANOVA and Dunnett's or Sidak's multiple comparison *post hoc* tests using GraphPad Prism (version 8). Differences were considered significant at $p < 0.05$.

Results

UA derivative 5 decreases the migratory and invasive potential of pancreatic cancer cells

Our previous results showed that derivative **5** potently reduced the viability of various cancer cell lines while non-cancerous cells were more resistant to the compound, suggesting its potential therapeutic use [24, 25]. Mechanisms of its action involved the release of calcium ions from the ER, which led to ER stress and massive cell vacuolization, G_0/G_1 cell cycle arrest and cell death of pancreatic cancer cells *in vitro* and *in vivo*, in a mouse xenograft model [25].

Here, the potential of derivative **5** in inhibiting pancreatic cancer cell migration and invasion was investigated. The wound healing assay revealed that migration of Mia PaCa-2 was reduced to 51 and 23% of control by derivative **5** used at 1 or 5 μg/mL with *p* values 0.0003 and $p<0.0001$, respectively (Fig. 1A, C). Migration of PANC-1 cells was reduced to 19 or 29% compared with controls by derivative **5** at 1 or 5 μg/mL, respectively (with $p<0.0001$) after the 48 h exposition (Fig. 1B, D). Differences in motility between cells treated with lower and higher concentrations of 5 were statistically insignificant. The effect of UA on the migration of both cell lines was negligible compared to control cells (Fig. 1).

In addition, derivative **5** reduced the invasion capacity of both cell lines when used at a higher concentration. The level of invading cells was lowered to 48.5% or 44% for Mia PaCa-2 and PANC-1 cells, respectively, when treated with 5 μg/mL derivative **5,** which were significant changes ($p<0.05$). The parental compound, UA, had a less profound effect; however, differences between UA-treated cells and control cells as well as between UA- and **5**-treated cells were statistically insignificant (Fig. 2).

Figure 1

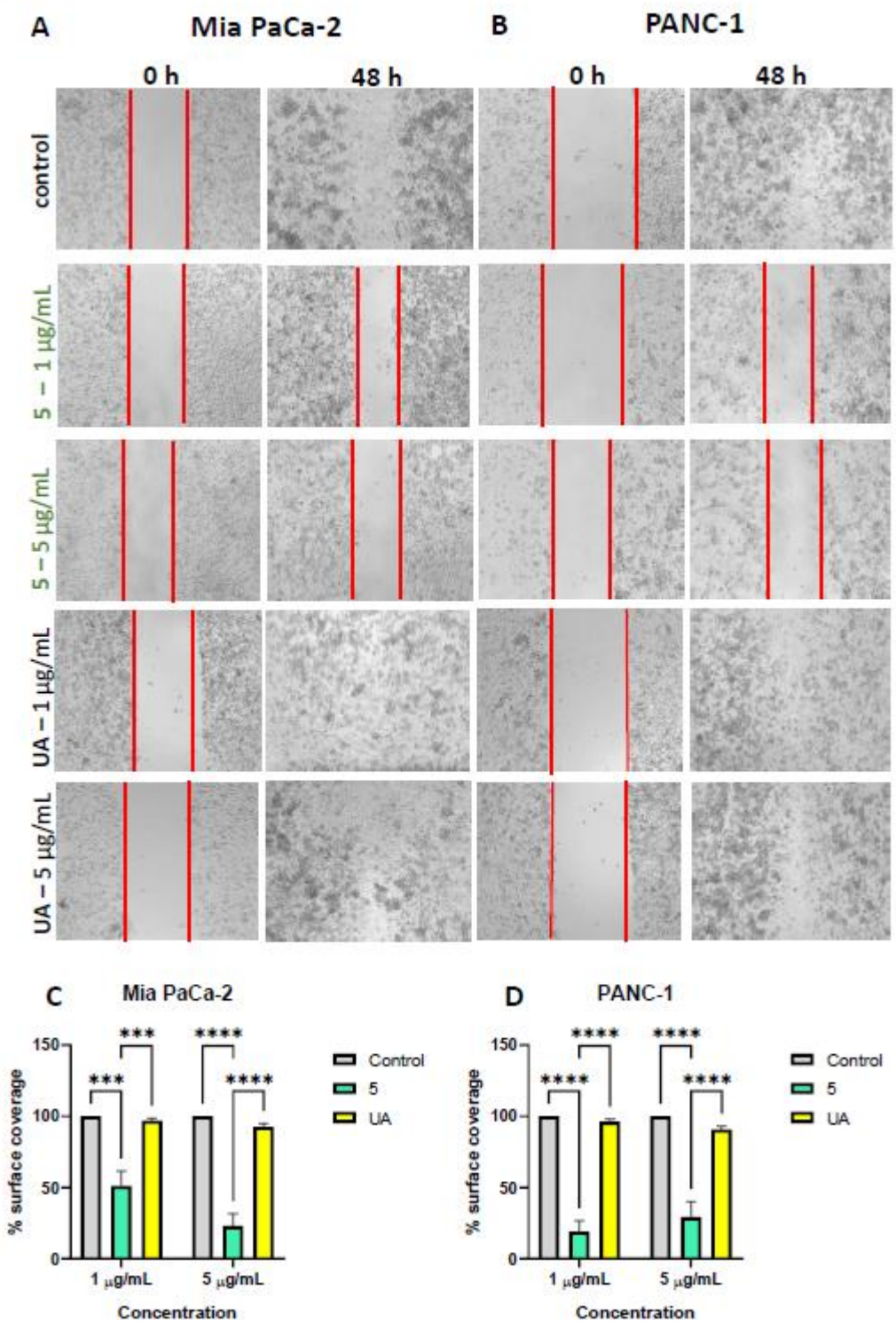

Fig. 1 Derivative **5** inhibits pancreatic cancer cell migration. Confluent Mia PaCa-2 (**A and C**) and PANC-1 (**B and D**) were wounded with a tip and treated with DMSO (control), derivative **5** or UA at the indicated concentration for 48 h. Migration through the wound was examined

under a light microscope (magnification 20×), and representative pictures are shown. Changes in surface areas were analyzed using the ImageJ program. Data are means ± SEM of three experiments, in each four randomly chosen fields were examined. Statistical significance was determined with ANOVA and Sidak's multiple comparison test; ***p<0.001, ****p<0.0001.

Figure 2

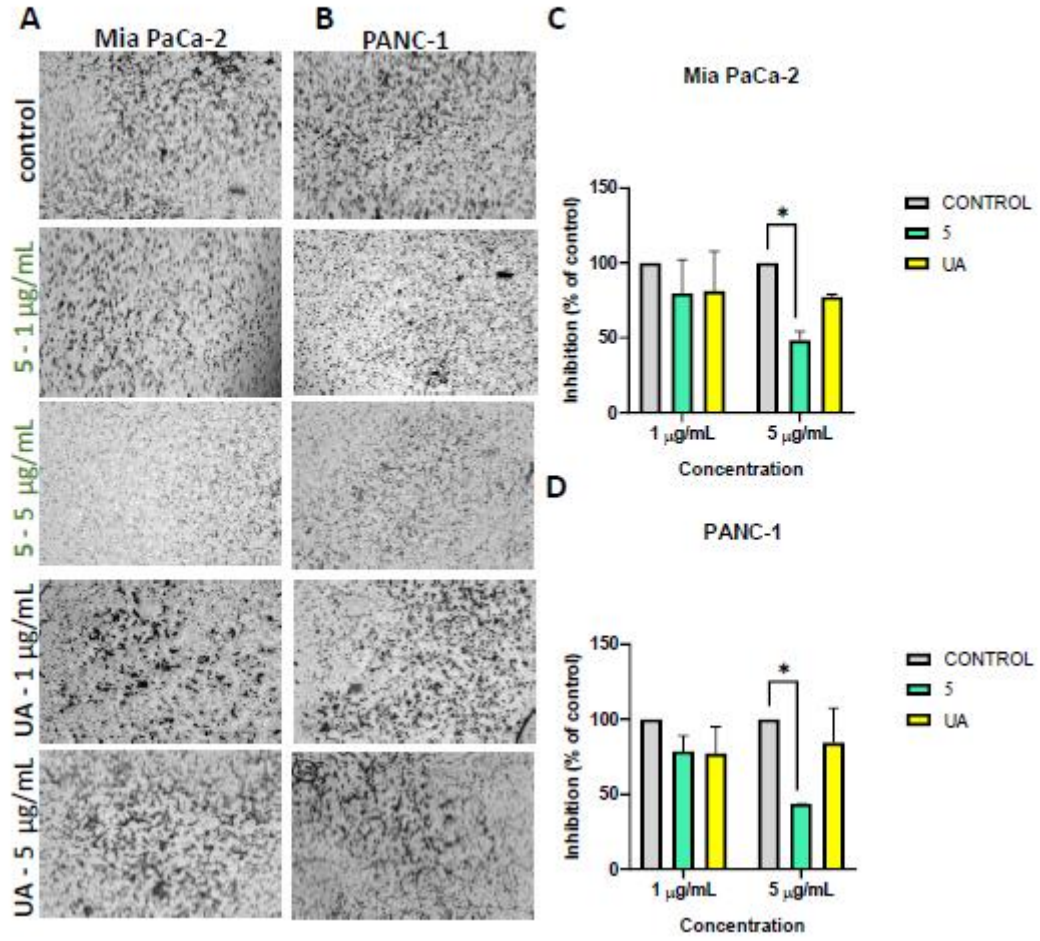

Fig. 2 Effect of derivative **5** and usnic acid (UA) on the invasion of Mia Paca-2 (**A and C**) and PANC-1 (**B and D**) cells. Boyden chamber assay was performed after 16 h treatment with **5** or UA at indicated concentrations or DMSO (control) and invaded cells were counted. Data are means ± SEM of three experiments. Statistical significance was determined with ANOVA and Sidak's multiple comparison test; *p<0.05.

Using the Western blot technique, the levels of EMT markers were determined after treatment with the derivative **5** or UA at the higher concentrations, which had a more evident effect on invasion. In Mia PaCa-2 cells, both **5** and UA slightly increased the E-cadherin level compared with the control (about 1.3 fold). In PANC-1 cells, only derivative **5** had such an effect on the E-cadherin level, while UA reduced it. The most spectacular effect was observed for Claudin-1 protein level, which was elevated 6.6-fold and 4.7-fold in derivative **5**-treated Mia PaCa-2 and PANC-1 cells, respectively. UA's impact on this protein was less potent: it reduced Claudin-1 in Mia PaCa-2 or had almost no effect in PANC-1 (Fig. 3, upper part).

The impact of tested compounds on proteins typical for mesenchymal cells (N-cadherin and Vimentin) was also cell-line specific. In Mia PaCa-2 cells, N-cadherin levels decreased by 85% and Vimentin levels by 60% when treated with derivative **5**. In UA-treated cells, these changes were weaker: N-cadherin and Vimentin levels were reduced by 40% and 10%, respectively. In PANC-1 cells, derivative **5** decreased N-cadherin by almost 30% and did not affect Vimentin level. Both proteins were slightly affected by UA (reduction by about 10%) (Fig. 3, middle part).

Transcription factors involved in EMT were also compared in control, **5** and UA-treated cells. As shown in Fig. 3, in MiaPaCa-2 cells, derivative **5** did not affect levels of Snail and ZEB-1; however, it reduced Slug levels by 40%. UA decreased Snail by 30%, Slug - by 10%, but increased ZEB-1 by 80% in these cells. In PANC-1 cells, derivative **5** had the strongest effect on Slug, which dropped by 80%. Snail level was also reduced (by 40%), while ZEB-1 increased by 80% in derivative **5**-treated cells. UA reduced levels of all transcription factors in PANC-1 cells: by 30, 40 or 60% in the case of Snail, Slug and ZEB-1. It is worth noting that the reduction of Snail and Slug levels was more pronounced by derivative **5**- than UA-treated PANC-1 cells (Fig. 3, lower part).

Figure 3

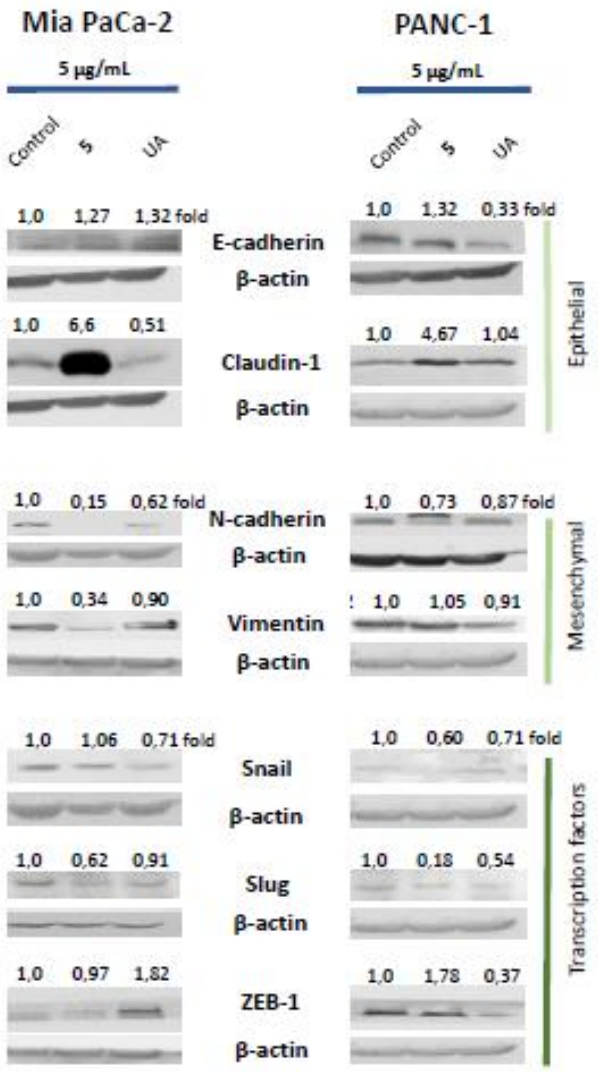

Fig. 3 Levels of proteins involved in the EMT process. Mia PaCa-2 and PANC-1 pancreatic cancer cells were treated with DMSO (control), derivative **5** or usnic acid (UA) for 48 h. Densitometric analysis results after correction for loading control (β-actin) and relative to respective controls are shown on top of bands. Representative results from three independent experiments are shown.

Derivative 5 changes mitochondrial morphology and ATP production in pancreatic cancer cells

One of the elements that determines the high aggressiveness of pancreatic cancer is its strong ability to form metastasis and relapses. Experimental data indicate that PDAC, especially with *KRAS* mutations, is characterized by fragmented mitochondria, which better sustain tumor needs. Moreover, increased mitochondrial fission in pancreatic cancer cells is associated with higher cell growth, migration, and drug resistance [30]. We examined the effect of compound **5** and UA on mitochondrial morphology in a cellular model of pancreatic cancer. We noticed changes in the length, but not the width, of mitochondria in Mia PaCa-2 cells treated with derivative **5** compared to control cells (Fig. 4). Mitochondria became longer after 24 and 48 hours of treatment (although in the latter case, 1 μg/mL induced insignificant changes). UA-induced changes were not statistically significant compared to control cells; however they were significant compared with **5**-treated cells (p=0.0002 and p=0.0005 in cells treated with 1 or 5 μg/mL concentrations for 24 h, respectively; p=0.0005 in cells treated with 5 μg/mL concentrations for 48 h; Fig. 4B, D). The width of mitochondria of Mia PaCa-2 cells was significantly reduced only by UA compared to derivative **5** used in higher concentration for a longer time (p=0.0076, Fig. 4E). In the case of the PANC-1 cell line, derivative **5** also caused an increase in the length of mitochondria. However, statistically significant changes were noted when cells were exposed to derivative **5** for a longer time compared to controls (p<0.0001 and p=0.0008 for 1 and 5 μg/mL concentrations, respectively) and compared to UA (p<0.0001 and p=0.0045 or 1 and 5 μg/mL concentrations, respectively; Fig. 5B, D). Treatment with derivative **5** for 24 h slightly increased mitochondrial length, which was significant only compared to UA treatment at concentration 5 μg/mL (p=0.024; Fig. 5A). The impact of tested compounds on mitochondrial width in PANC-1 cells was less potent and statistically significant reduction was observed after 24 h treatment with derivative **5** (p=0.0179) or UA (p=0.0253) at higher

Figure 4

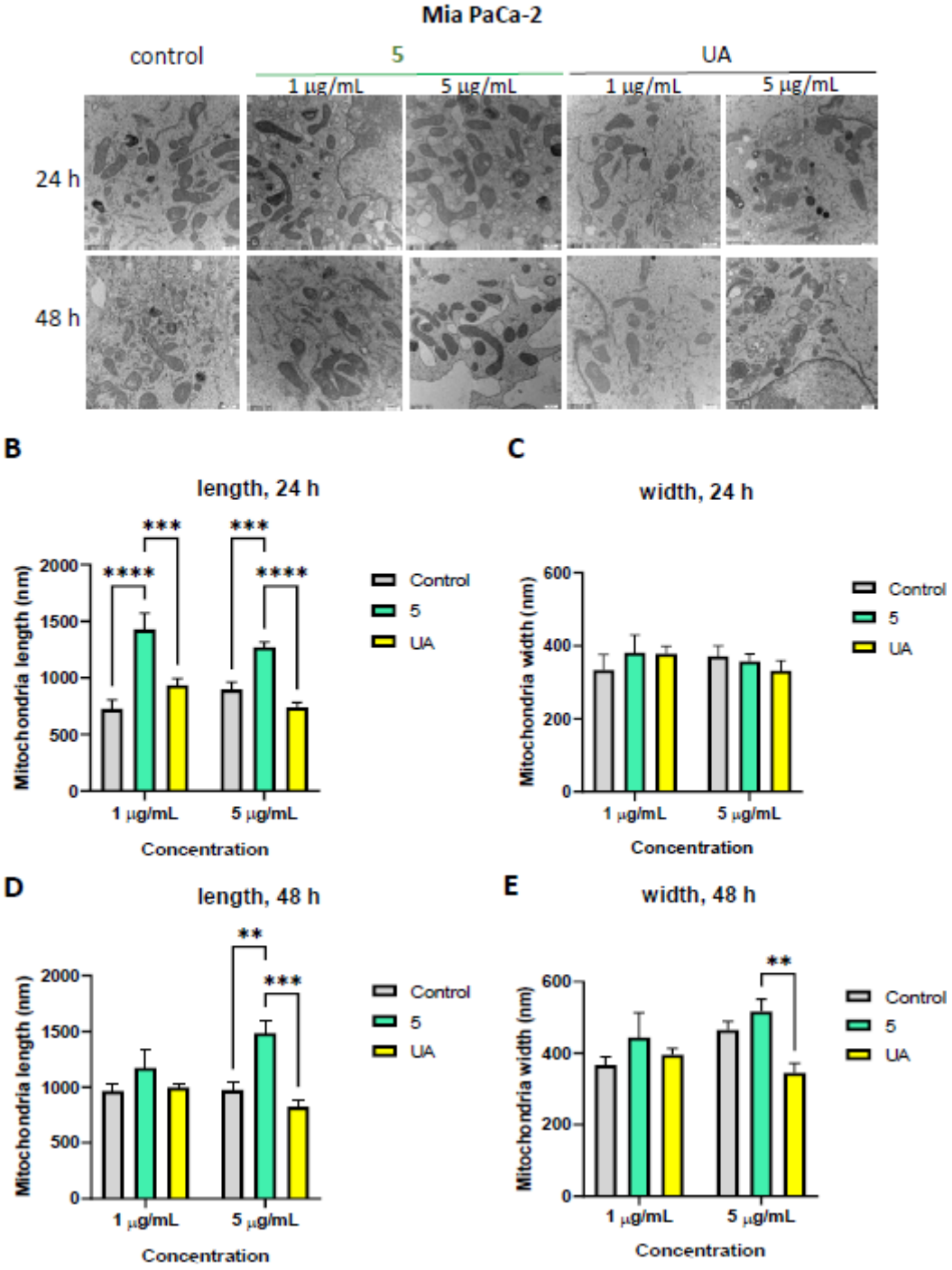

Fig. 4 Morphology of mitochondria in Mia PaCa-2 cells examined under TEM (**A**). Representative photographs of cells at 18500× magnification. Cells were treated with DMSO (control), derivative **5** or usnic acid (UA) at indicated concentrations. Mitochondrial length and width were measured after 24-h treatment (**B and C**, respectively) or 48-h treatment (**D and E**,

respectively). Data are means ± SEM of three experiments, in each a minimum of six mitochondria were observed per cell, replicated across three independent trials per experimental variant. Statistical significance between control and derivative **5** or UA-treated cells was determined with ANOVA and Sidak's multiple comparison test; $^{**}p<0.01$, $^{***}p<0.001$, $^{****}p<0.0001$. No markings were used in the absence of statistical significance.

Figure 5

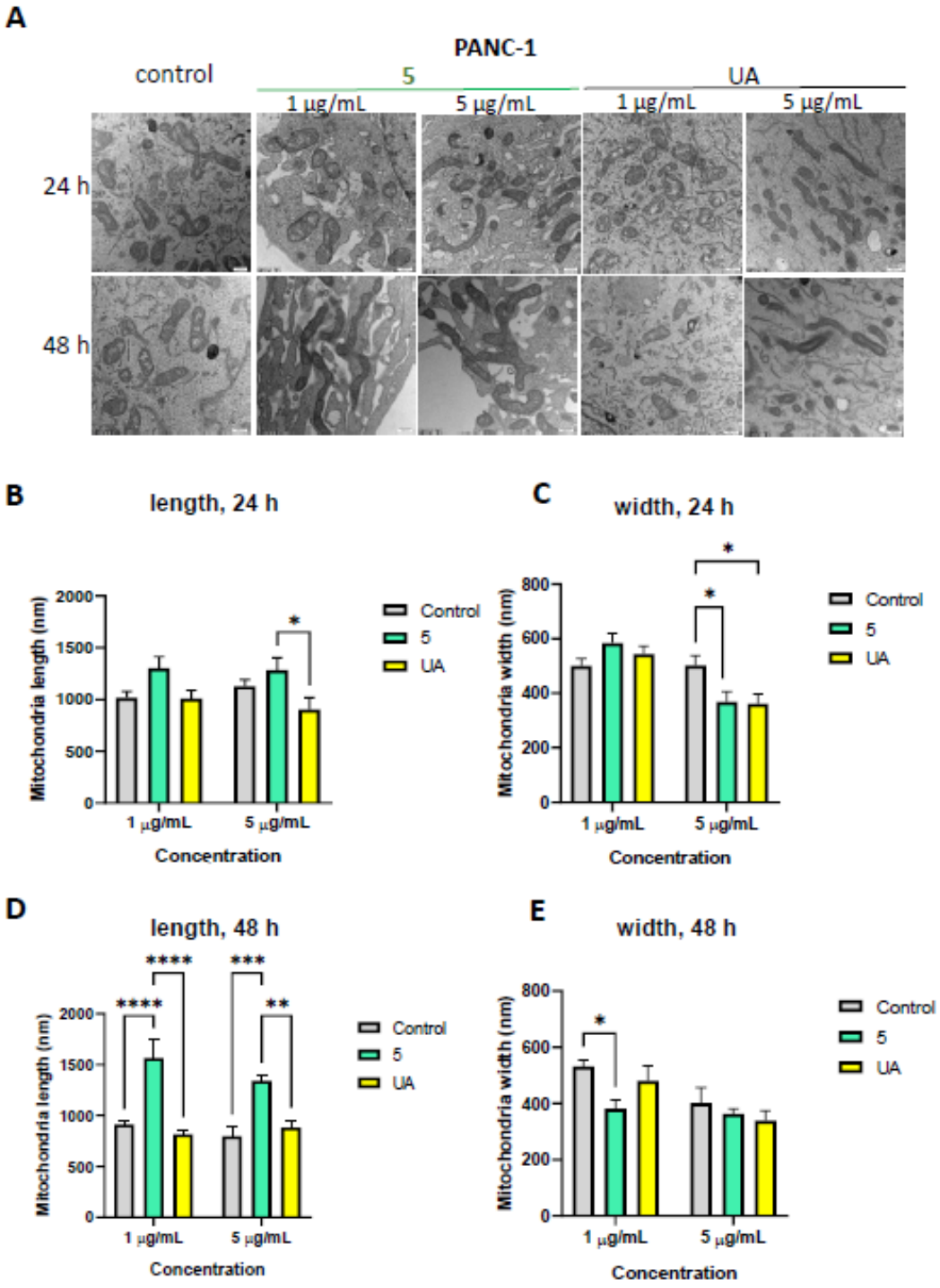

Fig. 5 Morphology of mitochondria in PANC-1 cells examined under TEM (**A**). Representative photographs of cells at 18500× magnification. Cells were treated with DMSO (control), derivative **5** or usnic acid (UA) at indicated concentrations. Mitochondrial length and width were measured after 24-h treatment (**B and C**, respectively) or 48-h treatment (**D and E**,

respectively). Data are means ± SEM of three experiments, in each a minimum of six mitochondria were observed per cell, replicated across three independent trials per experimental variant. Statistical significance between control and derivative **5** or UA-treated cells was determined with ANOVA and Sidak's multiple comparison test; *p<0.05, **p<0.01, ***p<0.001, ****p<0.0001. No markings were used in the absence of statistical significance.

concentrations and after 48-h treatment with derivative 5 (p=0.0261) at 1 μg/mL (Fig. 5C, D). UA had almost no effect on mitochondrial morphology compared to control cells (Fig. 5).

As changes in the mitochondrial length were more pronounced in Mia PaCa-2 cells, we used this cell line to elucidate whether they correlate with ATP production. As shown in Fig. 6A, ATP levels decreased to 86%, 79%, and 55% of the control level in Mia PaCa-2 cells treated for 48 h with derivative **5** at 0.25, 0.5 or 1 μg/mL concentrations, respectively. Changes observed for 0.5 and 1 μg/mL derivative **5** were statistically significant with p values of 0.007 or below 0.0001, respectively.

3BrPA potentiates the energetic drop and antiproliferative activity of derivative 5

As derivative **5** impacts the morphology of mitochondria and reduces ATP level, we hypothesized that additional blocking of glycolysis can potentiate energetic crisis and cell death. We used 3BrPA, a widely used glycolysis inhibitor, and first determined its impact on ATP levels in Mia PaCa-2 cells. 3BrPA dose-dependently reduced ATP level in these cells: to 90% (p=0.015), 68% and 48% of control (in both cases p<0.0001) when used at 25, 50 or 75 μM concentration, respectively (Fig. 6B). Next, we combined 50 μM 3BrPA with derivative **5** used at 0.1, 0.25, 0.5 or 1 μg/mL concentrations, and observed higher reduction of the ATP level than in case of any of the compounds used alone, to 48, 34, 21 and 16% of control level (Fig. 6C). The combination index (CI) was calculated as 0.57 which indicates synergistic activity of 3BrPA and derivative **5** in decreasing ATP levels in cancer cells.

The effect of combined treatment on cell death induction was evaluated. The percentage of live, apoptotic and necrotic Mia PaCa-2 cells was determined using flow cytometry detection of Annexin V bound to externalized phosphatidylserine in apoptotic cells and membrane permeabilization by the accumulation of 7-aminoactinomycin D (7-AAD) dye. Derivative **5** alone decreased live cells and increased the fraction of apoptotic cells in a dose-dependent

Figure 6

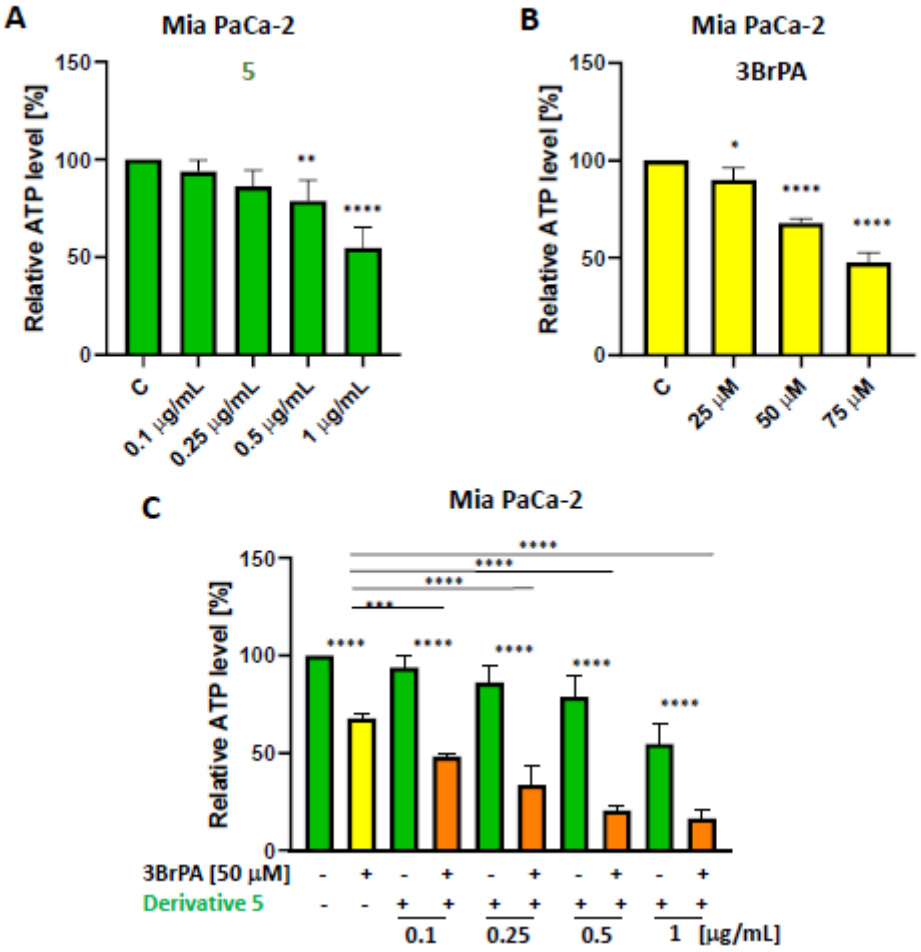

Fig. 6 Derivative **5** and 3BrPA combination more effectively reduces ATP than any of the compounds used alone. Cells were treated with indicated concentrations of derivative **5** alone (**A**), 3BrPA (**B**) alone or a combination of 50 µM 3BrPA with 0.1, 0.25, 0.5 or 1 µg/mL derivative **5** for 48 h (**C**). ATP level was measured using the ATPlite Luminescence Assay System (PerkinElmer) and was calculated relative to the value for control cells (100%). Data are means ± SEM of three experiments. Statistical significance was determined with ANOVA and Dunnett's (A, B) or Sidak's (C) multiple comparison tests; *p<0.05, **p<0.01, ***p<0.001, ****p<0.0001.

manner: 0.25 µg/mL concentration had almost no effect on live and death fractions while 0.5 and 1 µg/mL derivative **5** increased apoptotic cells to 15% and 48%, respectively, with no effect on necrosis induction after 48 h of treatment. 3BrPA alone, on the other hand, did not induce apoptosis but increased the fraction of necrotic cells, which was the lowest for 50 µM 3BrPA (3.5%) and the highest for 100 µM 3BrPA (85%). Thus, for the combined treatment, we used 50 µM 3BrPA and lower concentrations of derivative **5** (0.25 or 0.5 µg/mL), which alone minimally induced cell death. As shown in Fig. 7C, 50 µM 3BrPA potentiated the reduction of live cells treated with derivative **5** at 0.25 µg/mL (to 71 vs. 95, combination vs. derivative **5** alone, $p<0.0001$). The percentage of dead cells increased in cells treated with a combination compared to those treated with any compound alone (in each case, $p<0.0001$). Interestingly, the mode of cell death changed from apoptotic, observed for derivative **5** at 0.5 µg/mL concentration alone, to necrotic in combination with 3BrPA (Fig. 7D).

Discussion

Pancreatic cancer is characterized by its aggressive nature and high metastatic potential, making it one of the most lethal malignancies worldwide [9, 31]. The ability of pancreatic cancer cells to migrate and invade surrounding tissues is a critical factor in disease progression and metastasis [32, 33]. Thus, recent research focuses on developing novel therapeutic agents that effectively target these processes. In this context, pyrazole UA derivative **5** is emerging as a promising compound with significant anti-migratory and anti-invasive properties against pancreatic cancer cells. The observed reductions in migration ability (50-80%) and invasion capacity (40-50%) in both Mia PaCa-2 and PANC-1 cell lines suggest that derivative **5** could potentially impede the metastatic spread of pancreatic cancer.

The EMT is a crucial process in cancer progression, enabling tumor cells to acquire a more invasive phenotype [34, 35]. A loss of epithelial markers, including E-cadherin, and tight

Figure 7

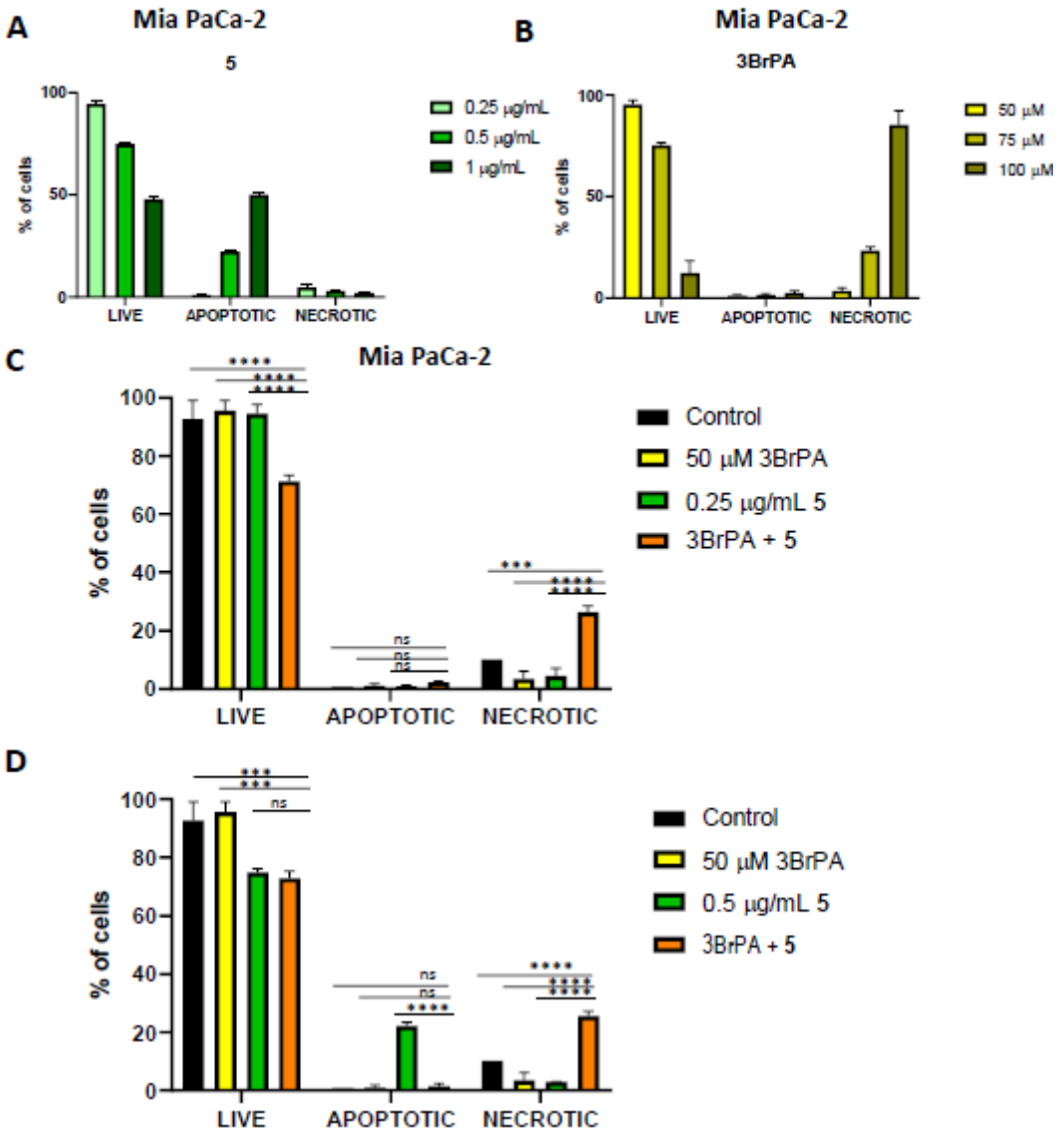

Fig. 7 Co-treatment with 3BrPA and derivative **5** changes the cell death profile. Percentage of live, apoptotic and necrotic cells after 48 h of treatment with derivative 5 (**A**), 3BrPA (**B**) and a combination of the two compounds (**C and D**). Data are means ± SEM of three experiments. Statistical significance was determined with ANOVA and Sidak's multiple comparison test: ***p<0.001, ****p<0.0001, ns.- non-significant.

junction proteins characterizes EMT. The ability of derivative **5** to alter EMT markers, increasing epithelial proteins while decreasing mesenchymal proteins, indicates its potential to reverse or inhibit this process. This effect, especially the significant increase in Claudin-1 protein levels, suggests that derivative **5** may help maintain epithelial integrity and reduce the metastatic potential of pancreatic cancer cells. Claudins are components of tight junctions that are responsible for contact between epithelial cells. Perturbation of the tight junction structure and loss of cell-to-cell association are essential for the invasion process. Downregulation of Claudin-1 gene (*CLDN1)* expression has been shown in numerous pancreatic cancer cell lines and tumor tissues, which correlated with cancer progression and shorter survival of pancreatic cancer patients [36, 37]. Overexpression of Claudin-1 in Mia PaCa-2 and FG cells inhibited their proliferation. Moreover, demethylation of the *CLDN1* promoter by DNMT inhibitor, SGI-1027, increased the protein level, which caused a decrease in cell viability both *in vitr*o and *in vivo*, and a reduction of EMT and stem cell markers. Thus, the authors postulated targeting Claudin-1 gene suppression as a strategy for effective pancreatic cancer therapy [37].

Among transcription factors involved in the repression of Claudin-1 or E-cadherin genes and activation of N-cadherin gene expression are Snail, Slug and ZEB-1 [36, 38-40]. Our results indicate that derivative **5** modulates their level, albeit to a different extent in the tested pancreatic cell lines. The most pronounced effect is observed in the case of the Slug transcription factor in both cell lines treated with derivative **5**.

Mitochondria play a vital role in cancer cell metabolism and survival [41-45]. They can change their morphology to optimize metabolic functions in response to cellular demands, and a balance between fission and fusion is involved in the regulation of bioenergetics adaptation to nutrient availability, proliferation, autophagy or apoptosis [46]. Recent evidence shows that mitochondrial fragmentation is associated with cancer progression and therapy resistance (reviewed in [47, 48]). Interestingly, pancreatic cancer cells exhibit highly fragmented

mitochondria, a phenomenon associated with increased mitochondrial fission and their number [17, 49]. It has been shown that shifting the balance toward mitochondrial fusion promoted mitophagy while reducing mitochondrial mass, oxygen consumption rate (OCR) and ATP production, all together retarded pancreatic tumor growth and metastasis [49]. Results of our work indicate that derivative **5** induces changes in mitochondrial morphology toward their elongation, which, similar to work by Yu et al. [49], correlates with the reduction of ATP levels in pancreatic cancer cells. This energy metabolism disruption could contribute to the compound's anti-cancer effects by limiting the energy available for cellular processes, including migration and invasion.

Correlation between increased fusion of mitochondria and decreased ATP may be related to increased mitophagy and reduction in mitochondria mass, as was reported by Yu et al. [49] or decreased glycolytic flux as reported by Nagdas et al. [17]. Lower ATP production from oxidative phosphorylation was also observed in breast cancer cells with deleted fission proteins, such as Drp1 or Fis1 [50]. Although altered respiration was accompanied by increased glycolytic ATP synthesis, it was not sufficient to fully compensate for drop in OXPHOS-mediated ATP production. Thus, reduction in mitochondria fission resulted in decreased maximal bioenergetics potential in these cells [50].

Cancer cells rely on aerobic glycolysis as an energy source; thus, inhibitors of glycolysis are regarded as promising selective anticancer agents. One such compound is 3BrPA, a small molecule alkylating agent. It targets glycolytic enzymes such as hexokinase II (HKII), which is selectively expressed in cancer cells and is the main driver of the “Warburg effect”, or glyceraldehyde-3-phosphate dehydrogenase (GAPDH) and 3-phosphoglycerate kinase (3-PGK) [51-55]. Moreover, recent reports showed that 3BrPA can inhibit other metabolic enzymes, such as lactate dehydrogenase (LDH), pyruvate dehydrogenase (PDH), or enzymes participating in the TCA cycle, glutaminolysis, and OXPHOS [54, 56]. Numerous data indicate

its anticancer activity, mostly by reducing ATP levels and thus, cell metabolism and anabolic processes (rev. in [57]) and leading to apoptosis or necrosis, depending on the concentration used. For example, in HL60 human myeloid leukemia cells, 3BrPA induced both apoptosis and necrosis at 20–30 μM and an almost exclusively necrotic death at 60 μM concentration [58]. 3BrPA has also been successfully tested in combination with other anticancer drugs. For instance, it has been shown that co-treatment with 3BrPA and cetuximab had a synergistic antiproliferative effect in colorectal cancer cells, suggesting potential for overcoming cetuximab resistance [59].

In the case of Mia PaCa-2 cells, we observed minimal effect on apoptotic cell number but slight necrosis induction by 50 μM 3BrPA, and significant necrosis when the compound was used at 75 or 100 μM concentration. It correlated with the extent of ATP level reduction. The combination of 3BrPA with derivative **5** potentiated a drop in ATP level and it was the synergistic effect. It is noteworthy that both compounds were used at low concentrations, which are not cytotoxic when used as single treatments. This is consistent with the advantage of combination therapies over monotherapies, giving the possibility to reduce doses of used therapeutics and thus cause fewer side effects and avoid drug resistance development by cancer cells while retaining anticancer potential.

In our model, 3BrPA and derivative **5** applied together at nontoxic concentrations induced necrotic cell death. It is particularly interesting and worth further research as necrosis is an immunogenic process, and thus has the potential to boost anti-cancer response *in vivo*.

Results presented in this work suggest that simultaneously targeting both mitochondrial function and glycolysis can be a powerful strategy against pancreatic cancer. This approach aligns with the growing understanding of cancer metabolism and the potential of metabolic targeting in cancer therapy. These findings highlight the multifaceted effects of derivative **5** on pancreatic cancer cells, targeting key processes involved in cancer progression and metastasis

(Fig. 8). The compound's ability to inhibit migration and invasion, modulate EMT, disrupt mitochondrial function, and synergize with a metabolic inhibitor, presents a promising avenue for further research in pancreatic cancer treatment.

We present results obtained *in vitro,* which is the main limitation of this work. In the future, the anti-metastatic activity of derivative **5,** as well as potentiation of its activity by glycolysis inhibition, should be tested *in vivo*. Our previous work showed that derivative **5** effectively reduced tumor growth in mice xenografted with Mia PaCa-2 cells and did not reveal toxicity when administered orally at 400 mg/kg three times a week for a month. However, the pharmacokinetics of this compound have not been investigated yet. Rather weak water solubility and the need to use it in high concentrations stimulate the need for development of drug delivery systems based on nanocarriers. Such constructs have been used to improve the therapeutic index of parent UA, which is comprehensively discussed by Zugic et.al. [60].

Conclusions

The pyrazole UA derivative **5** demonstrates significant potential as a novel therapeutic agent for pancreatic cancer, addressing several critical aspects of this aggressive malignancy. Derivative **5** effectively reduces the migration and invasion of pancreatic cancer cells, which indicates its anti-metastatic potential. By altering EMT markers, especially increasing Claudin-1 levels, the compound may prevent or reverse the EMT process, maintaining epithelial integrity and reducing metastatic potential. Changes in mitochondrial morphology and reduced ATP production indicate the compound's ability to interfere with cancer cell energy metabolism, limiting resources for cellular processes like migration and invasion. The combination of derivative **5** with the glycolysis inhibitor, 3BrPA, shows promising results in reducing ATP levels and increasing cell death, suggesting a potent dual-targeting strategy. By simultaneously targeting migration, invasion, EMT, and energy metabolism, derivative **5** addresses multiple

aspects of pancreatic cancer progression. These findings collectively position pyrazole UA derivative **5** as a promising candidate for further investigation in pancreatic cancer treatment, potentially offering a new approach to combat this lethal malignancy.

Figure 8

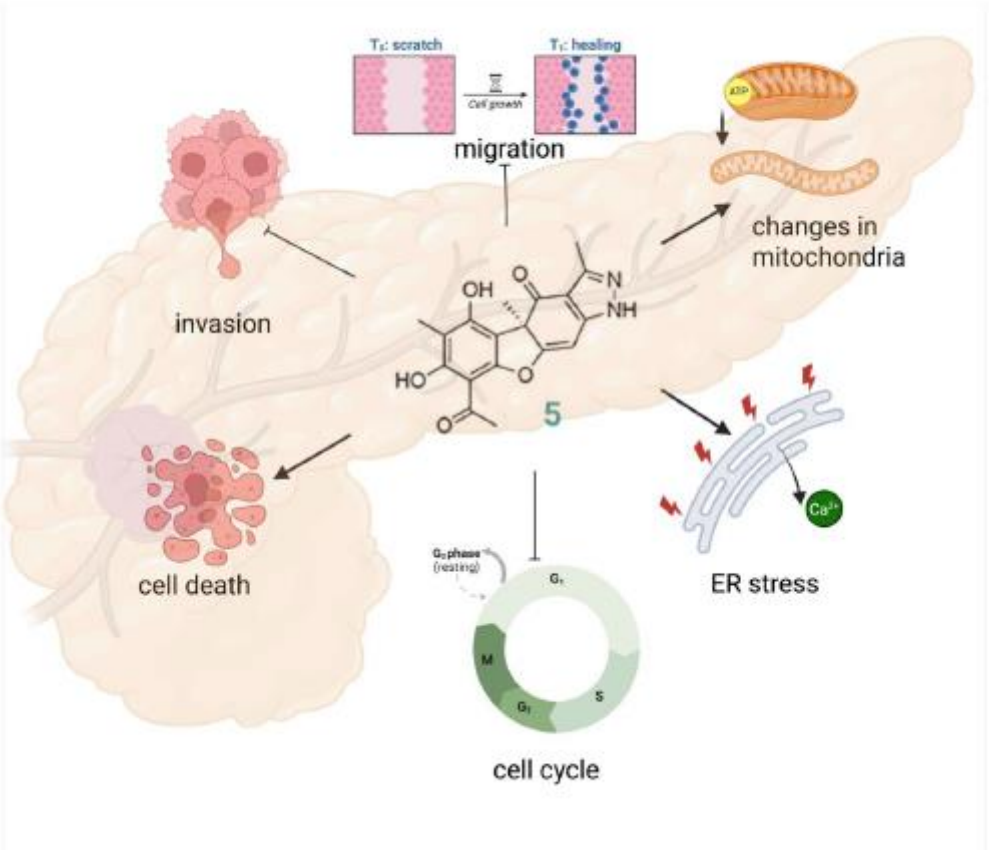

Fig. 8. Summary of the mechanisms of derivative **5** action in pancreatic cancer cells. The pyrazole derivative of UA inhibits the proliferation of cancer cells, inducing G_0/G_1 phase cell cycle arrest and cell death. It also reduces migration and invasion of pancreatic cancer cells, induces morphological alterations in their mitochondria, as well as energetic and ER stress that altogether lead to cell death (based on results presented in this work and in (24)). Created with BioRender.com.

Abbreviations

7-AAD	7-Aminoactinomycin D
3BrPA	3-Bromopyruvate
CI	Combination index
DNMT	DNA methyltransferase
ER	Endoplasmic reticulum
EMT	Epithelial-mesenchymal transition
GAPDH	Glyceraldehyde-3-phosphate dehydrogenase
HK II	Hexokinase II
LDH	Lactate dehydrogenase
OCR	Oxygen consumption rate
OXPHOS	Oxidative phosphorylation
PDAC	Pancreatic ductal adenocarcinoma
3-PGK	3-Phosphoglycerate kinase
PDH	Pyruvate dehydrogenase
TCA	Tricarboxylic acid
TEM	Transmission electron microscopy
UA	Usnic acid

Declarations

Ethics approval Not applicable.

Consent for publication Not applicable.

Data availability

The data supporting the findings of this study are available from the corresponding author upon reasonable request.

Competing interests A. H-A., M. G., T. A. R. have patent related to this work (patent no PL 246171 issued to the University of Gdańsk). The authors have no other competing interests to declare.

Funding

This research was supported by the National Science Centre, Poland (project no. 2017/26/M/NZ7/00668 to A.H.-A) and University of Gdańsk, Poland (grants no. 539-D130-B859-21 and no. 539-D130-B953-22 to M.G.).

Author contributions

MG and AH-A conceived the experiments; TAR synthesized **5**; MG designed and performed the experiments; MG, AH and AH-A analyzed and interpreted the data. MG and AH-A wrote the original draft of the manuscript. MG, AH, TAR and AH-A reviewed and edited the manuscript. All authors read and approved the final manuscript.

Acknowledgments

The authors thank Dr. M. Narajczyk (Bioimaging Laboratory, Faculty of Biology, University of Gdańsk) for technical assistance.

References

1. Bray F, Laversanne M, Sung H, Ferlay J, Siegel RL, Soerjomataram I, Jemal A. Global cancer statistics 2022: GLOBOCAN estimates of incidence and mortality worldwide for 36 cancers in 185 countries. CA Cancer J Clin. 2024;74(3):229-263.
2. Rahib L, Smith BD, Aizenberg R, Rosenzweig AB, Fleshman JM, Matrisian LM. Projecting cancer incidence and deaths to 2030: the unexpected burden of thyroid, liver, and pancreas cancers in the United States. Cancer Res. 2014;74(11):2913-2921.
3. Mustafa M, Abbas K, Alam M, Habib S, Zulfareen, Hasan GM, Islam S, Shamsi A, Hassan I. Investigating underlying molecular mechanisms, signaling pathways, emerging therapeutic approaches in pancreatic cancer. Front Oncol. 2024;14:1427802.
4. Wood LD, Klimstra DS. Pathology and genetics of pancreatic neoplasms with acinar differentiation. Semin Diagn Pathol. 2014;31(6):491-497.
5. Jaffee EM, Hruban RH, Canto M, Kern SE. Focus on pancreas cancer. Cancer Cell. 2002;2(1):25-28.
6. Jones S, Zhang X, Parsons DW, Lin JC, Leary RJ, Angenendt P, Mankoo P, Carter H, Kamiyama H, Jimeno A *et al*. Core signaling pathways in human pancreatic cancers revealed by global genomic analyses. Science. 2008;321(5897):1801-1806.
7. Wang S, Zheng Y, Yang F, Zhu L, Zhu XQ, Wang ZF, Wu XL, Zhou CH, Yan JY, Hu BY *et al*. The molecular biology of pancreatic adenocarcinoma: translational challenges and clinical perspectives. Signal Transduct Target Ther. 2021;6(1):249.

8. Pajewska M, Partyka O, Czerw A, Deptala A, Cipora E, Gaska I, Wojtaszek M, Sygit K, Sygit M, Krzych-Falta E *et al*. Management of metastatic pancreatic cancer-comparison of global guidelines over the last 5 years. Cancers (Basel). 2023;15(17):4400.
9. Chen X, Liu F, Xue Q, Weng X, Xu F. Metastatic pancreatic cancer: mechanisms and detection (Review). Oncol Rep. 2021;46(5):231.
10. Lee ES, Lee JM. Imaging diagnosis of pancreatic cancer: a state-of-the-art review. World J Gastroenterol. 2014;20(24):7864-7877.
11. Kleeff J, Korc M, Apte M, La Vecchia C, Johnson CD, Biankin AV, Neale RE, Tempero M, Tuveson DA, Hruban RH *et al*. Pancreatic cancer. Nat Rev Dis Primers. 2016;2:16022.
12. Karandish F, Mallik S. Biomarkers and targeted therapy in pancreatic cancer. Biomark Cancer. 2016;8(Suppl 1):27-35.
13. Nichetti F, Rota S, Ambrosini P, Pircher C, Gusmaroli E, Droz Dit Busset M, Pusceddu S, Sposito C, Coppa J, Morano F *et al*. NALIRIFOX, FOLFIRINOX, and gemcitabine with nab-paclitaxel as first-line chemotherapy for metastatic pancreatic cancer: a systematic review and meta-analysis. JAMA Netw Open. 2024;7(1):e2350756.
14. Beutel AK, Halbrook CJ. Barriers and opportunities for gemcitabine in pancreatic cancer therapy. Am J Physiol Cell Physiol. 2023; 324(2):C540-C552.
15. Bengtsson A, Andersson R, Ansari D. The actual 5-year survivors of pancreatic ductal adenocarcinoma based on real-world data. Sci Rep. 2020;10(1):16425.
16. Hollinshead KER, Parker SJ, Eapen VV, Encarnacion-Rosado J, Sohn A, Oncu T, Cammer M, Mancias JD, Kimmelman AC. Respiratory supercomplexes promote

mitochondrial efficiency and growth in severely hypoxic pancreatic cancer. Cell Rep. 2020;33(1):108231.

17. Nagdas S, Kashatus JA, Nascimento A, Hussain SS, Trainor RE, Pollock SR, Adair SJ, Michaels AD, Sesaki H, Stelow EB *et al*. Drp1 promotes KRas-driven metabolic changes to drive pancreatic tumor growth. Cell Rep. 2019;28(7):1845-1859.

18. Kashatus JA, Nascimento A, Myers LJ, Sher A, Byrne FL, Hoehn KL, Counter CM, Kashatus DF. Erk2 phosphorylation of Drp1 promotes mitochondrial fission and MAPK-driven tumor growth. Mol Cell. 2015;57(3):537-551.

19. Viale A, Pettazzoni P, Lyssiotis CA, Ying H, Sanchez N, Marchesini M, Carugo A, Green T, Seth S, Giuliani V *et al*. Oncogene ablation-resistant pancreatic cancer cells depend on mitochondrial function. Nature. 2014;514(7524):628-632.

20. Araujo AA, de Melo MG, Rabelo TK, Nunes PS, Santos SL, Serafini MR, Santos MR, Quintans-Junior LJ, Gelain DP. Review of the biological properties and toxicity of usnic acid. Nat Prod Res. 2015;29(23):2167-2180.

21. Gimla M, Herman-Antosiewicz A. Multifaceted properties of usnic acid in disrupting cancer hallmarks. Biomedicines. 2024;12(10):2199.

22. Neff GW, Reddy KR, Durazo FA, Meyer D, Marrero R, Kaplowitz N. Severe hepatotoxicity associated with the use of weight loss diet supplements containing ma huang or usnic acid. J Hepatol. 2004;41(6):1062-1064.

23. Guzow-Krzeminska B, Guzow, K., Herman-Antosiewicz, A. Usnic acid derivatives as cytotoxic agents against cancer cells and the mechanisms of their activity. Current Pharmacology Reports 2019;5:429–439.

24. Gunawan GA, Gimla M, Gardiner MG, Herman-Antosiewicz A, Reekie TA. Divergent reactivity of usnic acid and evaluation of its derivatives for antiproliferative activity against cancer cells. Bioorg Med Chem. 2023;79:117157.

25. Gimla M, Pyrczak-Felczykowska A, Malinowska M, Hac A, Narajczyk M, Bylinska I, Reekie TA, Herman-Antosiewicz A. The pyrazole derivative of usnic acid inhibits the proliferation of pancreatic cancer cells in vitro and in vivo. Cancer Cell Int. 2023;23(1):210.

26. Pyrczak-Felczykowska A, Kaczorowska AK, Gieldon A, Braczko A, Smolenski RT, Antosiewicz J, Reekie TA, Herman-Antosiewicz A. Natural product as a lead for impairing mitochondrial respiration in cancer cells. J Enzyme Inhib Med Chem. 2025;40(1):2465575.

27. Chou TC. Theoretical basis, experimental design, and computerized simulation of synergism and antagonism in drug combination studies. Pharmacol Rev. 2006;58(3):621-681.

28. Chou TC. Drug combination studies and their synergy quantification using the Chou-Talalay method. Cancer Res. 2010;70(2):440-446.

29. Pyrczak-Felczykowska A, Narlawar R, Pawlik A, Guzow-Krzeminska B, Artymiuk D, Hac A, Rys K, Rendina LM, Reekie TA, Herman-Antosiewicz A *et al*. Synthesis of usnic acid derivatives and evaluation of their antiproliferative activity against cancer cells. J Nat Prod. 2019;82(7):1768-1778.

30. Carmona-Carmona CA, Dalla Pozza E, Ambrosini G, Errico A, Dando I. Divergent roles of mitochondria dynamics in pancreatic ductal adenocarcinoma. Cancers (Basel). 2022;14(9):2155.

31. Miquel M, Zhang S, Pilarsky C. Pre-clinical models of metastasis in pancreatic cancer. Front Cell Dev Biol. 2021;9:748631.

32. Alabas E, Ata Ozcimen A. The supression of migration and metastasis via inhibition of vascular endothelial growth factor in pancreatic adenocarcinoma cells applied danusertib. Turk J Gastroenterol. 2024;35(2):150-157.

33. Shi X, Wang X, Yao W, Shi D, Shao X, Lu Z, Chai Y, Song J, Tang W, Wang X. Mechanism insights and therapeutic intervention of tumor metastasis: latest developments and perspectives. Signal Transduct Target Ther. 2024;9(1):192.

34. den Hollander P, Maddela JJ, Mani SA. Spatial and temporal relationship between epithelial-mesenchymal transition (EMT) and stem cells in cancer. Clin Chem. 2024;70(1):190-205.

35. Youssef KK, Narwade N, Arcas A, Marquez-Galera A, Jimenez-Castano R, Lopez-Blau C, Fazilaty H, Garcia-Gutierrez D, Cano A, Galceran J *et al*. Two distinct epithelial-to-mesenchymal transition programs control invasion and inflammation in segregated tumor cell populations. Nat Cancer. 2024;5(11):1660-1680.

36. Liu M, Yang J, Zhang Y, Zhou Z, Cui X, Zhang L, Fung KM, Zheng W, Allard FD, Yee EU *et al*. ZIP4 promotes pancreatic cancer progression by repressing ZO-1 and Claudin-1 through a ZEB1-dependent transcriptional mechanism. Clin Cancer Res. 2018;24(13):3186-3196.

37. Zhu L, Tang N, Hang H, Zhou Y, Dong J, Yang Y, Mao L, Qiu Y, Fu X, Cao W. Loss of Claudin-1 incurred by DNMT aberration promotes pancreatic cancer progression. Cancer Lett. 2024;586:216611.

38. Ikenouchi J, Matsuda M, Furuse M, Tsukita S. Regulation of tight junctions during the epithelium-mesenchyme transition: direct repression of the gene expression of claudins/occludin by Snail. J Cell Sci. 2003;116(Pt 10):1959-1967.

39. Martinez-Estrada OM, Culleres A, Soriano FX, Peinado H, Bolos V, Martinez FO, Reina M, Cano A, Fabre M, Vilaro S. The transcription factors Slug and Snail act as repressors of Claudin-1 expression in epithelial cells. Biochem J. 2006;394(Pt 2):449-457.

40. Dongre A, Weinberg RA. New insights into the mechanisms of epithelial-mesenchymal transition and implications for cancer. Nat Rev Mol Cell Biol. 2019;20(2):69-84.

41. Ahn M, Ali A, Seo JH. Mitochondrial regulation in the tumor microenvironment: targeting mitochondria for immunotherapy. Front Immunol. 2024;15:1453886.

42. Carlosama C, Arevalo C, Jimenez MC, Lasso P, Uruena C, Fiorentino S, Barreto A. Triple negative breast cancer migration is modified by mitochondrial metabolism alteration induced by natural extracts of C. spinosa and P. alliacea. Sci Rep. 2024;14(1):20253.

43. Li Z, Zhang W, Guo S, Qi G, Huang J, Gao J, Zhao J, Kang L, Li Q. A Review of advances in mitochondrial research in cancer. Cancer Control. 2024;31:10732748241299072.

44. Lin P, Lu Y, Zheng J, Lin Y, Zhao X, Cui L. Strategic disruption of cancer's powerhouse: precise nanomedicine targeting of mitochondrial metabolism. J Nanobiotechnology. 2024;22(1):318.

45. Biswas P, Palazzo J, Schlanger S, Jayaram DT, Islam S, Page RC, Stuehr DJ. Visualizing mitochondrial heme flow through GAPDH in living cells and its regulation by NO. Redox Biol. 2024;71:103120.

46. Boland ML, Chourasia AH, Macleod KF. Mitochondrial dysfunction in cancer. Front Oncol. 2013;3:292.

47. Trotta AP, Chipuk JE. Mitochondrial dynamics as regulators of cancer biology. Cell Mol Life Sci. 2017;74(11):1999-2017.

48. Chen H, Chan DC. Mitochondrial dynamics in regulating the unique phenotypes of cancer and stem cells. Cell Metab. 2017;26(1):39-48.

49. Yu M, Nguyen ND, Huang Y, Lin D, Fujimoto TN, Molkentine JM, Deorukhkar A, Kang Y, San Lucas FA, Fernandes CJ *et al*. Mitochondrial fusion exploits a therapeutic vulnerability of pancreatic cancer. JCI Insight. 2019;5(16):e126915.

50. Minarrieta L, Annis MG, Audet-Delage Y, Kuasne H, Pacis A, St-Louis C, Nowakowski A, Biondini M, Khacho M, Park M *et al*. Mitochondrial elongation impairs breast cancer metastasis. Sci Adv. 2024;10(45):eadm8212.

51. Sun Y, Liu Z, Zou X, Lan Y, Sun X, Wang X, Zhao S, Jiang C, Liu H. Mechanisms underlying 3-bromopyruvate-induced cell death in colon cancer. J Bioenerg Biomembr. 2015;47(4):319-329.

52. Dell'Antone P. Targets of 3-bromopyruvate, a new, energy depleting, anticancer agent. Med Chem. 2009;5(6):491-496.

53. Lis P, Jurkiewicz P, Cal-Bakowska M, Ko YH, Pedersen PL, Goffeau A, Ulaszewski S. Screening the yeast genome for energetic metabolism pathways involved in a phenotypic response to the anti-cancer agent 3-bromopyruvate. Oncotarget. 2016;7(9):10153-10173.

54. Pereira da Silva AP, El-Bacha T, Kyaw N, dos Santos RS, da-Silva WS, Almeida FC, Da Poian AT, Galina A. Inhibition of energy-producing pathways of HepG2 cells by 3-bromopyruvate. Biochem J. 2009;417(3):717-726.

55. Roy S, Dukic T, Bhandary B, Tu KJ, Molitoris J, Ko YH, Shukla HD. 3-Bromopyruvate inhibits pancreatic tumor growth by stalling glycolysis, and dismantling mitochondria in a syngeneic mouse model. Am J Cancer Res. 2022;12(11):4977-4987.

56. Jardim-Messeder D, Moreira-Pacheco F. 3-Bromopyruvic acid inhibits tricarboxylic acid cycle and glutaminolysis in HepG2 Cells. Anticancer Res. 2016;36(5):2233-2241.

57. Azevedo-Silva J, Queiros O, Baltazar F, Ulaszewski S, Goffeau A, Ko YH, Pedersen PL, Preto A, Casal M. The anticancer agent 3-bromopyruvate: a simple but powerful molecule taken from the lab to the bedside. J Bioenerg Biomembr. 2016;48(4):349-362.

58. Calvino E, Estan MC, Sanchez-Martin C, Brea R, de Blas E, Boyano-Adanez Mdel C, Rial E, Aller P. Regulation of death induction and chemosensitizing action of 3-bromopyruvate in myeloid leukemia cells: energy depletion, oxidative stress, and protein kinase activity modulation. J Pharmacol Exp Ther. 2014;348(2):324-335.

59. Mu M, Zhang Q, Zhao C, Li X, Chen Z, Sun X, Yu J. 3-Bromopyruvate overcomes cetuximab resistance in human colorectal cancer cells by inducing autophagy-dependent ferroptosis. Cancer Gene Ther. 2023;30(10):1414-1425.

60. Zugic A, Tadic V, Savic S. Nano- and microcarriers as drug delivery systems for usnic acid: review of literature. Pharmaceutics. 2020;12(2):156.

12.3.1. Oświadczenia autorów

Gdańsk, 06.03.2025 r.

mgr Mariola Gimła
Katedra Biologii i Genetyki Medycznej
Wydział Biologii
Uniwersytet Gdański

Oświadczenie o wkładzie w publikację

Oświadczam, że mój wkład w publikację:

Gimła, M., Hac, A., Reekie, T., A., Herman-Antosiewicz, A. The usnic acid pyrazole derivative inhibits pancreatic cancer cell migration and invasion, alters mitochondrial functioning and a glycolysis inhibitor enhances its cytotoxic activity (2025)

polegał na:

- Kierowaniu projektami badawczymi ze źródeł Uniwersytetu Gdańskiego
- Zaplanowniu i przeprowadzeniu eksperymentów
- Analizie i interpretacji otrzymanych danych
- Przygotowaniu figur
- Napisaniu wstepnej wersji pracy
- Poprawieniu ostatecznej wersji manuskryptu

Mariola Gimła

Gdańsk, 06.03.2025 r.

dr Aleksandra Hać
Katedra Biologii i Genetyki Medycznej
Wydział Biologii
Uniwersytet Gdański

Oświadczenie o wkładzie w publikację

Oświadczam, że mój wkład w publikację:

Gimła, M., Hac, A., Reekie, T., A., Herman-Antosiewicz, A. The usnic acid pyrazole derivative inhibits pancreatic cancer cell migration and invasion, alters mitochondrial functioning and a glycolysis inhibitor enhances its cytotoxic activity (2025)

polegał na:

- Udziale w interpretacji wyników i przygotowaniu manuskryptu publikacji

Wydział Biologii
KATEDRA BIOLOGII I GENETYKI MEDYCZNEJ
dr Aleksandra Hać

March 14, 2025

Tristan A. Reekie
School of Science
University of New South Wales Canberra
Australian Capital Territory
Canberra, 2600, Australia

Author contributions

I hereby declare that my contribution in the manuscript:

Gimła, M., Hac, A., Reekie, T., A., Herman-Antosiewicz, A. The usnic acid pyrazole derivative inhibits pancreatic cancer cell migration and invasion, alters mitochondrial functioning and a glycolysis inhibitor enhances its cytotoxic activity (2025)

included:

- synthesized derivative 5
- reviewed and edited the manuscript

signature

Gdańsk, 05.03.2025 r.

prof. dr hab. Anna Herman-Antosiewicz
Katedra Biologii i Genetyki Medycznej
Wydział Biologii
Uniwersytet Gdański

Oświadczenie o wkładzie w publikację

Oświadczam, że mój wkład w manuskrypt publikacji:

Gimła, M., Hac, A., Reekie, T., A., Herman-Antosiewicz, A. The usnic acid pyrazole derivative inhibits pancreatic cancer cell migration and invasion, alters mitochondrial functioning and a glycolysis inhibitor enhances its cytotoxic activity (2025)

polegał na:

- analizie i interpretacji otrzymanych danych
- udziale w przygotowaniu rycin
- udziale w napisaniu wstępnej wersji pracy
- opiece merytorycznej nad mgr Mariolą Gimłą
- kierowaniu projektem Harmonia

Wydział Biologii
KATEDRA BIOLOGII i GENETYKI MEDYCZNEJ
Anna Herman-Antosiewicz
prof. dr hab. Anna Herman-Antosiewicz

Osiągnięcia naukowe

Artykuły naukowe

1. Fornalik Michał, Moska Sandra, **Gimła Mariola**, Yabluchanskiy Andriy, Bonin Pinto Camila (2025) Donepezil for cancer-related cognitive impairment: systematic review and meta-analysis, *Clin Exp Med.* 25: 196. DOI: 10.1007/s10238-025-01708-w.

2. **Gimła Mariola**, Herman-Antosiewicz Anna (2024) Multifaceted properties of usnic acid in disrupting cancer hallmarks, *Biomedicines* 12(10): 2199. DOI:10.3390/biomedicines12102199.

3. **Gimła Mariola**, Pyrczak-Felczykowska Agnieszka, Malinowska Marcelina, Hać Aleksandra, Narajczyk Magdalena, Bylińska Irena, Reekie Tristan, Herman-Antosiewicz Anna (2023) The pyrazole derivative of usnic acid inhibits the proliferation of pancreatic cancer cells in vitro and in vivo, *Cancer Cell International* 23(1): 210.
   DOI:10.1186/s12935-023-03054.

4. Gunawan Gregory A., **Gimła Mariola**, Gardiner Michael G., Herman-Antosiewicz Anna, Reekie Tristan A.: Divergent reactivity of usnic acid and evaluation of its derivatives for antiproliferative activity against cancer cells (2023) *Bioorganic & Medicinal Chemistry* 79(117157): 1-12. DOI:10.1016/j.bmc.2023.117157.

Patenty

1. *Pirazolowa pochodna kwasu usninowego, sposób otrzymywania pirazolowej pochodej kwasu usninowego i medyczne wykorzystanie pochodnej kwasu usninowego w terapii nowotworów, szczególnie nowotworów szyjki macicy*
   Herman-Antosiewicz Anna, Reekie Tristan, Pawlik Anna, **Gimła Mariola**, Brodecki Maciej, Żuczek Klaudia
   Wynalazek Chroniony, Numer zgłoszenia: P.440801,
   Numer patentu/prawa: **Pat.246171**,
   Data zgłoszenia: 30-03-2022,
   Data udzielenia prawa: 05-05-2024,
   Publikacja patentu/wzoru: [WUP 09-12-2024]

2. *Pochodna kwasu usninowego, sposób otrzymywania tej pochodnej, medyczne zastosowanie w terapii nowotworów, zastosowanie in vitro odczynnika*
   Herman-Antosiewicz Anna, Reekie Tristan, **Gimła Mariola**, Żuczek Klaudia
   Wynalazek Chroniony, Numer zgłoszenia: P.440802,
   Numer patentu/prawa: **Pat.246172**,
   Data zgłoszenia 30-03-2022,
   Data udzielenia prawa: 05-05-2024,
   Publikacja patentu/wzoru: [WUP 09-12-2024]

3. *Pochodna kwasu usninowego, sposób otrzymywania pochodnej kwasu usninowego i medyczne wykorzystanie pochodnej kwasu usninowego w terapii nowotworów oraz zastosowanie do indukcji stresu związanego z retikulum endoplazmatycznym*
   Herman-Antosiewicz Anna, **Gimła Mariola**, Pawlik Anna, Malinowska Marcelina, Hać Aleksandra, Guzow-Krzemińska Beata, Ryś Kamil
   Wynalazek Chroniony, Numer zgłoszenia: 436476,
   Numer patentu/prawa: **239308**,
   Data zgłoszenia: 24-12-2020,

Data udzielenia prawa: 22-11-2021,
Publikacja patentu/wzoru: [WUP 22-11-2021]

Konferencje naukowe

1. **Gimła Mariola,** Herman-Antosiewicz Anna: The pyrazole derivative of usnic acid inhibits the metastatic potential of pancreatic cancer cells *in vitro*. International Sopot Youth Conference "Where the world is heading?", Sopot, 2024.
2. **Gimła Mariola,** Herman-Antosiewicz Anna: The pyrazole derivative of usnic acid suppresses metastatic capabilities of pancreatic cancer cells *in vitro.* Oklahoma Cell Biology Symposium, Oklahoma City, USA, 2024.
3. **Gimła Mariola,** Herman-Antosiewicz Anna: Pyrazole usnic acid derivative as an antiproliferative agent towards pancreatic cancer cells. International Conference on Cancer and Oncology Research, Rzym, Włochy, 2023.
4. **Gimła Mariola,** Hać Aleksandra, Herman-Antosiewicz Anna: Anti-metastatic potential of usnic acid derivative against pancreatic cancer cells. 12th European Workshop on Cell Death - Cell death - Inflammation – Cancer (EWCD 2022), Fiuggi, Włochy, 2022.
5. **Gimła Mariola**, Reekie Tristan, Hać Aleksandra, Herman-Antosiewicz Anna: Usnic acid derivative as an effective antiproliferative agent towards pancreatic cancer cells. 8th Central European Congress of Life Science (Eurobiotech 2022), Kraków, 2022.
6. **Gimła Mariola,** Reekie Tristan, Hać Aleksandra, Herman-Antosiewicz Anna: Antiproliferative potential of usnic acid derivative against cancer cells. 6th International Conference of Cell Biology, Kraków, 2020.
7. Budka Justyna**, Gimła Mariola,** Herman-Antosiewicz Anna, Hać Aleksandra: Anticancer potential of selected flavonol derivatives. Molecular Biology and Immunology of Cancer - R&D Perspectives: ScanBalt Forum, Gdańsk, 2019.

8. **Gimła Mariola,** Budka Justyna, Herman-Antosiewicz Anna, Hać Aleksandra: Synthetic flavonol derivatives affect crucial cellular processes in cancer cells. Molecular Biology and Immunology of Cancer - R&D Perspectives: ScanBalt Forum, Gdańsk, 2019.
9. **Gimła Mariola,** Wydra Piotr, Jarząb Mirosław, Lipińska Barbara: Comparison of biochemical properties of human HtrA2 proapoptotic protease and its frui homolog dOmi. III International Conference of Cell Biology, Kraków, 2017.

Projekty naukowe

1. Projekt: „Wpływ pochodnej kwasu usninowego na proces inwazji w komórkowym modelu nowotworu trzustki" finansowany przez Uniwersytet Gdański (nr. 539-D130-B859-21), 2021.

2. Projekt: „Działanie terapii łączonej na zmiany metabolizmu energetycznego w komórkowym modelu nowotworu trzustki" finansowany przez Uniwersytet Gdański (nr. 539-D130-B953-22), 2022.